Title
Age-related decline of occluding junctions in Drosophila melanogaster

Author
Hodge, Rachel Ann

Publication Date
2022

Peer reviewed|Thesis/dissertation

UNIVERSITY OF CALIFORNIA

Los Angeles

Age-related decline of occluding junctions in *Drosophila melanogaster*

A dissertation submitted in partial satisfaction of the

requirements for the degree Doctor of Philosophy

in Molecular Biology

by

Rachel Ann Hodge

2022

ABSTRACT OF THE DISSERTATION

Age-related decline of occluding junctions in

Drosophila melanogaster

by

Rachel Ann Hodge

Doctor of Philosophy in Molecular Biology

University of California, Los Angeles, 2022

Professor Margot Elizabeth Quinlan, Chair

Intestinal barrier function declines across species with age, including *Drosophila melanogaster,* and the causes are unknown. Occluding junctions, referred to as tight junctions (TJs) in mammals and septate junctions (SJs) in arthropods, contribute significantly to the maintenance of intestinal barrier function. The tricellular septate junction (tSJ) is at the point where three adjacent cells meet. Our lab previously demonstrated that aging results in mis-localization of the tricellular SJ (tSJ)-specific component Gliotactin (Gli) in enterocytes (ECs) of the fly intestine. Because we found Gli is required at the tSJ to maintain intestinal homeostasis, we decided to investigate the tSJ protein Bark beetle (Bark) to find if it is similarly required. Like Gli, Bark appears to mislocalize away from the tSJ in aged fly intestines. EC-specific *bark* depletion in young flies disrupted intestinal stem cell homeostasis, compromised intestinal barrier function,

and shortened lifespan. We concluded that Bark is required at the tSJ to maintain intestinal homeostasis, and that mislocalization of Bark in aged flies may contribute to the overall intestinal aging phenotype. Additionally, we had previous evidence that suggested age-related SJ protein mislocalization is due to changes in vesicular trafficking. Our preliminary data indicates early and late endosomes may increase in size or aggregation in the aged fly intestine, and SJ proteins Mesh and Gli may respectively accumulate in each compartment. The endocytosis pathway also appears to be required for normal SJ protein localization in the intestine. Future studies will further characterize age-related changes in vesicular trafficking in the fly intestine, which may be beneficial for prevention of age-related intestinal barrier decline in humans.

The dissertation of Rachel Ann Hodge has been approved.

Dana Leanne Jones

Volker Hartenstein

Alvaro Sagasti

Elaine Yih-Nien Hsiao

Margot Elizabeth Quinlan, Chair

University of California, Los Angeles

2022

This thesis is dedicated to every one of my scientific mentors:

Nancy Suttle, Rick Navarre, Peri LoBue, Pat Kite, Karen Shepherd, Kim Wolff, Stuart Ravnik, Lynn Tam, Andrew Pieper, Pin Xu, Paula Huntington, Thomas Miller, Aldo Compagnoni, Jeffrey Zigman, Bharath Manivasagam, Aryeh Warmflash, George Britton, Kinshuk Mitra, Utpal Banerjee, Carrie Spratford, Alvaro Sagasti, Aaron van Loon, Larry Zipursky, Ying Lin, Saumya Jain, Jeffrey Long, Diana Azurdia, Margot Quinlan, Volker Hartenstein, Elaine Hsiao, Martin Resnik-Docampo, Rafael Demarco, Cecilia D'Alterio, Kathleen Cunningham, Marie Clémot, and Leanne Jones.

Thank you for your patience and wisdom.

Table of Contents

List of Figures

Chapter 1: Introduction

Chapter 2: The septate junction component Bark beetle is required to maintain intestinal homeostasis

List of Tables

Acknowledgments

I would first like to thank the entire Jones Lab for their support, scientific insight, and humor. Thank you to Martin Resnik-Docampo, who generously passed this project down to me; Cecilia D'Alterio, our amazing lab manager for many years; Rafael Demarco, Kathleen Cunningham, and Marie Clémot for their mentorship; my fellow Jones Lab graduate students, Jordan Kryza and Nick Jackson, for going on this grad school journey with me. I want to especially thank my advisor, Leanne Jones, for her outstanding guidance, knowledge, and scientific leadership.

Next, I would like to thank the leaders and administrators of the UCLA MCDB department, Molecular Biology PhD program, and Biosciences PhD program for their commitment to creating a world-class research environment: Utpal Banerjee, Amander Clark, Luisa Iruela-Arispe, Hilary Coller, Jeffrey Long, Alvaro Sagasti, Diana Azurdia, Gregory Payne, Ashley Straight, Stephanie Cuellar, Helen Houldsworth, Nadia Avila, and Nancy Jensen.

The Hartenstein lab is especially thanked for their generosity in offering research space and resources. The Walker lab, Banerjee lab, Reiff lab, Terasaki Life Sciences building staff, UCLA BSCRC Microscopy Core, and UCLA *Drosophila* Media Facility are also thanked for their guidance and technical support.

In addition, I want to thank all of my previous mentors at UCLA, Rice University, UT Southwestern Medical Center, and the Plano Independent School District, whom this dissertation is dedicated to. I am so incredibly grateful that I got the chance to learn from each of them.

My friends in and outside of science are also thanked for supplying joy when I most needed it, especially: Abby McCracken, Darien Wulf, Orsolya Ficsor, Cher Tang, Alitha Partono, Peggie Chien, and Amara Thind.

Finally, I would like to thank my parents, Bill and Janet Hodge, who worked tirelessly to enable the beginning of my scientific journey. It is absolutely certain that I could not have accomplished this without their support.

Chapter 2 is adapted from a manuscript in preparation:

R. A. Hodge, M. Ghannam, E. Edmond, F. de la Torre, C. D'Alterio, N.H. Kaya, M. Resnik-Docampo, T. Reiff and D. L. Jones (2022). The septate junction component *Bark beetle* is required for *Drosophila* intestinal barrier function and homeostasis. *In preparation.*

M. Ghannam, N.H. Kaya and T. Reiff performed experiments and data analysis related to Bark beetle's role in enteroblasts. E. Edmond and F. de la Torre performed the experiment demonstrating Bark depletion by RNAi expression. C. D'Alterio performed fly husbandry and demonstrated anti-Bark antibody and Bark::GFP colocalization. M. Resnik-Docampo, T. Reiff and D. L. Jones provided guidance. All other experiments and data analysis were performed by R. A. Hodge.

This work was supported by the UCLA Summer Mentored Research Fellowship (SMRF), the UCLA Cell and Molecular Biology Training Program (Ruth L. Kirschstein National Research Service Award GM007185), and the NIH: AG040288, AG028092 and DK105442 (D.L.J.).

Chapter 3 is unpublished work. Experiments and data analysis were primarily performed by R.A. Hodge. C. Ochoa performed some experiments demonstrating the requirement for endocytosis in septate junction protein localization.

This work was supported by the UCLA Cell and Molecular Biology Training Program (Ruth L. Kirschstein National Research Service Award GM007185), and the NIH: AG040288, AG028092 and DK105442 (D.L.J.).

Vita

Education

University of California Los Angeles, Los Angeles, CA (2017 – present)
Doctor of Philosophy in Molecular Biology
Rice University, Houston, TX (2013 - 2017)
Bachelor of Arts: Biochemistry & Cell Biology
Minor: Ecology & Evolutionary Biology

Experience

- June 2018 to present: Jones Lab, University of California Los Angeles, Los Angeles, CA
- August 2015 to May 2017: Warmflash Lab, Rice University, Houston, TX
- June 2016 to August 2016: Banerjee Lab, University of California Los Angeles, Los Angeles, CA
- June 2015 to August 2015: Zigman Lab, UT Southwestern Medical Center, Dallas, TX
- October 2013 to April 2015: Miller Lab, Rice University, Houston, TX
- June 2012 to July 2012: Pieper Lab, UT Southwestern Medical Center, Dallas, TX

Presentations

63rd Annual *Drosophila* Research Conference: San Diego, CA

Title: The septate junction protein Bark beetle is required for *Drosophila* intestinal barrier function and homeostasis

April 2022

"Flying Through the Gut" Seminar: Virtual

Title: Age-related occluding junction decline in the *Drosophila melanogaster* intestine

March 2022

Cell and Developmental Biology Club: University of California – Los Angeles, Los Angeles, CA (Virtual)

Title: Age-related occluding junction decline in the *Drosophila melanogaster* intestine

January 2022

American Society for Cell Biology Conference: Virtual

Title: The septate junction protein Bark beetle is required for *Drosophila* intestinal barrier function and homeostasis

December 2021

Molecular, Cell, and Developmental Biology Retreat: University of California – Los Angeles, Los Angeles, CA

Title: Age-related occluding junction decline in the *Drosophila melanogaster* intestine

December 2021

Molecular Biology Interdepartmental Program (MBIDP) Retreat: University of California – Los Angeles, Los Angeles, CA

Title: Age-related occluding junction decline in the *Drosophila melanogaster* intestine

September 2021

Molecular Biology Interdepartmental Program (MBIDP) Retreat: University of California – Los Angeles, Los Angeles, CA (Virtual)

Title: Age-related occluding junction decline in the *Drosophila melanogaster* intestine

September 2020

Molecular Biology Interdepartmental Program (MBIDP) Recruitment Weekend: University of California – Los Angeles, Los Angeles, CA

Title: Age-related occluding junction decline in the *Drosophila melanogaster* intestine

January 2020, February 2020

Molecular Biology Interdepartmental Program (MBIDP) Student Seminar: University of California – Los Angeles, Los Angeles, CA

Title: Age-related occluding junction decline in the *Drosophila melanogaster* intestine

October 2019

Awards and Honors

Summer Mentored Research Fellowship: University of California – Los Angeles, Los Angeles, CA

July 2021

Graduate Poster Prize: University of California – Los Angeles, Los Angeles, CA

Molecular, Cell, and Developmental Biology Department Retreat

December 2019

Cell and Molecular Biology Training Program Fellowship: University of California – Los Angeles, Los Angeles, CA

June 2018 to October 2019

Roy Trustee Distinguished Scholarship: Rice University, Houston, TX

August 2013 to May 2017

Nicandros Century Scholarship: Rice University, Houston, TX

August 2013 to May 2015

Publications

- **Rachel Hodge,** Emma Edmond, Fernando de la Torre, Martin Resnik-Docampo, Mirna Ghannam, Nida Kaya, Tobias Reiff, and Leanne Jones (manuscript in progress): The septate junction protein Bark beetle is required for *Drosophila* intestinal barrier function and homeostasis.
- George Britton, Idse Heemskerk, **Rachel Hodge,** Amina A. Qutub, and Aryeh Warmflash (2019): A novel self-organizing embryonic stem cell system reveals signaling logic underlying the patterning of human ectoderm. Development 146 (20): dev179093
- Pin Xu, Brad A. Grueter, Jeremiah K. Britt, Latisha McDaniel, Paula J. Huntington, **Rachel Hodge**, Stephanie Tran, Brittany L. Mason, Charlotte Lee, Linh Vong, Bradford B. Lowell, Robert C. Malenka, Michael Lutter, and Andrew A. Pieper (2013): Double deletion of melanocortin 4 receptors and SAPAP3 corrects compulsive behavior and obesity in mice. PNAS 110 (26): 10759-10764

Chapter 1: Introduction

The *Drosophila* posterior midgut (PMG) is analogous to the mammalian small intestine

The *Drosophila melanogaster* posterior midgut (PMG) is analogous to the human small intestine (Apidianakis & Rahme, 2011), since both are responsible for nutrient absorption. The PMG epithelium is composed primarily of post-mitotic enterocytes (ECs), polyploid cells with microvilli which facilitate the absorption of nutrients from food. ECs, along with secretory enteroendocrine (EE) cells, are maintained by a pool of intestinal stem cells (ISCs). ISCs primarily generate daughter enteroblasts (EBs), which then differentiate into either mature ECs or EEs (Apidianakis & Rahme, 2011) (**Fig. 1-1**). EB fate is specified by activation of the Notch signaling pathway (Ohlstein & Spradling, 2007; Micchelli & Perrimon, 2006), leading to the expression of the transcription factor *klumpfuss (klu)* in EBs. EE and EC fate decisions become stochastic upon loss of lineage specifying *klu,* and EB fates can be tracked using specific *klu*-based lineage tracing tools (e.g. klu^{ReDDM}) (Reiff *et al.*, 2019; Korzelius *et al.*, 2019). Due to *Drosophila*'s short life cycle and readily available genetic tools, including genetic drivers specific to subtypes of intestinal cells, it is a tractable model system for the mammalian small intestine.

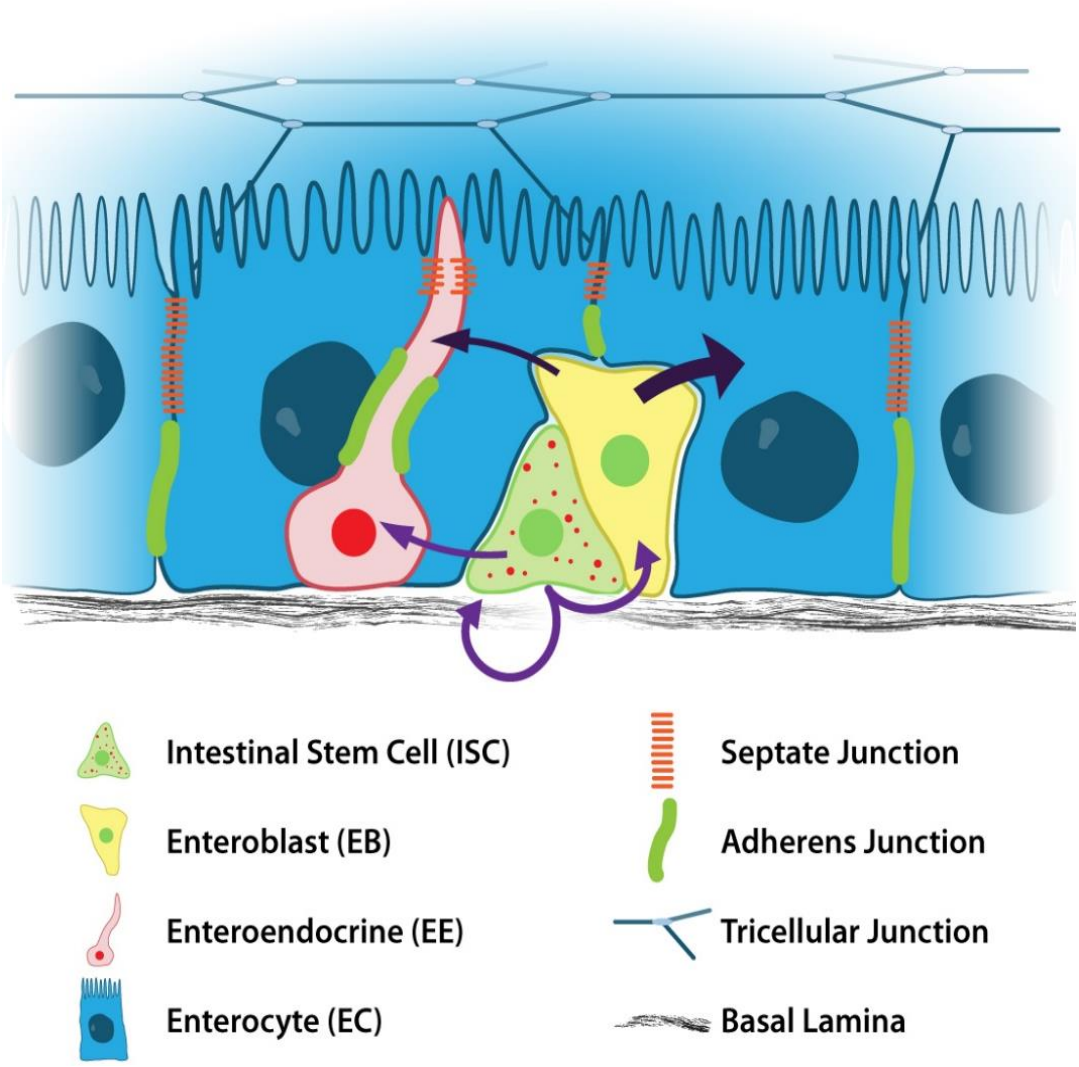

Figure 1-1: The *Drosophila melanogaster* posterior midgut. The posterior midgut (PMG) is a monolayer epithelium composed primarily of absorptive enterocytes (ECs). ECs and secretory enteroendocrine cells (EEs) are continuously turned over by intestinal stem cells (ISCs). ISCs can asymmetrically divide to produce daughter enteroblasts (EBs) which further differentiate into post-mitotic ECs or EEs. ECs and EEs have septate junctions (SJs, orange) and adherens junctions (AJs, green). (Chris Koehler).

Barrier function is required in epithelia

Barrier function in the intestinal epithelium allows selective paracellular transport of water, ions, and nutrients while maintaining food matter and microbes inside the intestinal lumen (Marchiando *et al*, 2010). This is thought to be particularly crucial to homeostasis because leakage of food matter or microbes could be harmful to interstitial tissues. There is a strong correlation between aging and decline in intestinal barrier integrity across multiple species, including rats, baboons, and *Drosophila melanogaster* (Kirkwood, 2004; Biteau *et al.*, 2008; Ren *et al.*, 2014; Schiffrin *et al.*, 2010; Tran & Greenwood-Van Meerveld, 2013; Rera *et al.*, 2012). Age-associated loss of the intestinal barrier in *Drosophila* is associated with systemic metabolic defects, such as changes in insulin/insulin-like growth factor signaling, intestinal dysbiosis, chronic expression of inflammatory genes, and an increase in proliferation of intestinal stem cells (ISCs) (Choi *et al.*, 2011; Clark *et al.*, 2015; Rera *et al.*, 2012; Guo *et al.*, 2014). In humans, inflammatory bowel disease (Michielan & D'Incà, 2015) and other gastrointestinal disorders such as celiac disease (Schuppan *et al.*, 2009) are correlated with increased intestinal permeability.

Assays for barrier function

Studies of epithelial barrier function use a variety of methods to track permeability changes *in vivo.* Trans-epithelial electrical resistance (TEER) can be utilized *ex vivo* to determine permeability in an epithelial monolayer (Mullin *et al.*, 2002; Tran & Greenwood-Van Meerveld, 2013), but this has limited applications in studying the complex effects of aging. In particular, the microbiome and immune system have been demonstrated to alter

intestinal permeability (Clark *et al.,* 2015; Rera *et al.*, 2012), which TEER cannot accurately account for.

Drosophila are an especially useful tool to survey intestinal barrier function due to their translucent abdomen allowing easy *in vivo* tracking. In 2011, the “Smurf assay” was developed as a noninvasive tool to track *Drosophila* intestinal barrier loss (Rera *et al.*, 2011). Flies are fed a nontoxic blue food dye, which is too large to be passively transported across healthy intestinal epithelia. In these individuals, dye is clearly visible only in the digestive tract when the abdomen is viewed under a light microscope (**Fig. 1-2,** left). However, with a stressor like age, intestinal injury, or acute cold stress, dye moves into the hemolymph and turns the fly’s body bright blue (a “Smurf”) (Rera *et al.*, 2011; MacMillan *et al.*, 2017; Resnik-Docampo *et al.*, 2017). Spontaneous “Smurfing,” indicating severe intestinal barrier loss, is associated with impending death within several days. The severity of this phenotype is apparent through its clear visual difference to non-Smurfs, and because both young and old Smurf flies have significantly shorter lives than age-matched counterparts (Rera *et al.*, 2012).

Because the Smurf assay is a noninvasive monitor of barrier function that can be easily used in a large sample size, it allows researchers to pinpoint when digestive barrier function fails. Following the development of the Smurf assay, it was adapted for use in zebrafish and *C. elegans* (Martins *et al.*, 2018). Variations have also been performed using fluorescently labeled dextran and D-mannitol, allowing quantification of dye movement and use in vertebrate model systems (MacMillan *et al.*, 2017; Condette *et al.*, 2014; Bagnat *et al.*, 2007). Given these benefits, our lab uses the *Drosophila* Smurf assay

to determine when severe intestinal barrier loss occurs during aging or upon disruption of intestinal homeostasis.

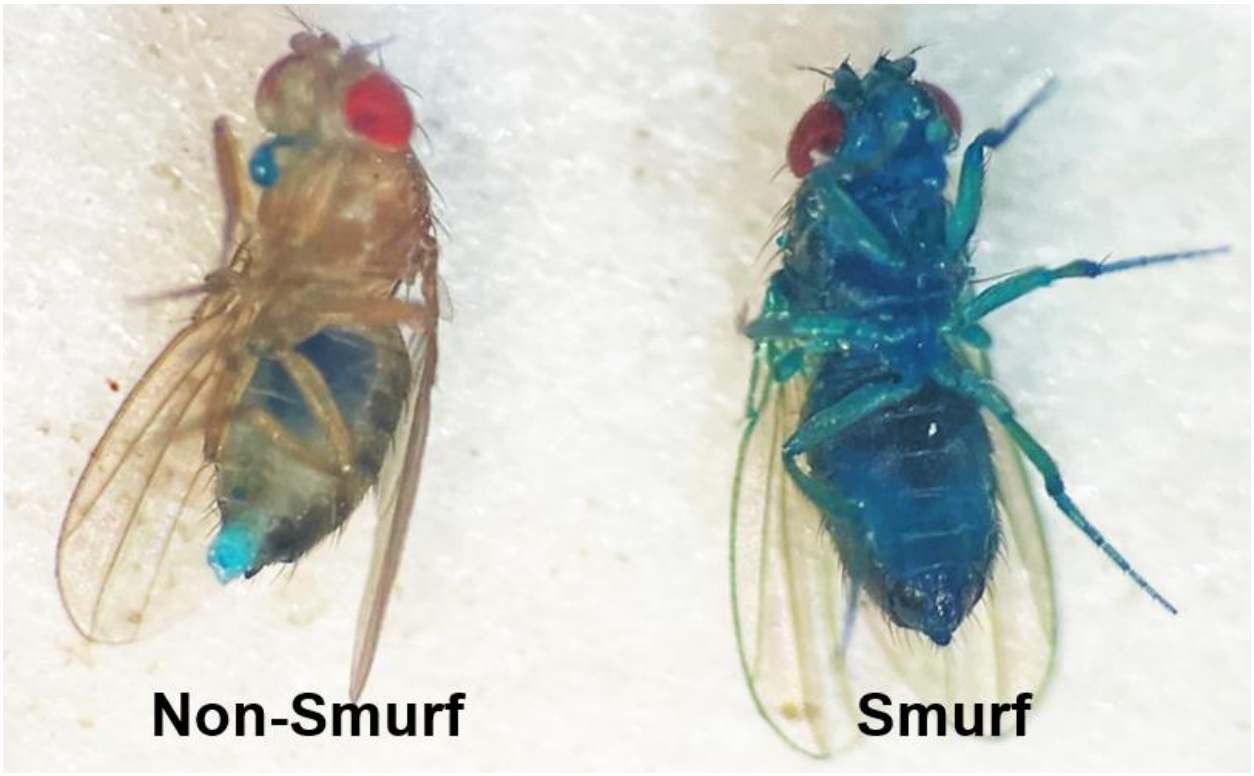

Figure 1-2: The Smurf assay indicates severe intestinal barrier loss. In the Smurf assay, flies are fed a non-toxic blue food dye. In flies with normal intestinal barrier function (i.e. young and without manipulation of the barrier), blue dye is visible through the translucent abdomen (left). In flies with severe intestinal barrier loss, blue dye spreads through the hemolymph, turning the entire body bright blue (right).

Occluding junctions contribute to barrier function

Multiple factors, including the microbiome, metabolism, and immune system in *Drosophila* (Clark *et al.*, 2015) and the mucus layer in mammals (Mu *et al.*, 2017), have been identified as key components of intestinal barrier maintenance. One of the most

well-characterized contributors to epithelial barrier function are intercellular occluding junctions, referred to as tight junctions (TJs) in vertebrates and septate junctions (SJs) in arthropods, play a major role in maintenance of the endothelial and epithelial barriers, including the intestinal barrier (Resnik-Docampo *et al.*, 2017; Salazar *et al.*, 2018; Izumi *et al.*, 2019). In *Drosophila*, maintenance of SJs in the intestine is required for normal barrier function. For example, our lab has previously demonstrated that SJ disruption by depletion of the SJ component Gliotactin (Gli) in adult fly ECs is sufficient to accelerate barrier loss and shorten lifespan (Resnik-Docampo *et al.*, 2017). Additionally, TJ integrity has been demonstrated to play an essential role in human health, since a variety of diseases are associated with TJ gene mutations. For example, mutations in claudin-14 or tricellulin are associated with non-syndromic deafness, and mutations in ZO-2 are associated with familial hypercholanaemia (Zihni *et al.*, 2016). Based on these studies, a greater understanding of occluding junction assembly and maintenance could be beneficial in treating genetic disorders associated with TJ gene mutations.

While TJs and SJs appear different ultrastructurally, they share many homologous proteins and both restrict passive paracellular transport. TJs use a branched network of independently sealing strands to create a semipermeable barrier at “kissing points” between adjacent membranes, and SJs reduce net solute diffusion by increasing diffusional distance across the junction with bridge-like structures called septa (Mariano *et al.*, 2011; Furuse & Tsukita, 2006). SJs are formed during late embryogenesis in *Drosophila* (Tepass & Hartenstein, 1994), and their components are continuously turned over across the cell’s lifetime (Oshima & Fehon, 2011).

TJ transmembrane proteins, which include claudins, occludin and JAM proteins, form the “kissing points” that adhere adjacent cell membranes. TJ cytosolic proteins, such as ZO proteins, link TJs to the cytoskeleton (Zihni *et al.*, 2016). While extensive studies using tools such as freeze-fracture electron microscopy have mapped the architecture of TJs, the ultrastructure of SJs is less well characterized. SJs are composed of a core complex of transmembrane proteins (Oshima & Fehon, 2011), as well as scaffolding proteins similar to ZO proteins (Willott *et al.*, 1993). The scaffolding proteins Discs large (Dlg) (homologous to mammalian ZO-1) and Scribbled (Scrib) are essential for the epithelial barrier, and are also required for the maintenance of basolateral epithelial polarity (Bilder *et al.*, 2000). The claudin-like proteins, including Snakeskin (Ssk), Mesh, and Tetraspanin 2A (Tsp2A) are thought to form the distinctive “ladder rungs” of the SJ visible in electron micrographs (Izumi *et al.*, 2012).

In *Drosophila melanogaster,* pleated SJs (pSJs) are found in ectodermally-derived epithelia, whereas smooth SJs (sSJs) are found in endodermally-derived tissue such as the midgut (Tepass & Hartenstein, 1994; Lane & Skaer, 1980; Resnik-Docampo *et al.*, 2018). pSJs and sSJs share most of the same protein components, and are named for their different visual appearances (**Fig. 1-3**). Like tight junctions, sSJs in *Drosophila* are oriented apically relative to adherens junctions (Resnik-Docampo *et al.*, 2018), making the *Drosophila* intestine a more ideal model for studying intestinal barrier function.

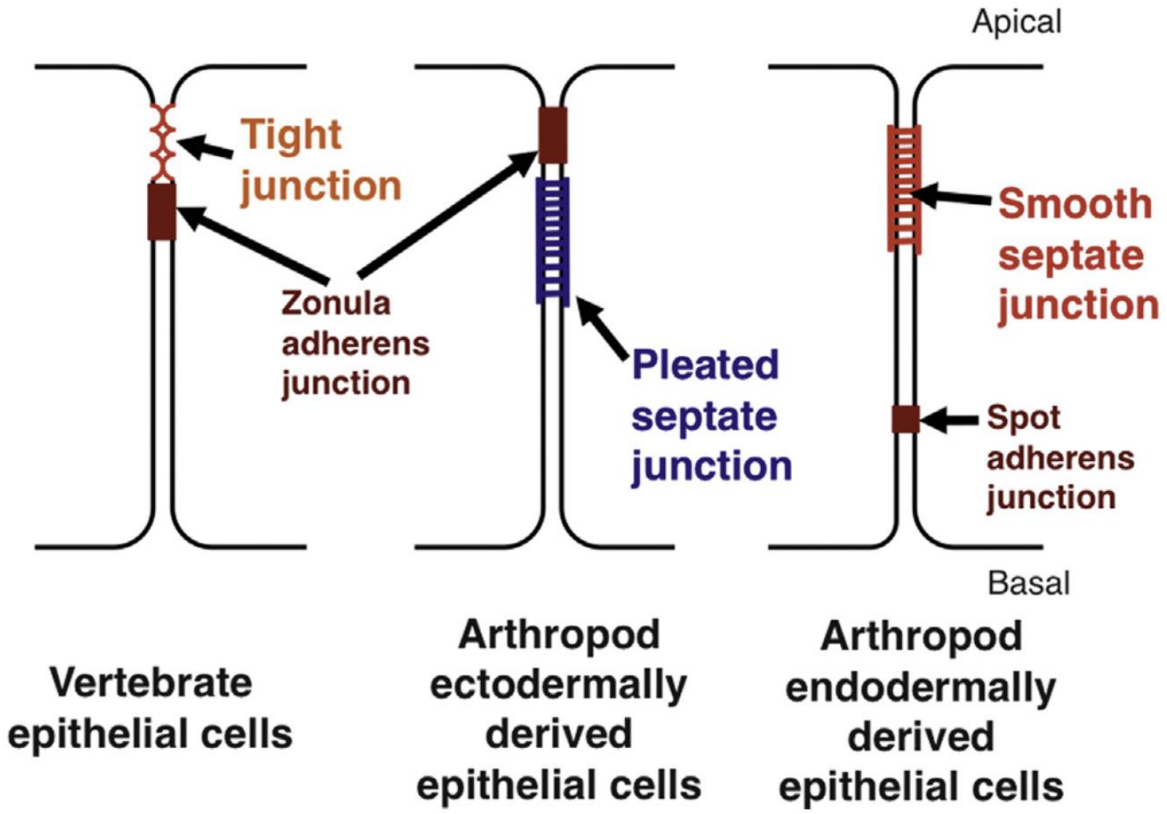

Figure 1-3: Organization of the vertebrate tight junction (TJ) and arthropod septate junction (SJ). In epithelial tissues, tight junctions (TJs) are oriented apically relative to adherens junctions (AJs), as are smooth septate junctions (sSJs). However, pleated septate junctions (pSJs) are oriented basally relative to AJs. (Izumi *et al.*, 2014).

Aging causes systemic dysfunction in the PMG

In the aged midgut, ISC proliferation increases dramatically, as measured by an increase in cells expressing the ISC/EB marker Escargot (esg) and a significant increase in mitotic events (Biteau *et al.*, 2008; Li & Jasper, 2016; Jiang *et al.*, 2009; Choi *et al.*, 2008; Park *et al.*, 2009). This increased proliferation causes psuedostratification of the epithelium, as well as an accumulation of cells that may be misdifferentiated (i.e., no

defined identity). Additional aging phenotypes in the PMG, which have been well-characterized, include an apparent loss of SJ physical integrity (visible gaps between membranes) (Resnik-Docampo *et al.*, 2017), dysbiosis, inflammation (Clark *et al.*, 2015), changes in insulin/insulin-like growth factor signaling (Choi *et al*., 2011; Clark *et al.*, 2015; Rera *et al*., 2012; Guo *et al*., 2014), activation of the JNK stressor pathway (Biteau *et al.,* 2008), and loss of the intestinal barrier (Resnik-Docampo *et al.*, 2017) (**Fig. 1-4**). "Smurfing," indicating severe intestinal barrier loss, generally occurs within several days before death. Depletion of SJ components via RNAi expression in the PMG recapitulates multiple aging phenotypes, including increased *esg*+ cells, increased JNK pathway activity, and severe intestinal barrier loss (Resnik-Docampo *et al.*, 2017). Notably, we performed a screen assessing JNK pathway activity and found that depletion of multiple SJ components, such as Bark beetle (Bark), is sufficient to significantly increase expression of the JNK pathway repressor *puckered* (*puc*) (Martín-Blanco *et al.*, 1998) (**Fig. 1-5**).

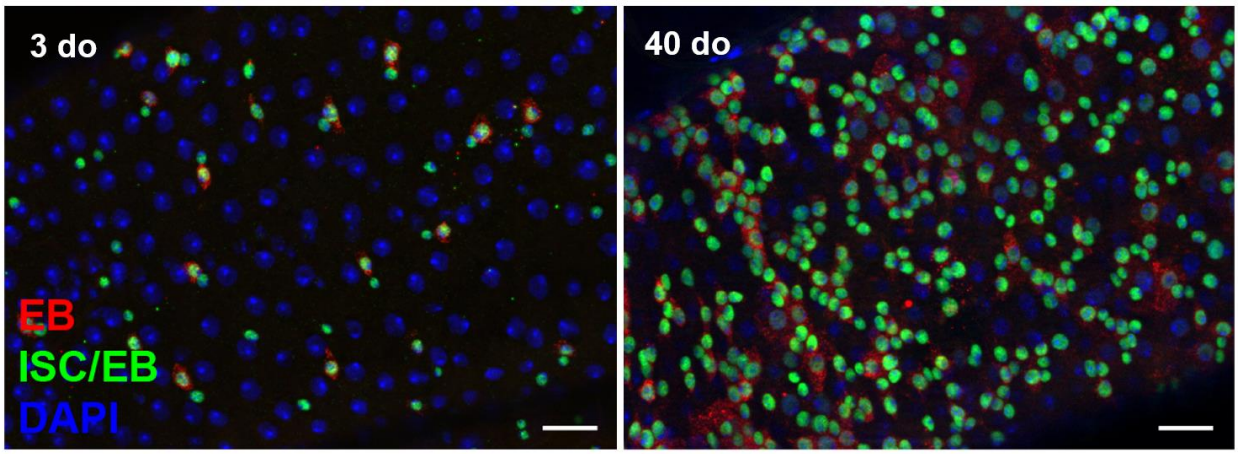

Figure 1-4: Effects of aging on intestinal stem cells (ISCs) and intestinal homeostasis. The *Drosophila* intestinal epithelium is comprised of ISCs, enteroblasts (EBs),

enteroendocrine cells (EEs) and enterocytes (ECs). GFP (green; *esg-GFP*) labels ISCs and EBs; Suppressor of Hairless-lacZ (*Su(H)*) (red, cytoplasmic) labels EBs. ECs can be identified by DAPI staining (blue) of their polyploid nuclei. With age, intestinal stem cells (ISCs, green, *esg*+) in the posterior midgut begin to proliferate in an irregular manner, giving rise to progenitor cells that simultaneously express markers of ISCs and differentiated ECs. (Chris Koehler).

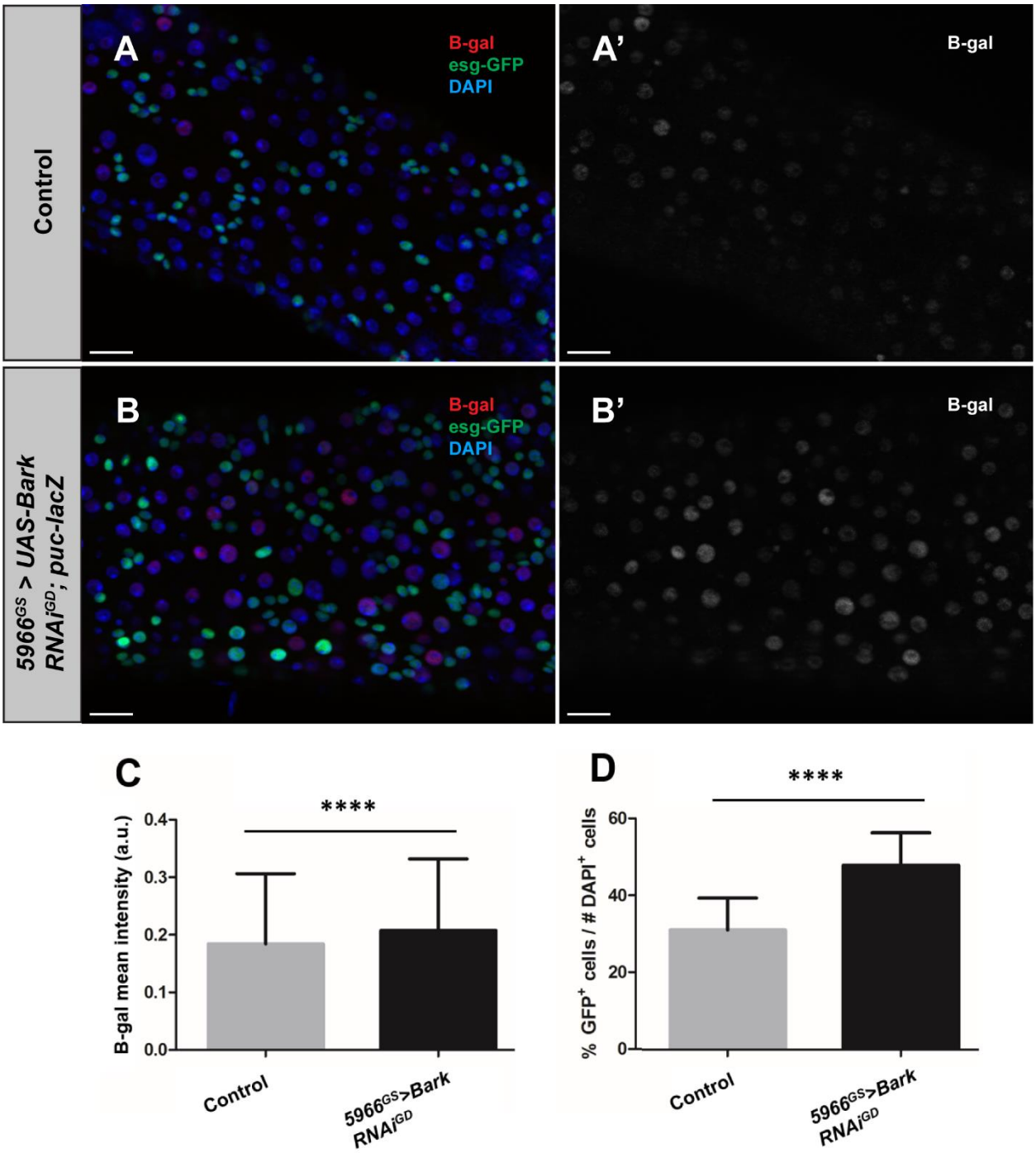

Figure 1-5: Depletion of the SJ component Bark beetle (Bark) significantly increases JNK pathway activity and number of *esg*+ cells. Young (2 do) flies with induced expression of *5966^{GS}>UAS-Bark RNAi^{GD}* for 9 days (**B**) have significantly higher JNK pathway activity (n = 4), as measured by mean fluorescence intensity of the reporter *puc-lacZ* in ECs

compared with uninduced controls (n = 6) (**A**). (**C, D**) Young (2 do) flies with induced expression of *5966^{GS}>UAS-Bark RNAi^{GD}* for 9 days have a significantly higher number of *esg*+ cells, based on expression of the *esg-GFP* enhancer trap. Four pictures were taken per PMG. Statistical significance was determined by Tukey's multiple comparisons test. ****, P < 0.0001. Scale bars, 20 μm.

Evidence for age-related decline of occluding junctions

Age-associated intestinal barrier decline in mammals and Drosophila

Age-related intestinal barrier decline has been demonstrated in mammals, although more extensive studies are still needed to fully understand limitations of the *Drosophila* model (Kirkwood, 2004; Biteau *et al.*, 2008; Ren *et al.*, 2014; Schiffrin *et al.*, 2010; Tran & Greenwood-Van Meerveld, 2013; Rera *et al.*, 2012). Notably, in the aged rat small intestine, the epithelium is visibly disrupted, including atrophy of intestinal villi. Additionally, genes for key tight junction proteins such as ZO-1 and occludin, are downregulated and tight junction strands are increasingly discontinuous, suggesting loss of physical integrity (Ren *et al.*, 2014). Additionally, in baboon colon samples cultured *ex vivo,* aged colons have increased permeability based on TEER. Downregulated tight junction gene expression and higher inflammatory cytokine levels are also observed (Tran & Greenwood-Van Meerveld *et al.*, 2013). Correspondingly, aged rat colon *ex vivo* culture also shows increased permeability (Mullin *et al.*, 2002). Human studies of intestinal barrier function loss, sometimes referred to as "leaky gut syndrome," are currently limited. However, studies have indicated that intestinal barrier loss in humans is associated with chronic inflammation (Marchiando *et al.*, 2010). Increased intestinal permeability has also

been associated with inflammatory bowel disease in humans, which includes Crohn's disease and ulcerative colitis (Marchiando *et al.*, 2010; Odenwald & Turner, 2017).

Septate junctions in the Drosophila intestine lose physical integrity with age

Electron micrographs of ECs in aged fly PMGs appear to show gap formation in sSJs, suggesting a loss of physical integrity (**Fig. 1-6**) (Resnik-Docampo *et al.*, 2017). Because aging and intestinal barrier loss are correlated in both *Drosophila* and mammals, and because occluding junctions are known to play a significant role in intestinal barrier maintenance, this apparent age-related structural deficiency could be a contributing factor to age-related barrier decline. Notably, a similar aging phenotype has been observed in rat small intestine tight junctions (TJs) (Ren *et al.*, 2014). TJ strands appear increasingly discontinuous, suggesting loss of TJ integrity which may contribute to age-associated intestinal barrier loss.

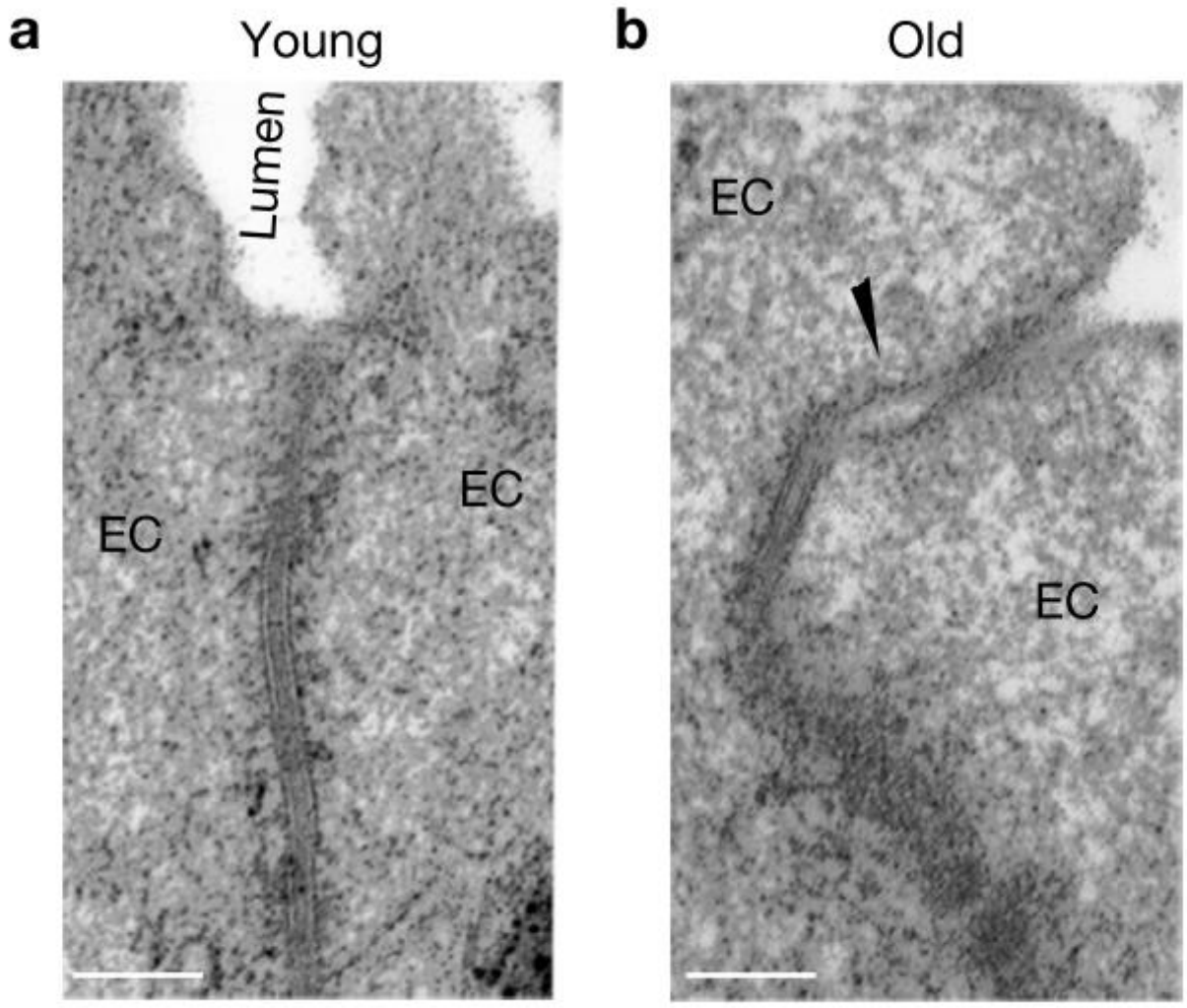

Figure 1-6: Apparent loss of structural integrity in sSJs in the aged fly posterior midgut. Figure adapted from Resnik-Docampo *et al.*, 2017. In young flies (left, 5 do), sSJs between ECs have their characteristic ladder-like appearance. In old flies (right, 45 do), sSJs appear to have gaps (arrowhead). This suggests a loss of junction physical integrity resulting in separation of the adjacent membranes.

Septate junction proteins in enterocytes of aged flies mislocalize with age

Following this observation that SJs appear to lose physical integrity with age in the fly PMG, our lab conducted a screen to observe SJ protein localization in young and old

fly PMGs. We established that many sSJ proteins change in localization in the old fly PMG. sSJ proteins increasingly localize to cytoplasmic puncta, and immunofluorescence staining reveals decreased fluorescence at the SJ relative to the cytoplasm (**Fig. 1-7**). Interestingly, the adherens junction (AJ) component Armadillo (Arm) did not significantly change its localization in the PMG with age (Resnik-Docampo *et al.*, 2017), although we have not yet characterized how additional aspects of AJs and the cytoskeleton may change with age in the PMG.

Surprisingly, no age-related change in pSJ protein localization was observed in the aged *Drosophila* hindgut (Resnik-Docampo *et al.*, 2017), which is analogous to the mammalian large intestine. While no electron microscopy was performed to observe the ultrastructure of aged hindgut SJs, this suggests that pSJs in the *Drosophila* hindgut maintain their structural integrity with age and do not contribute to age-related barrier failure. We have hypothesized that this is due to currently uncharacterized differences between sSJs and pSJs, although further investigation of other tissues containing both junction types will be required to confirm this. Since the *Drosophila* foregut also has pSJs, and due to more thorough prior studies of occluding junctions and barrier function in the PMG and mammalian small intestine, we decided to concentrate our efforts on the PMG.

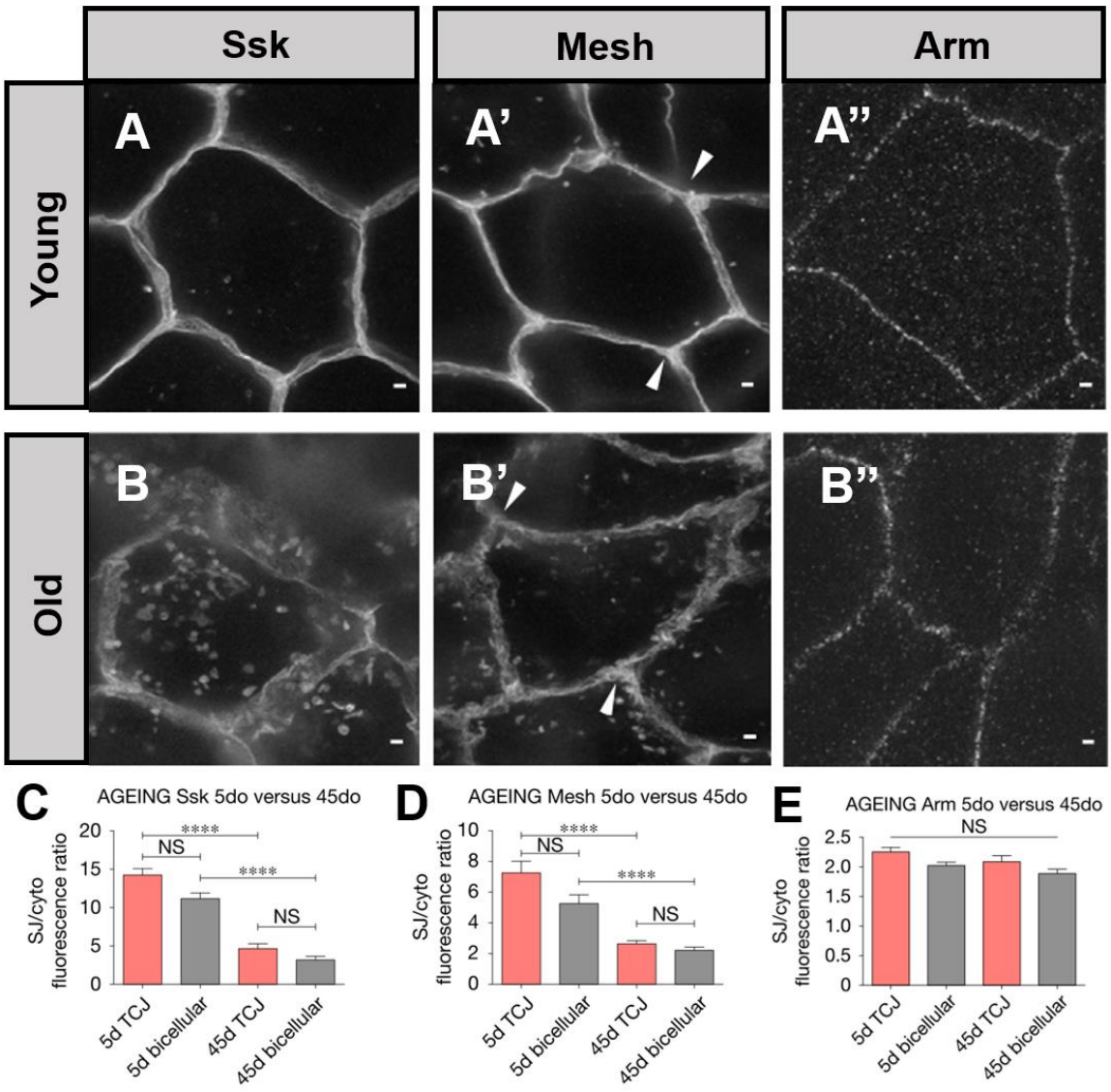

Figure 1-7: sSJ proteins mislocalize in ECs of aged fly PMGs. In ECs of young (10 do) fly PMGs, sSJ proteins such as Ssk and Mesh localize to the bSJ normally based on stimulated emission depletion (STED) imaging (**A, A'**). Some cytoplasmic protein is also visible. In ECs of old (45 do) fly PMGs, Ssk and Mesh protein increasingly localize to the cytoplasm compared with the bSJ (**B-D**). No age-related change is observed in the localization of the adherens junction component Armadillo (**A'', B'', E**). Figure adapted from Resnik-Docampo *et al.,* 2017.

The tricellular junction (TCJ) is a component of occluding junctions

In *Drosophila*, a specialized SJ region referred to as the tricellular junction (TCJ) is found where three adjacent cell corners meet (**Fig. 1-8**). TCJs are also present in the mammalian TJ, and include tricellulin and angulin-1 (also known as lipolysis-stimulated lipo-protein receptor [LSR]). The *Drosophila* tSJ protein Gliotactin (Gli) is homologous to tricellulin, while angulin-1 has some similarity to the *Drosophila* tricellular septate junction (tSJ) protein Bark beetle (Bark) (Sugawara *et al.*, 2021; Ikenouchi *et al*., 2005). Our lab showed that the tSJ protein Gli increasingly localizes to cytoplasmic puncta in ECs in the aged fly midgut based on immunofluorescence intensity. Gli protein at the TCJ simultaneously decreases (Resnik-Docampo *et al.*, 2017). Bark, another TCJ-specific protein [also referred to as Anakonda (Aka)], forms a complex with Gli at the pSJ and is required for correct Gli localization in the fly embryonic epithelium (Byri *et al*, 2015.; Hildebrandt *et al.*, 2015). A more recently discovered tSJ-specific protein, M6, was found to be essential along with Bark for tSJ assembly in the pupal notum (de Bournonville & Le Borgne *et al.*, 2020).

Our lab has demonstrated that Gli is required in the tSJs of ECs to maintain intestinal homeostasis, including in the contexts of ISC proliferation, intestinal barrier function, and having a normal lifespan. Depletion of Gli by induced RNAi expression in ECs mimics multiple aspects of the *Drosophila* intestinal aging phenotype: overproliferation of ISCs, severe intestinal barrier loss, and JNK pathway activation in ECs (Resnik-Docampo *et al.*, 2017). This indicates that age-related mislocalization of Gli in ECs may contribute to the overall aging phenotype. Additionally, despite tSJs being a relatively small portion of the entire SJ, disruption of the tSJ has a robust phenotype,

suggesting that the integrity of the tSJ may be an especially important part of SJ maintenance despite its relatively small surface area.

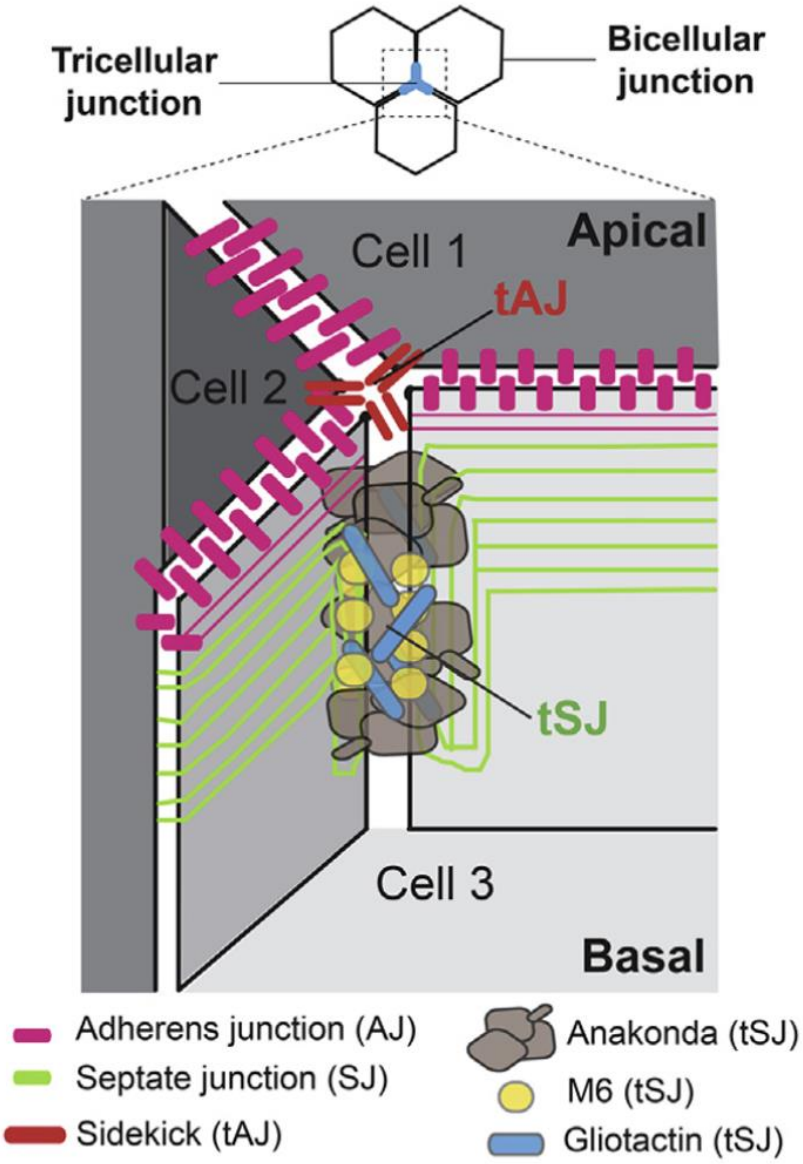

Figure 1-8: Structure of the tricellular septate junction (tSJ). Figure adapted from de Bournonville & Le Borgne *et al.*, 2020. The tSJ is the region of the SJ where three adjacent epithelial cells meet, and is known to contribute to intestinal barrier maintenance. Bark

beetle (Bark, also referred to as Anakonda, Aka) is believed to form a trimer that makes a diaphragm-like structure in the tSJ channel. Gliotactin (Gli) is thought to be associated with the limiting strands found on each side of the tSJ, and a recent study suggested it may be responsible for linking the tSJ with the bicellular SJ (bSJ) (Esmangart de Bournonville & Le Borgne, 2020). M6, another tSJ-specific protein, is required for tSJ assembly. The pleated septate junction (pSJ), shown here, is found in ectoderm-derived epithelia and is basal relative to the adherens junction (AJ); the smooth septate junction (sSJ) is found in endoderm-derived epithelia and is apical relative to the AJ.

Chapter 2: The septate junction component Bark beetle is required to maintain intestinal homeostasis

Introduction

The intestinal barrier allows selective paracellular transport of water, ions, and nutrients while maintaining food and microbes inside the intestinal lumen (Marchiando *et al.*, 2010). Barrier integrity is crucial to intestinal homeostasis because leakage of potentially harmful antigens or microbes could be detrimental to interstitial tissues. There is a strong correlation between aging and decline in intestinal barrier integrity across multiple species, including *Drosophila melanogaster* (Kirkwood, 2004; Biteau *et al.*, 2008; Ren *et al.*, 2014; Schiffrin *et al.*, 2010; Tran & Greenwood-Van Meerveld, 2013; Rera *et al.*, 2012). Age-associated loss of the intestinal barrier in *Drosophila* is associated with systemic metabolic defects, such as changes in insulin/insulin-like growth factor signaling, intestinal dysbiosis, chronic expression of inflammatory genes, and an increase in proliferation of intestinal stem cells (ISCs) (Choi *et al.*, 2011; Clark *et al.*, 2015; Rera *et al.*, 2012; Guo *et al.*, 2014). Intercellular occluding junctions, referred to as tight junctions (TJs) in vertebrates and septate junctions (SJs) in arthropods, play a major role in maintenance of the intestinal barrier (Resnik-Docampo *et al.*, 2017; Salazar *et al.*, 2018; Izumi *et al.*, 2019). While TJs and SJs appear different ultrastructurally, they share many homologous proteins, and both TJs and SJs restrict passive, paracellular transport. TJs use a branched network of independently sealing strands to create a semipermeable barrier at “kissing points” between adjacent membranes, while SJs reduce net solute diffusion by increasing diffusional distance across the junction with bridge-like structures called septa (Mariano *et al.*, 2011; Furuse & Tsukita, 2006). In *Drosophila melanogaster,* pleated SJs (pSJs) are found in epithelia derived from ectoderm, whereas smooth SJs (sSJs) are found in endoderm-derived tissues, such as the midgut (Tepass & Hartenstein,

1994; Lane & Skaer, 1980; Resnik-Docampo *et al.*, 2018). Similar to TJs, sSJs in *Drosophila* are located apical to adherens junctions (Resnik-Docampo *et al.*, 2018), making the *Drosophila* midgut a tractable model system for studying mammalian TJs, such as those that maintain the mammalian intestinal barrier.

The *Drosophila* posterior midgut (PMG) is functionally analogous to the human small intestine (Apidianakis & Rahme, 2011). The PMG epithelium is composed primarily of absorptive enterocytes (ECs), polyploid cells with microvilli that extend into the gut lumen and facilitate the absorption of nutrients. ECs and secretory enteroendocrine (EE) cells are maintained by a pool of ISCs that are able to self-renew by producing new ISCs. ISCs primarily generate daughter enteroblasts (EBs), which then differentiate into either mature ECs or EE cells (Apidianakis & Rahme, 2011). EB fate is specified by activation of the Notch signaling pathway (Ohlstein & Spradling, 2007; Micchelli & Perrimon, 2006), leading to the expression of the transcription factor *klumpfuss (klu)* in EBs. EE cell and EC fate decisions become stochastic upon loss of lineage specifying *klu,* and EB fates can be tracked using specific *klu*-based lineage tracing tools (e.g. klu^{ReDDM}) (Reiff *et al.*, 2019; Korzelius *et al.*, 2019).

In aged flies, ISC proliferation increases dramatically, as measured by an increase in cells that are positive for the mitotic marker phospho-histone H3 (pHH3). (Biteau *et al.*, 2008; Li & Jasper, 2016; Jiang *et al.*, 2009; Choi *et al.*, 2008; Park *et al.*, 2009). The increase in progenitor cells is coupled with a delay in differentiation, resulting in an accumulation of cells co-expressing the ISC/EB markers Escargot, Delta, and reporters of the Notch signaling pathway (Biteau *et al.*, 2008). Smooth SJs are found between adjacent ECs and between ECs and EE cells, and our lab has demonstrated previously

that integrity of sSJs between ECs is required for maintenance of the intestinal barrier in the midgut (Resnik-Docampo *et al.*, 2017). Thus, additional intestinal phenotypes exhibited by aged flies include loss of sSJ physical integrity (visible gaps between membranes) (Resnik-Docampo *et al.*, 2017) and loss of the intestinal barrier (Rera *et al.*, 2012). Indeed, electron micrographs of ECs in aged flies revealed gaps between adjacent ECs, suggesting a loss of sSJ integrity over time (Resnik-Docampo *et al.*, 2017). Gaps in SJs correlated with changes in localization of key sSJ components in PMGs from old flies. Immunofluorescence (IF) imaging revealed decreased staining intensity for several sSJ components at the junction, relative to the cytoplasm, with a concomitant increase in staining intensity in the cytoplasm, relative to what was observed for cells in intestines from young flies (Resnik-Docampo *et al.*, 2017).

In *Drosophila*, a specialized junction, referred to as the tricellular junction (TCJ), is found where three adjacent cells meet. Similar to sSJ proteins, the tricellular septate junction (tSJ) protein Gliotactin (Gli) was lost from the tSJ and increasingly localized to cytoplasmic puncta in ECs from aged flies (Resnik-Docampo *et al.*, 2017). Bark beetle (Bark), another tSJ-specific protein, also referred to as Anakonda (Aka), is required for proper Gli localization to the tSJ in the fly embryonic epithelium. Bark is similar to the mammalian angulin-1, which was recently found to be required to seal tight junction TCJs independently of tricellulin, the mammalian homolog of Gli (Sugawara *et al.*, 2021). Bark and Gli colocalize at the tSJ in both pSJs and sSJs (Byri *et al.*, 2015; Hildebrandt *et al.*, 2015). Because Gli is required at tSJs between ECs to maintain intestinal homeostasis (Resnik-Docampo *et al.*, 2017), and because proper Gli localization was disrupted in aged flies, we wanted to determine whether Bark also plays a role in the adult intestine. Here,

we show that Bark localizes to the tSJ and that it is required in both EBs and mature ECs to maintain intestinal homeostasis.

Results

Bark is expressed in the adult intestine

Bark is a type I transmembrane protein with a tripartite extracellular domain; it has been proposed that Bark forms a trimer, which acts as a diaphragm in the center of the tSJ canal (Byri *et al.*, 2015). Bark was demonstrated to be required for proper localization of Gli and maturation of the pSJ in the embryonic epithelium (Byri *et al.*, 2015). In order to determine whether Bark has a role in the adult intestine, PMGs from young (2 do) flies expressing a GFP-tagged form of Bark (hereafter referred to as Bark::GFP, see Materials and Methods) (Sarov *et al.*, 2016) were stained with anti-Bark antibody (Hildebrandt *et al.*, 2015). Bark localized to tSJs in both the PMG and hindgut, similar to what was observed in the embryonic epithelium (Byri *et al.*, 2015) **(Figs. 2-1, 2-S1, and 2-2A).**

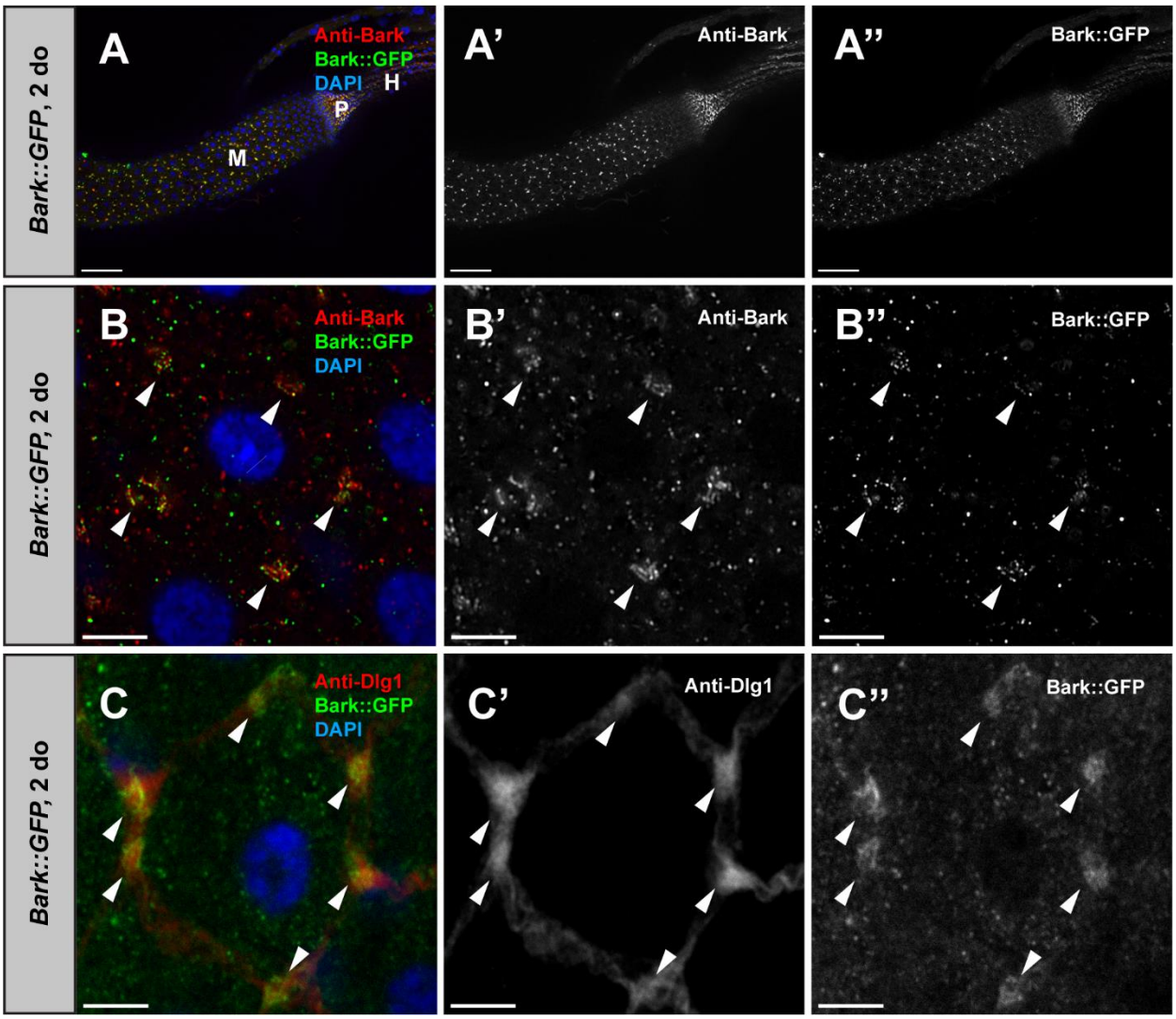

Figure 2-1: Anakonda/Bark beetle (Bark) localizes to the tricellular septate junction (tSJ) in the adult *Drosophila* intestine. (**A-A"**) Representative staining for Bark (antisera, red) (*Bark::GFP*, GFP, green) in the posterior midgut (M) of young (2 do) flies. Pylorus (P) and hindgut (H) to the right. DNA is stained with DAPI (blue). Scale bars, 50 µm. (**B-B"**) High magnification view of an enterocyte (EC) showing staining of endogenous Bark protein and GFP-tagged bark at the tSJ (arrowheads). (**C-C"**) High magnification view of an EC showing GFP-tagged bark colocalizes with the bicellular septate junction (bSJ) protein Discs large 1 (Dlg1, red) at the tSJ (arrowheads). Scale bars, 5 µm.

Specifically, in the PMG, Bark localized to the tSJ between adjacent ECs and ECs and EE cells. By contrast, in aged (40 day old, do) flies, Bark localization decreased at the tSJ between adjacent ECs and appeared to spread along the bicellular junction, with modest accumulation in the cytoplasm (**Fig. 2-2**). Loss of Bark from the tSJ in PMGs from aged flies is similar to what was observed for Gli; however, previous studies indicated significantly more accumulation of Gli in the cytoplasm, when compared to Bark (Resnik-Docampo *et al.*, 2017).

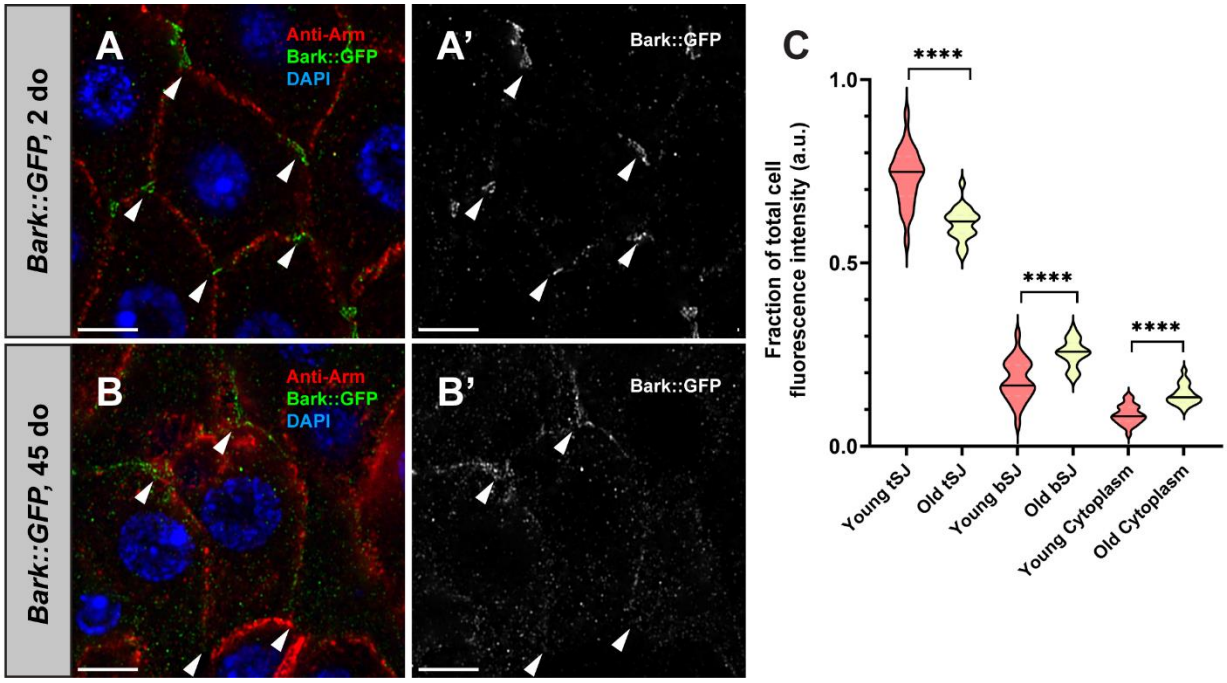

Figure 2-2: Bark becomes mislocalized in aged flies. **(A)** In young (2 do) flies, Bark localizes to the tSJ (arrowheads) in ECs, whereas it is no longer detected at the tSJ in the aged (45 do) flies **(B-B').** Adherens junctions (Armadillo, Arm, red); Bark (GFP, green); DNA (DAPI, blue). Scale bars, 5 µm. (**C**) Quantification reveals that Bark is increased at the bicellular septate junction (bSJ) or in the cytoplasm of old flies. 3 cells were analyzed per PMG. Young *Bark::GFP* PMGs, n = 26; old *Bark::GFP* PMGs, n = 22.

3 cells were measured per PMG. Each clearly visible tSJ in the cell was measured. 6 measurements were taken of the BCJ and cytoplasm in each cell, respectively. Quantification of fluorescence intensity ratios for Bark (**C**) in the bicellular junction (BCJ), tSJ, and cytoplasm. Statistical significance determined by Mann-Whitney test. ns, not significant; *, $P < 0.05$; **, $P < 0.001$; ****, $P < 0.0001$.

Given the previously described relationship between Bark and Gli, where Bark is required for recruitment of Gli to the tSJ in developing embryonic epithelia (Byri *et al.*, 2015), we wanted to determine whether Bark is required for Gli localization in the adult PMG. As mutations in *bark* are embryonic lethal, we took advantage of an inducible gene expression system, GeneSwitch (GS), to deplete *bark* from ECs, specifically in young adult flies. The GeneSwitch (GS) system permits cell type-specific gene expression following feeding flies the progesterone analog mifepristone (RU-486) (Brand & Perrimon, 1993; Osterwalder *et al.*, 2001). Similar to previously published results in the embryonic epithelium (Byri *et al.*, 2015), RNAi-mediated, EC-specific depletion of *bark* resulted in a decrease in Gli::GFP staining intensity at the tSJ (**Fig 2-S2A-B**). However, in contrast to the findings in the embryonic epithelium, depletion of *Gli* using a similar strategy resulted in an increase in Bark::GFP staining intensity at the bicellular junction, somewhat reminiscent of the aging phenotype (**Fig 2-S2D-E**). A similar mutually dependent relationship between Gli and Bark has been observed in the pupal notum (Esmangart de Bournonville & le Borgne, 2020). Taken together, these data suggest that the mechanisms for assembly and maintenance of the tSJ may differ by tissue type or with age.

bark is required in ECs for the maintenance of intestinal homeostasis

Given that the changes in Gli::GFP upon depletion of *bark*, and vice versa, resemble what occurs at the tSJ in an aged midgut, we wanted to determine whether depletion from ECs in PMGs from young flies led to other aging phenotypes. Following depletion of *bark* from ECs for 5 days in young flies, the number of $pHH3^{+}$ cells was significantly higher than in controls (**Fig. 3A-C**), suggesting that Bark is required in ECs to maintain intestinal homeostasis, similar to Gli (Resnik-Docampo *et al.*, 2017). Immunostaining confirmed depletion of Bark protein from ECs, validating the RNAi line **(Fig. 2-S3A-B).** In addition, the number of $pHH3^{+}$ cells increased with extended induction times (**Fig. 2-S3E-G**), and similar results were obtained using additional, independent *RNAi* lines **(Fig. 2-3C, Fig. 2-S3C-D**)**,** as well as alternative, inducible systems to deplete *bark* from ECs **(Fig. 2-S3H-K).**

Next, we wanted to determine whether Bark is required for maintenance of the intestinal barrier, similar to Gli (Resnik-Docampo *et al.*, 2017). The GeneSwitch system was used to deplete *bark* in ECs throughout the adult lifespan. Integrity of the intestinal barrier and lifespan were assayed in parallel by feeding the flies a non-absorbable, non-toxic blue food dye, as described previously (Rera *et al.*, 2011, 2012). In flies with an intact intestinal barrier, the dye remains in the lumen of the digestive tract; however, when the intestinal barrier is severely compromised, the dye visibly leaks into the hemolymph (Rera *et al.*, 2011). Consistent with a model where Bark plays an integral role in tSJs, depletion of *bark* in ECs led to significant loss of the intestinal barrier after 19 days. Furthermore, as has been shown previously, loss of barrier integrity correlated with shortened lifespan when compared to control flies (**Fig. 3D-E**) (Rera *et al.*, 2012)**.** These

data indicate that Bark is required in ECs for regulating intestinal homeostasis, maintaining the intestinal barrier, and for a normal lifespan.

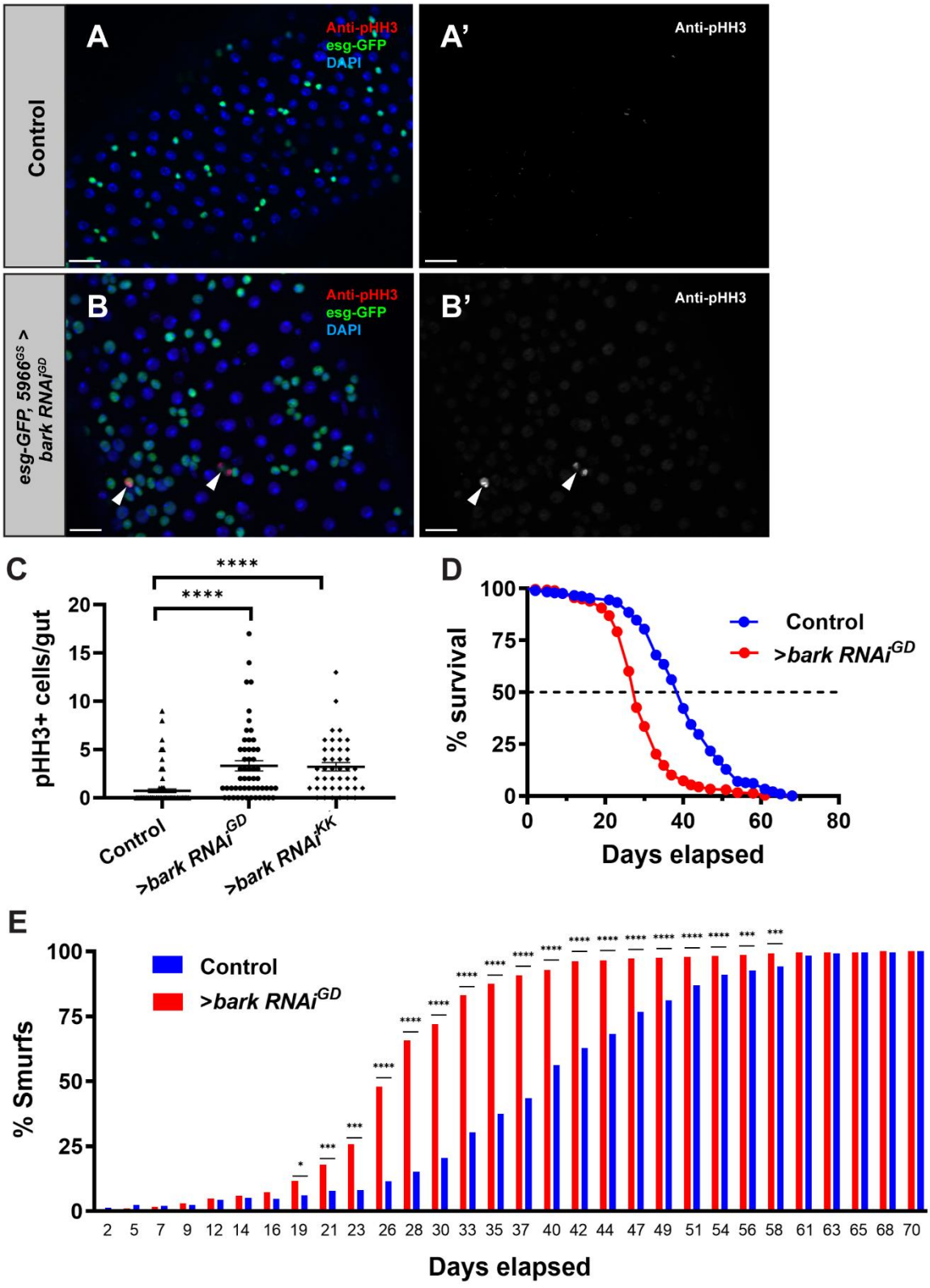
Control
A
Anti-pHH3
esg-GFP
DAPI
A'
Anti-pHH3
esg-GFP, 5966GS > bark RNAiGD
B
Anti-pHH3
esg-GFP
DAPI
B'
Anti-pHH3
C
****
****
pHH3+ cells/gut
20
15
10
5
0
Control
>bark RNAiGD
>bark RNAiKK
D
% survival
100
75
50
25
0
Control
>bark RNAiGD
0
20
40
60
80
Days elapsed
E
% Smurfs
100
75
50
25
0
Control
>bark RNAiGD
2 5 7 9 12 14 16 19 21 23 26 28 30 33 35 37 40 42 44 47 49 51 54 56 58 61 63 65 68 70
Days elapsed

Figure 2-3: Bark is required at the tSJ in enterocytes to maintain intestinal homeostasis. (**A-B**) Depletion of Bark in ECs of young (2 do) flies by *5966^{GS}:bark RNAi^{GD}* expression for 5 days results in an increase in mitotic activity (n = 54), compared to outcrossed controls (n = 48). Genotypes: (**A**) *w; esg-GAL4, UAS-GFP, 5966^{GS}*. (**B**) *w; esg-GAL4, UAS-GFP, 5966^{GS}:bark RNAi^{GD}*. All flies are fed RU-486 to induce transgene expression. ISCs/EBs (GFP, green); mitotic cells (phosphorylated histone H3, pHH3, red), DNA (DAPI, blue). Scale bars, 20 μm. (**C)** Quantification of mitotic events. *w; esg-GAL4, UAS-GFP, 5966^{GS}:bark RNAi^{KK}* flies are also included (n = 42). Error bars represent mean with SEM. Significance was determined by Mann-Whitney test. ****, P < 0.0001. (**E**) Intestinal barrier ('Smurf') assay shows loss of barrier function upon depletion of Bark (red, n = 301) and (**D**) statistically significant (****) shortening of lifespan, when compared to outcrossed controls (blue, n = 299). Genotypes: Red, *w; esg-GAL4, UAS-GFP, 5966^{GS}>UAS-bark RNAi^{GD};* blue, *w; esg-GAL4, UAS-GFP, 5966^{GS}.* *, P < 0.05; ***, P < 0.001, ****, P < 0.0001. Statistical significance determined by Fisher's exact test (Smurf assay) and non-parametric log-rank Mantel-Cox test (lifespan assay).

bark overexpression in ECs disrupts intestinal homeostasis

We next investigated the effect of EC-specific overexpression of Bark protein on PMG homeostasis, and if Bark overexpression is sufficient to rescue age-associated phenotypes in the PMG. Because our previous study showed no significant decrease in transcription of SJ proteins in aged PMGs (Resnik-Docampo *et al.*, 2017), we did not anticipate that simple Bark overexpression would rescue aging phenotypes; however, we wanted to eliminate the possibility that age-related intestinal barrier decline was due to simple reduction of Bark protein in the EC.

We confirmed that flies expressing *esg-GFP, 5966^{GS}:UAS-Bark* which are induced with RU-486 feeding overexpress Bark protein, and this causes Bark protein to localize to the tSJ in addition to the bicellular SJ and the EC cytoplasm (**Fig. 2-4A-B**). Overexpression of *bark* in young PMGs leads to a significant increase in ISC proliferation (**Fig. 2-4C-E**), indicating that *bark* overexpression disrupts intestinal homeostasis. Similarly, comparing *esg-GFP, 5966^{GS}:UAS-Bark* flies with outcrossed controls in a Smurf assay reveals that *bark* overexpression throughout adulthood slightly accelerates age-associated barrier loss and decreases lifespan, rather than rescuing age-associated barrier loss and/or extending lifespan (**Fig. 2-4F-G**). Therefore, as our previous RNAseq data (Resnik-Docampo *et al.*, 2017) suggested, merely increasing expression of an SJ protein such as Bark is not sufficient to preserve intestinal homeostasis or prevent age-associated barrier loss. Beginning *bark* overexpression in ECs beginning in midlife, as well as modulating *bark* overexpression induction, have not yet been investigated and could prove beneficial to homeostasis and barrier function.

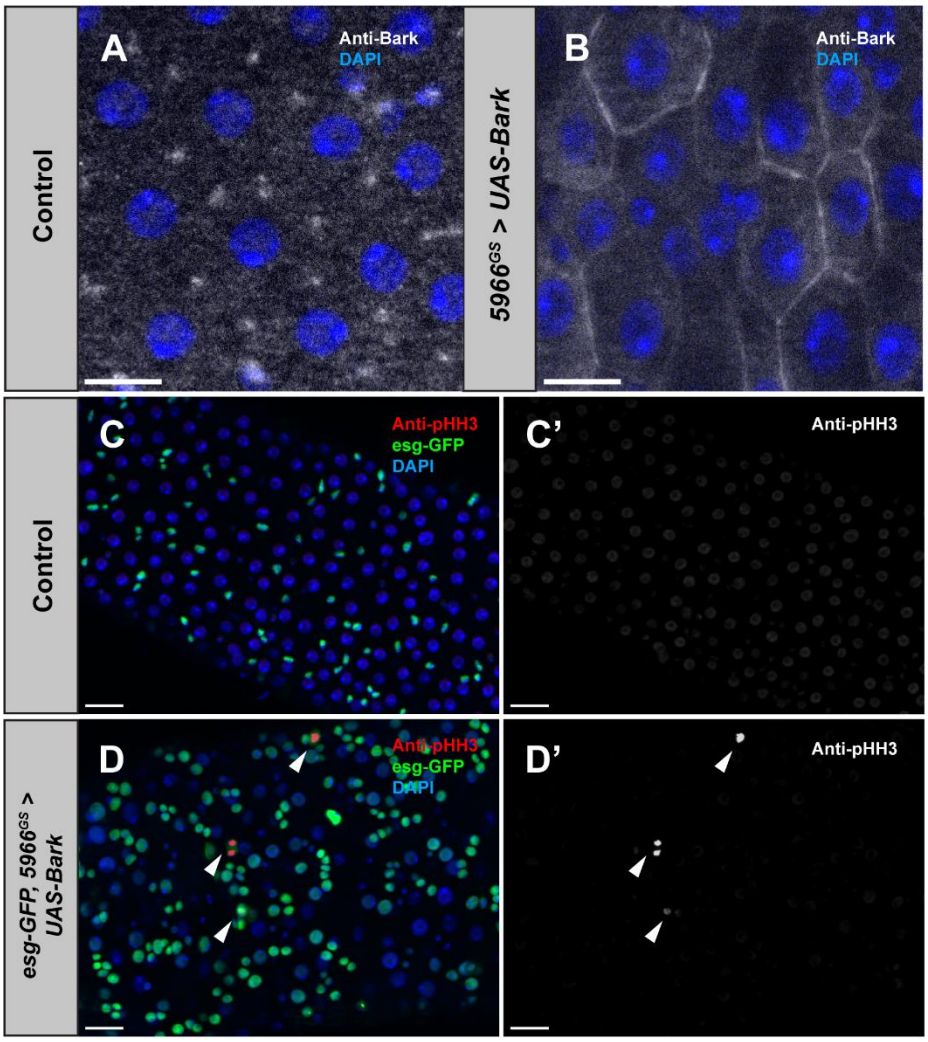
A
Anti-Bark
DAPI
Control
B
Anti-Bark
DAPI
5966GS > UAS-Bark
C
Anti-pHH3
esg-GFP
DAPI
Control
C'
Anti-pHH3
D
Anti-pHH3
esg-GFP
DAPI
esg-GFP, 5966GS > UAS-Bark
D'
Anti-pHH3

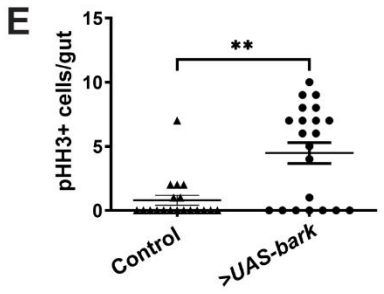
E
pHH3+ cells/gut
15
10
5
0
**
Control
>UAS-bark

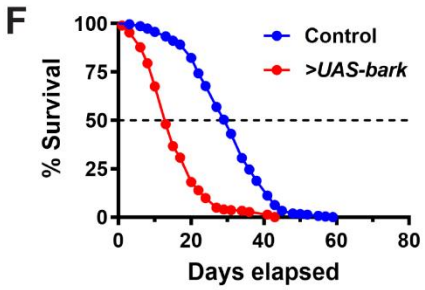
F
% Survival
100
75
50
25
0
Control
>UAS-bark
0
20
40
60
80
Days elapsed

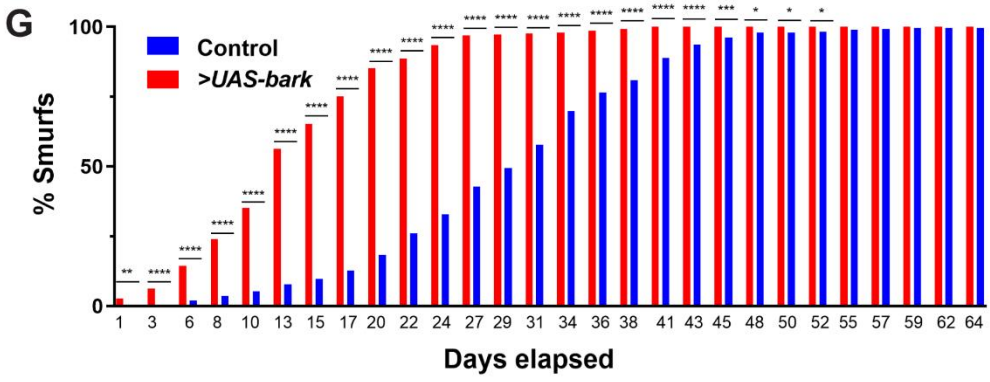
G
% Smurfs
100
50
0
Control
>UAS-bark
1 3 6 8 10 13 15 17 20 22 24 27 29 31 34 36 38 41 43 45 48 50 52 55 57 59 62 64
Days elapsed

Figure 2-4: Increased Bark protein by enterocyte-specific expression of *UAS-Bark* disrupts intestinal homeostasis. (**A-B**) Young (2 do) flies expressing *Su(H)lacZ; esg-GFP, 5966^{GS}; UAS-Bark* were induced via RU-486 feeding for 5 days. Dissection of the PMG reveals *UAS-Bark* expression induces an increase in Bark protein based on immunofluorescence staining, including along the bicellular junction (BCJ), which appears similar to the aged phenotype shown in Fig. 2-2 (n = 8) (**B**). Outcrossed controls show normal Bark protein localization to the tSJ with no apparent increase in Bark protein level (n = 9) (**A**). Scale bar, 10 microns. (**C-D**) Induced *5966^{GS}:UAS-Bark* expression (n = 21) increases number of mitotic events in the PMG, based on antibody staining for pHH3 and compared with outcrossed controls (n = 19). (**E**) Quantification of mitotic events in *5966^{GS}:UAS-Bark* and outcrossed control fly PMGs. Significance was determined by Mann-Whitney test. Error bars represent mean with SEM. **, P < 0.01. (**G**) Intestinal barrier ('Smurf') assay shows loss of barrier function upon *UAS-bark* expression (red, n = 300) and (**F**) statistically significant (****) shortening of lifespan, when compared to outcrossed controls (blue, n = 300). Genotypes: Red, *w; esg-GAL4, UAS-GFP, 5966^{GS}>UAS-bark;* blue, *w; esg-GAL4, UAS-GFP, 5966^{GS}.* *, P < 0.05; **, P < 0.01; ***, P < 0.001, ****, P < 0.0001. Statistical significance determined by Fisher's exact test (Smurf assay) and non-parametric log-rank Mantel-Cox test (lifespan assay).

bark **is required in EBs for proper differentiation**

A hallmark of the aging PMG is accumulation of EB-like cells that express hallmarks of both ISCs and ECs (Dutta *et al.*, 2015). Although Bark expression was detected at tSJs between ECs and EEs, single cell sequencing data revealed expression of *bark* in EBs(Dutta *et al.*, 2015; Hung *et al.*, 2021). Therefore, we wanted to investigate a role for

bark in committed EC progenitors using lineage tracing in combination with conditional expression of *bark* RNAi. Briefly*, klu*^{ReDDM} allows EB-specific manipulation and tracing of differentiated ECs, taking advantage of different fluorophore stability (Reiff *et al.*, 2019; Korzelius *et al.*, 2019). Depleting *bark* in *klu*^{ReDDM} results in accumulation of *klu*$^{+}$ EBs (**Fig. 2-5B-D**), although not at the expense of EC differentiation (**Fig. 2-5E**). Similar results were obtained when ISC- and EB-specific *esg*^{ReDDM} was used (**Fig. 2-S4**) (Antonello *et al.*, 2015). As a consequence of disrupted cellular homeostasis, specific depletion of *bark* from EBs reduced lifespan compared to outcrossed controls (**Fig. 2-5G**). In addition, depletion of *bark* in EBs led to an increase in newly generated EEs, identified by antibody staining for the EE cell lineage marker Prospero (Pros, **Fig. 2-5F**).

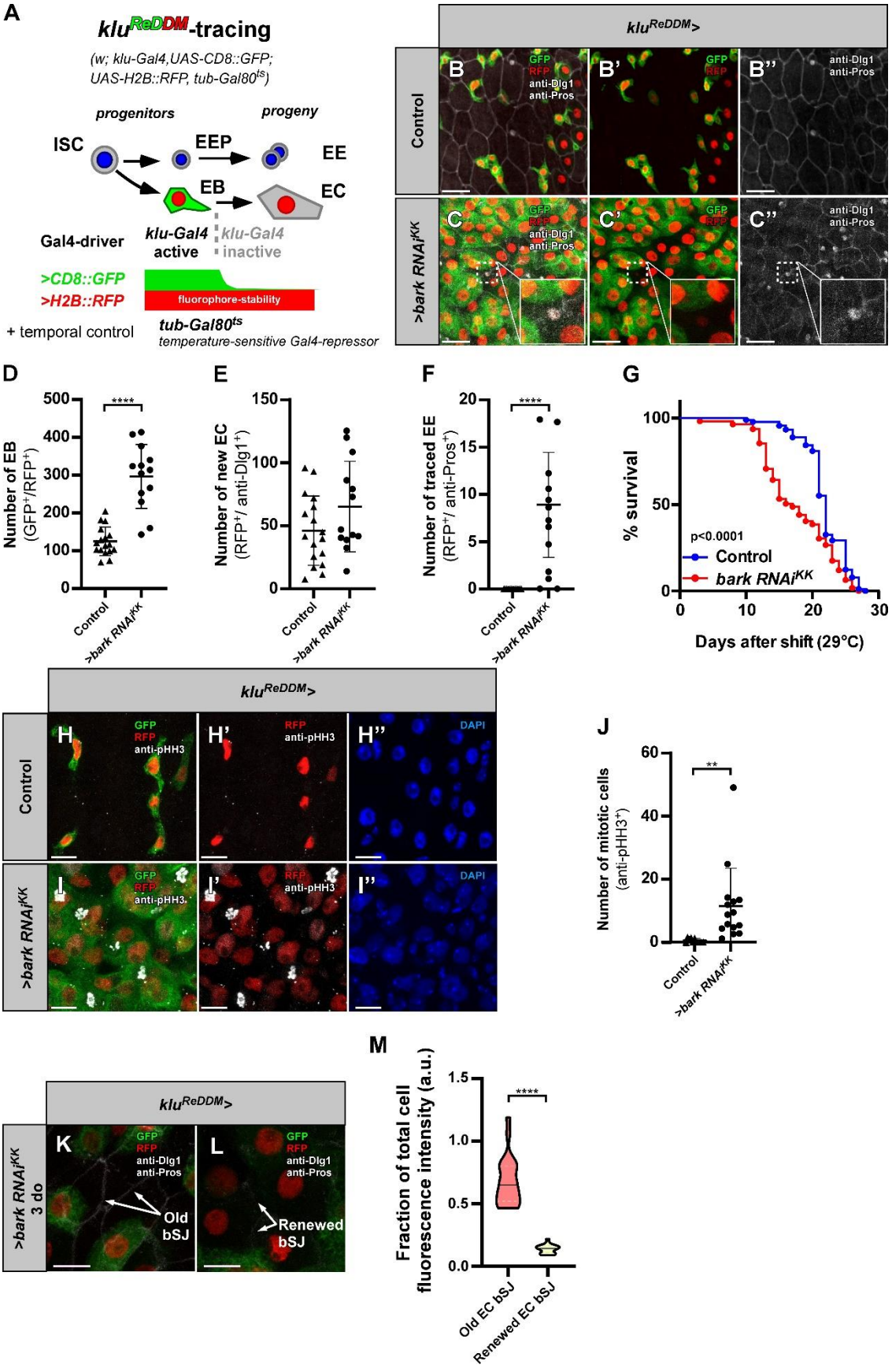
A
klu^ReDDM-tracing
(w; klu-Gal4,UAS-CD8::GFP;
UAS-H2B::RFP, tub-Gal80^ts)
progenitors
progeny
ISC
EEP
EE
EB
EC
Gal4-driver
klu-Gal4 active
klu-Gal4 inactive
>CD8::GFP
>H2B::RFP
fluorophore-stability
+ temporal control
tub-Gal80^ts
temperature-sensitive Gal4-repressor
klu^ReDDM>
Control
>bark RNAi^KK
B
B'
B''
C
C'
C''
GFP
RFP
anti-Dlg1
anti-Pros
D
Number of EB
(GFP+/RFP+)
E
Number of new EC
(RFP+/ anti-Dlg1+)
F
Number of traced EE
(RFP+/ anti-Pros+)
****
G
% survival
p<0.0001
Control
bark RNAi^KK
Days after shift (29°C)
H
H'
H''
I
I'
I''
DAPI
anti-pHH3
J
Number of mitotic cells
(anti-pHH3+)
**
K
L
Old bSJ
Renewed bSJ
>bark RNAi^KK 3 do
M
Fraction of total cell fluorescence intensity (a.u.)
Old EC bSJ
Renewed EC bSJ

Figure 2-5: EB specific depletion of bark results in EB accumulation, EE fate plasticity and reduced Dlg1 levels at bSJs of new ECs. **(A)** *klu^{ReDDM}* (*w; klu-GAL4, UAS-CD8::GFP; UAS-H2B::RFP, tub-GAL80^{ts}*) tracing. Expression of two fluorophores (*CD8::GFP* and *H2B::RFP*) is driven by EB-specific driver *klu-GAL4*. EBs differentiating to epithelial ECs lose *CD8::GFP*, while stable *H2B::RFP* persists. The expression of UAS-driven transgenes is temporally controlled by a ubiquitously expressed temperature-sensitive *GAL80^{ts}* repressor, which is inactivated by temperature shift to 29°C. **(B-C'')** Confocal images of control PMG **(B-B'')** and >*bark-RNAi^{KK}* **(C-C'')** in the R5 region after 7 days of tracing**. (D-F)** Quantifications of the number of EBs **(D)**, new ECs **(E)** and traced EEs **(F)** upon *bark* knockdown after 7 days of tracing. (n = 17, 13). Statistical significance determined by Mann-Whitney test. **, P < 0.01. Scale bar 20 µm. Depletion of *bark* induces EB to EE differentiation (inset, GFP-/RFP$^+$/anti-Pros$^+$, **F**) but no significant change in the number of ECs (GFP$^-$/RFP$^+$/ anti-Dlg1$^+$, **E**). Additionally, *bark* knockdown increased the number of progenitor cells (GFP$^+$/RFP$^+$, **D**). **(G)** Survival (in percentage) over time upon *bark* knockdown using *klu^{ReDDM}*. Survival curves were plotted combining data from >80 flies per one genotype group: Control (blue, n=89), *bark RNAi^{KK}* (red, n=109). *bark* knockdown in EBs reduces lifespan significantly. Statistical significance determined by non-parametric log-rank Mantel-Cox test. ****, P < 0.0001. **(H-I'')** Knockdown of *bark* **(I-I'')** leads to an increase in the number of proliferating cells (marked by pHH3) as compared to the controls **(H-H'')**. **(J)** Quantification of the number of mitotic cells upon *bark* depletion after 7 days of tracing. (n = 11, 15). Statistical significance determined by Mann-Whitney test. ****, P < 0.0001. Scale bar 10 µm. **(K, L)** Knockdown of *bark* leads to a reduced Dlg1 fluorescence intensity at the bSJ between renewed EC

(white arrows, **L**) as compared to the Dlg1 fluorescence intensity bSJ between old EC (white arrow, **K**). **(M**) Quantification of the Dlg1 fluorescence intensity ratio at the bSJ between old ECs and bSJ between renewed ECs upon *bark* knockdown after 3 days of tracing. (n= 24, 22). Statistical significance determined by Mann-Whitney test. ****, P < 0.0001. Scale bar 10 µm.

Cell fate decisions after ISC division strongly depend on the Notch signaling pathway, whereby low Notch activation was shown to drive EE differentiation (Micchelli & Perrimon, 2006; Ohlstein & Spradling, 2007, 2005). By using *Su(H)-GBE-GFP* as a reporter of Notch activation (Furriols & Bray, 2000), we found that depletion of *bark* using *klu-GAL4* led to a reduction in *Su(H)-GBE-GFP* fluorescence intensity (**Fig. 2-6C)** and smaller EB nuclei (**Fig. 2-6D).**

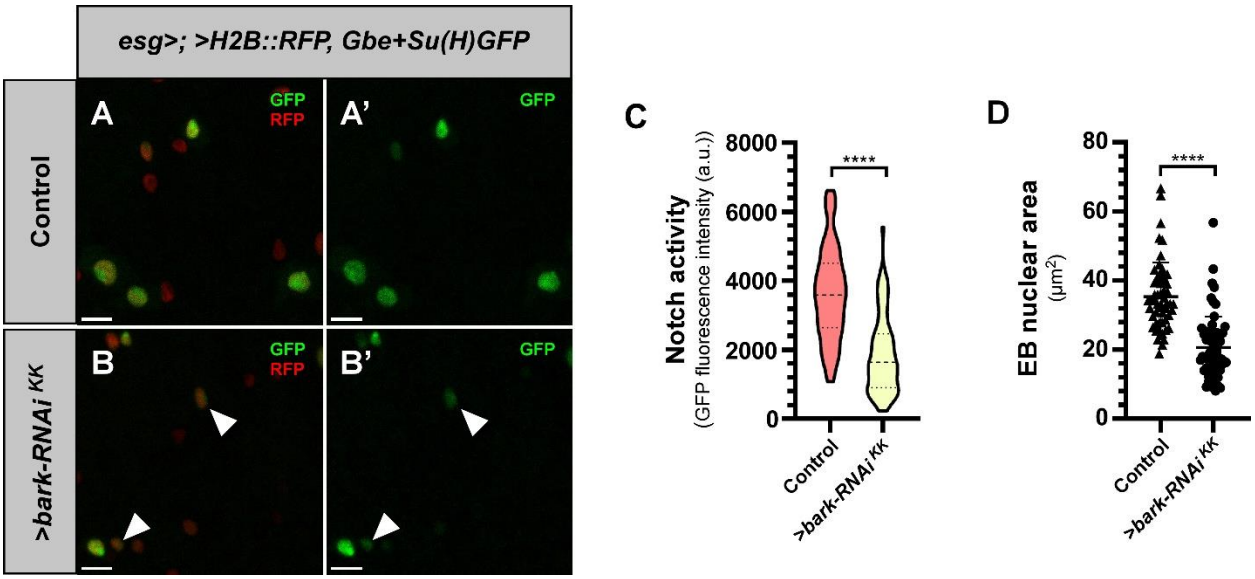

Figure 2-6: Knockdown of *bark* in ISCs/EBs results in reduced Notch pathway activation and EB nuclear size. **(A)** Expression of *H2B::RFP* fluorophore is driven by ISC- and EB-specific driver *esg-GAL4*. H2B::RFP persists in epithelial ECs differentiated from EBs.

Gbe+Su(H)GFP is a readout of Notch activity, and marker of the EB lineage (arrowheads, B); GFP intensity was analyzed upon >*bark-RNAi*^{KK} (**B**). **(C, D)** Quantification of GFP fluorescence intensity and **(D)** EB nuclear size following 7 days of induction. Knockdown of *bark* decreases the GFP intensity (**C**) and EB nuclear size (GFP^{+} cells, **D**) compared to controls (**B, B'**, n= 73, 70). Statistical significance determined by Mann Whitney test. ****, P < 0.0001. Scale bar 10 µm.

Our data indicates that EBs upon *bark* depletion exhibit increased cellular plasticity toward the EE lineage, which has previously been observed upon loss of EB lineage specifying *klu* (Reiff *et al.*, 2019; Korzelius *et al.*, 2019). Similar results were obtained when *bark* was depleted from ISCs and EBs simultaneously, using the *esg-GAL4* driver, in combination with the ReDDM lineage tracing cassette (**Fig. 2-S4**). Taken together, our findings suggest that Bark plays a role in the EB-EC differentiation path and that depletion of *bark* leads to accumulation of EBs with reduced Notch activity, stimulating a change in lineage towards EE fate.

Discussion

Occluding junctions, known as tight junctions in mammals and septate junctions in arthropods, play a significant role in maintaining the intestinal barrier (Marchiando *et al.*, 2010; Resnik-Docampo *et al.*, 2017; Salazar *et al.*, 2018), which passively restricts paracellular flow across the intestinal epithelium. Interestingly, loss of the intestinal barrier has been described as a result of aging and is associated with impending death across species (Rera *et al.*, 2012). Due to the strong correlation between aging and loss of the intestinal barrier (Kirkwood, 2004; Biteau *et al.*, 2008; Ren *et al.*, 2014; Schiffrin *et al.*, 2010; Tran & Greenwood-Van Meerveld, 2013; Rera *et al.*, 2012), we wanted to

characterize the impact of aging on occluding junctions, using the *Drosophila* intestine as a model system. Here, we describe the expression, localization and role of the tSJ component Bark in the adult PMG.

Bark localized to the tSJ in both the PMG and hindgut (**Figs. 2-1, 2-S1**); however, analysis of PMGs from aged flies indicated that Bark was lost from the tSJ over time (**Fig. 2-2**). Concomitant with the decreased staining intensity at the tSJ, we observed an increase in staining along the bicellular junction (**Fig. 2-2**). Depletion of *bark* from ECs in young flies led to an increase in ISC proliferation, loss of the intestinal barrier, and shortened lifespan (**Fig. 2-3**). These results are similar to what we reported previously for another tSJ component, Gli (Resnik-Docampo *et al.*, 2017). Although our study utilizes RNAi-mediated depletion of tSJ components, we have shown previously that transcription of *bark* does not decrease with age in the PMG (Resnik-Docampo *et al.*, 2017); therefore, our approach may not accurately recapitulate the impact of aging on the tSJ. However, these studies are a relevant first step toward understanding the importance of Bark and other SJ proteins in intestinal homeostasis.

Our finding that Bark is lost from the tSJ in PMGs from aged flies, in combination with the observation that depletion of *bark* from ECs in young flies recapitulates some prevalent intestinal phenotypes that are apparent with age, supports the hypothesis that loss of SJ components may contribute to age-related loss of intestinal barrier function (Resnik-Docampo *et al.*, 2017; Salazar *et al.*, 2018). Overexpression of *bark* in young flies or over the course of the adult lifetime was severely disruptive to homeostasis, including intestinal barrier function (**Fig. 2-4**). One possible mechanism leading to age-related changes in the localization of SJ proteins could be alterations in vesicular

trafficking, including increased endocytosis of SJ proteins and/or decreased delivery of recycled or newly synthesized SJ proteins to the plasma membrane. This hypothesis, along with previous RNAseq data indicating that *bark* transcription is upregulated with age (Resnik-Docampo *et al.*, 2017), could explain why simple *bark* overexpression fails to rescue aging phenotypes. Manipulation of transport machinery, rather than production of SJ proteins, could be explored as an approach to restore Bark and other SJ proteins at the SJ in aged flies, although manipulation of transport machinery would likely result in pleiotropic, unrelated phenotypes.

In addition to analyzing a role for Bark in ECs, we show that EB-specific depletion of *bark* results in accumulation of EB-like cells, resembling defects observed in flies that are aged or have damaged intestinal epithelia (Biteau *et al.*, 2010; Zhai *et al.*, 2015). The accumulation of EB-like cells correlated with a decrease in lifespan, as reported previously (**Fig. 2-5D, G**) (Antonello *et al.*, 2015). EBs depleted for *bark* are capable of forming ECs in normal numbers (**Fig. 2-5E**), although the new ECs, originating from Bark-depleted EBs, are abnormally small and show irregular Dlg-1 localization (**Fig. 2-5B-C")**. Therefore, we speculate that depletion of *bark* from EBs results in failure to form a tight, functional bSJ and/or tSJ; whether normal levels of Bark protein are observed in ECs derived from *klu*+ EBs/EC progenitors has not yet been assessed. Our findings demonstrate an essential role for Bark during tSJ establishment when differentiating EBs integrate into the intestinal epithelium. An ultrastructural study of how early ECs undergo epithelial integration, while simultaneously preserving intestinal barrier function, will be an important component of future studies.

In our evaluation of the relationship between Gli and Bark protein in the PMG tSJ, we found that depletion of one component results in changes in staining intensity of the other at tSJs in adult PMGs (**Fig. 2-S2).** Our findings are different from previous studies that examined the relationship between Bark and Gli in the embryonic epithelium (Byri *et al.*, 2015) that found Bark is required for Gli to localize to the TCJ, but the reverse was not true. However, another study revealed Gli and Bark are mutually dependent for localization to the tSJ in the pupal notum (Esmangart de Bournonville & le Borgne, 2020). Differences could be due to relationships between Gli and Bark in embryonic versus more mature tissues, the use of null alleles versus RNAi-mediated depletion, length of RNAi depletion time, and/or the use of antibodies targeting the proteins directly, rather than GFP tags. Because a similar Gli-Bark relationship was found in both the PMG and pupal notum (Esmangart de Bournonville & le Borgne, 2020), which have sSJs and pSJs respectively, it does not seem likely that this is due to different roles for Gli and Bark in sSJs and pSJs. An ultrastructural study could better pinpoint the nature of Gli-Bark interaction in the PMG. Investigation of Gli and Bark's relationship to another tSJ protein, M6 (Wittek *et al.*, 2020; Esmangart de Bournonville & le Borgne, 2020) in the *Drosophila* PMG may also help further illuminate these differing results.

In summary, we have found that Bark protein is required in the tSJs of ECs and EBs in the *Drosophila* posterior midgut to maintain homeostasis in the contexts of ISC proliferation, EB fate, intestinal barrier function, and lifespan. Because Bark also mislocalizes from the tSJ in the aged fly PMG, our study suggests that this mislocalization may contribute to the overall intestinal aging phenotype. Additionally, Bark and the tSJ protein Gliotactin appear mutually dependent on one another for proper tSJ localization

in the adult PMG, unlike in the embryonic epithelium (Byri *et al.*, 2015). Given the importance of intestinal barrier function, and age-related intestinal barrier loss across species (Kirkwood, 2004; Biteau *et al.*, 2008; Ren *et al.*, 2014; Schiffrin *et al.*, 2010; Tran & Greenwood-Van Meerveld, 2013; Rera *et al.*, 2012), our discovery of an essential role for Bark during homeostatic cellular turnover sheds light on fascinating future research lines. This study could help generate insight into the role of tSJs in the human gut and possible pathologies associated with tSJ dysfunction.

Acknowledgments

The authors thank the Vienna *Drosophila* RNAi Center (VDRC), the Bloomington *Drosophila* Stock Center (NIHP400D018537), the Transgenic RNAi Project (TRiP) at Harvard Medical School (NIK/NIGMS R01-GM084947) and Thomas Klein for reagents. We also thank the UCLA MCDB/BSCRC Microscopy Core and Center for Advanced Imaging (CAi) at Heinrich Heine University (DFG INST 208/539-1 FUGG) for imaging training and facilities. In addition, we are grateful to Jones laboratory members for comments and feedback on experiments and the manuscript. Special thanks are also given to Volker Hartenstein for sharing laboratory space and equipment. This work was supported by the Eli and Edythe Broad Center of Regenerative Medicine and Stem Cell Research at the University of California, Los Angeles and the NIH: R01AG028092, R01DK105442, R01GM135767 (D.L.J.). MG is funded by the Deutsche Forschungsgemeinschaft (DFG-Sachbeihilfe RE 3453/6–1).

Methods

Set 1: Fig. 1C, Fig. 4-5, Fig. S3H-K, Fig. S4

Set 2: Fig. 1A-B, Fig. 2-3, Fig. S1-S2, Fig. S3A-G

Fly food and husbandry:

Set 1: Fly food contained 7.12% corn meal, 4.5% malt extract, 4% sugar beet syrup, 1.68% dried yeast, 0.95% soy flour, 0.5% agarose, 0.45% propionic acid, and 0.15% NIPAGIN powder (antimycotic agent). *GAL80^{ts}* flies were kept at 18°C (permissive temperature) until shifted to 29°. Otherwise, flies and crosses were kept at 25°C. All analyses were performed on 3-7 day old (do) mated females that were shifted to 29°C for 7 days for tracing. For survival analysis (**Fig. 2-5G**, *klu^{ReDDM} bark* knockdown), 3-5 do flies (males and females) were shifted to 29°C and monitored for their survival.

Set 2: Flies were cultured in vials containing standard cornmeal medium (1.1% agar, 2.9% baker's yeast, 9.2% maltose, and 7.1% cornmeal; all concentrations given in wt/vol). Propionic acid (0.5%) and TegoSept (methylparaben, Sigma, 0.16%) were added to adjust pH and prevent fungal growth, respectively. Newly eclosed adults were kept for an additional 1–2 days before inducing transcription activation by placement on food containing the steroid hormone mifepristone (RU-486; Sigma M8046) in a 25 µg/ml concentration and flipped every 2 days thereafter. All analyses for these studies were performed on female flies, as age-related gut pathology has been well established in females (Biteau *et al.*, 2008; Rera *et al.*, 2012).

Fly stocks used:

Stock	Source
5966-GAL4^{GS}	Gift from H. Jasper[1]
esg-GFP; UAS-H2B::RFP	T. Reiff
Gbe+Su(H)dsRed	Gift from T. Klein[2]
Gli::GFP	DGRC 115-332
Myo1A-Gal4	Jiang & Edgar, 2009
P{bark.Ty1-Tev-SGFP-FLAG}	VDRC
Su(H)lacZ; esg:GFP, 5966GAL4GS	Gift from B. Ohlstein[3]
tub-GAL80^{ts}	BL 7017
UAS-bark-RNAi^{GD}	VDRC 52608GD
UAS-bark-RNAi^{KK}	VDRC 107348KK
UAS-Gli RNAi	VDRC 37115GD
UAS-N-RNAi	VDRC 14477GD
w; esg-Gal4,UAS-CD8::GFP; UAS-H2B::RFP, tub-Gal80ts	T. Reiff
w; klu-Gal4,UAS-CD8::GFP; UAS-H2B::RFP, tub-Gal80ts	T. Reiff
w; klu-Gal4,UAS-CD8::RFP; UAS-H2B::RFP, tub-Gal80ts	T. Reiff
w^{1118}	Gift from L. Wang[4]
yw hsflp; Sco/Cyo Dfd-GMR nuGFP; UAS-Aka attP2y (L057)	Gift from S. Luschnig[5]

Table 2-1: List of *Drosophila* stocks used.

[1]Genentech and Buck Institute for Research on Aging, USA; [2]University of Düsseldorf, Germany; [3]UT Southwestern Medical Center, USA; [4]UCLA, USA; [5]University of Münster, Germany

Immunohistochemistry:

Set 1: Dissected guts were fixed in 4% PFA in 1XPBS for 45 min. After fixation the guts were washed with 1XPBS for 10 min and stained with primary antibodies, diluted in 0.5%

PBT (0.5% Triton (Sigma-Aldrich) in 1XPBS) + 5% normal goat serum (ThermoFisher Scientific, Berman, Germany). Primary antibody staining was performed at 4°C overnight on an orbital shaker. On the next day, guts were washed with 1XPBS for 10 min and incubated with secondary antibodies and DAPI (1:1000; 100 µg/mL stock solution in 0.18 M Tris pH 7.4; DAPI No. 18860, Serva, Heidelberg) for at least 3 h at RT. After washing with 1XPBS for 10 min the stained guts were mounted in Fluoromount-G Mounting Medium (Electron Microscopy Sciences). Stained posterior midguts were imaged in the R5 region using LSM 710 confocal microscope (Carl Zeiss) using 'Plan-Apochromat 20 × /0.8 M27′ and 'C-Apochromat 40 × /1.20 W Corr M27′ objectives. Image resolution was set to at least 2048 × 2048 pixels. Focal planes were combined into Z-stacks and images were then processed by Fiji software. Final images were assembled using Canvas X-Pro. We would like to acknowledge the Center for Advanced Imaging (CAi) at Heinrich Heine University for providing support with imaging and access to the LSM 710 microscope system (DFG INST 208/539-1 FUGG).

Set 2: All images were taken in the P3–P4 regions of the *Drosophila* PMG, located by centering the pyloric ring in a ×40 field of view (fov) and moving 1–2 fov toward the anterior. PMGs were dissected into ice-cold PBS/4% formaldehyde and incubated for 1 h in fixative at room temperature. Samples were then washed three times, for 10 min each, in PBT (PBS containing 0.5% Triton X-100), 10 min in Na-deoxycholate (0.3%) in PBT (PBS with 0.3% Triton X-100), and incubated in block (PBT-0.5% bovine serum albumin) for 30 min at room temperature. Samples were immunostained with primary antibodies overnight at 4ºC, washed 3 × 10 min at room temperature in PBT (PBS containing 0.5% Triton X-100), incubated with secondary antibodies (1:500, Invitrogen)

at room temperature for 2 h, washed 3 × 10 min with PBT and mounted in Vecta-Shield/DAPI (Vector Laboratories, H-1200). Images were acquired on a Zeiss LSM780 or LSM880 inverted confocal microscope (UCLA MCDB/BSCRC Microscopy Core), and on a Zeiss Axio Observer Z1 with Apotome 2 using the ZEN Black v.2.0 (Zeiss) software. Images were processed with Fiji/ImageJ and Zen software. Final figures were assembled using Adobe Illustrator.

Antibody	Manufacturer	Catalog #	Species	Clonality	Dilution
Anti-Armadillo	DSHB	N2 7A1	Mouse	Monoclonal	1:20
Anti-Bark	Gift from R. Schuh[1]	n/a	Guinea pig	Polyclonal	1:1000
Anti-Dlg	DSHB	4F3	Mouse	Monoclonal	1:250
Anti-GFP	Aves Labs	GFP-1010	Chicken	Polyclonal	1:500
Anti-GFP	Abcam	ab13970	Chicken	Polyclonal	1:200
Anti-GFP	Molecular Probes	A-11122	Rabbit	Polyclonal	1:3000
Anti-pHH3	Millipore	06-570	Rabbit	Polyclonal	1:200
Anti-Pros	DSHB	MR1A	Mouse	Monoclonal	1:250
Anti-Chicken Alexa488	Invitrogen	A-11039	Goat	Polyclonal	1:500
Anti-Guinea Pig Alexa568	Invitrogen	A-11075	Goat	Polyclonal	1:500
Anti-Mouse Alexa568	Invitrogen	A-11004	Goat	Polyclonal	1:500
Anti-Mouse Alexa647	Invitrogen	A-21235	Goat	Polyclonal	1:500
Anti-Rabbit Alexa647	Invitrogen	A-31573	Donkey	Polyclonal	1:500

Table 2-2: List of antibodies used.

[1]Max Planck Institute for Multidisciplinary Sciences, Germany

Statistical Analysis: GraphPad Prism 8.0.2 was used to run statistical analysis and create graphs of quantifications. For single comparisons, data sets were analyzed by two-sided unpaired *t*-test or Mann-Whitney test. Multiple comparisons were analyzed by one-way ANOVA or Kruskal-Wallis tests. For survival analyses, Mantel-Cox log-rank test was performed. Significant differences are displayed as * for $P \leq 0.05$, ** for $P \leq 0.01$, *** for $P \leq 0.001$ and **** for $P \leq 0.0001$.

Quantification of Proliferation, Cell Size and Fluorophore Intensity Measurements:

Quantification of mitotic events, as measured by $pHH3^{+}$ cells per gut, was performed by acquiring 4 independent images at 40X magnification per gut in the P3-P4 region. Images were taken in directly adjacent fields of view on each side of the gut. Quantification of progenitor cell number and epithelial renewal and fluorescence intensity measurements were performed as described previously (Zipper *et al.*, 2020).

Set 1: Fiji (ImageJ 1.51 n, Wayne Rasband, National Institutes of Health, USA) was used to calculate maximum intensity images from z-stack images. GFP positive progenitor cells and RFP positive differentiated cells (EC and/or EE) of esg^{ReDDM} (Antonello *et al.*, 2015), klu^{ReDDM}, and $Myo\text{-}Gal4^{ts}$ were counted manually. Nuclear size measurements were performed in Fiji by outlining the nucleus manually and measuring the area. Mean intensities of the manually selected nuclear area were measured using Fiji by manually selecting the area of interest.

Set 2: Quantification of antibody fluorescence at the tSJ, bSJ and cytoplasm was performed with the ZEN Blue software. Images were acquired on a Zeiss LSM880 inverted confocal microscope equipped with AiryScan at 100X. Full z-stacks were used,

and anti-Armadillo staining was used to mark membranes. 3 cells were measured per PMG. Each clearly visible tSJ in the cell was measured. 6 measurements were taken of the bicellular junction and cytoplasm in each cell, respectively.

Smurf assay: Flies were maintained on standard medium prepared with FD&C Blue Dye no. 1 from Spectrum, added at a concentration of 2.5% (wt/vol). Loss of intestinal barrier function was determined ("Smurf" status) when dye was clearly observed outside the digestive tract (Rera *et al.*, 2011). Flies were checked three times weekly for loss of barrier function and/or death.

Survival Analysis: Flies were kept at 18°C and 3-5 days old flies were then shifted to 29°C. Not more than 10 flies (1:1 ratio of females: males) were kept per vial and flipped every other day to avoid bacterial contamination in the food. Flies were checked daily to record death events. At least 80 flies were assessed per genotype. Survival curves were plotted using Prism GraphPad software.

Supplemental information

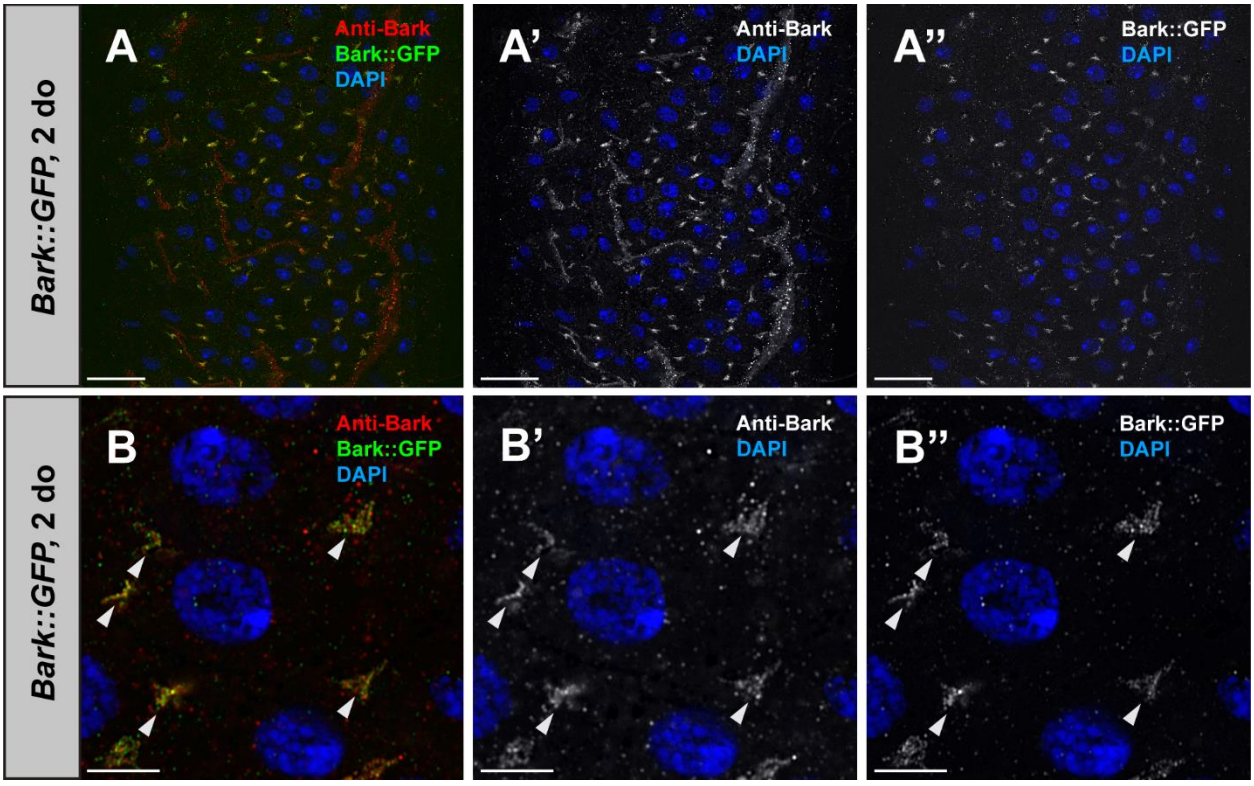

Figure 2-S1: Bark is expressed at the tSJ in the adult *Drosophila* hindgut. (**A-A"**) Representative staining for Bark (antisera, red) (*Bark::GFP*, GFP, green) in the hindgut of young (2 do) flies. DNA is stained with DAPI (blue). Scale bars, 20 µm. (**B-B"**) High magnification view of the hindgut showing staining of Bark at the tSJ (arrowheads). Scale bars, 5 µm.

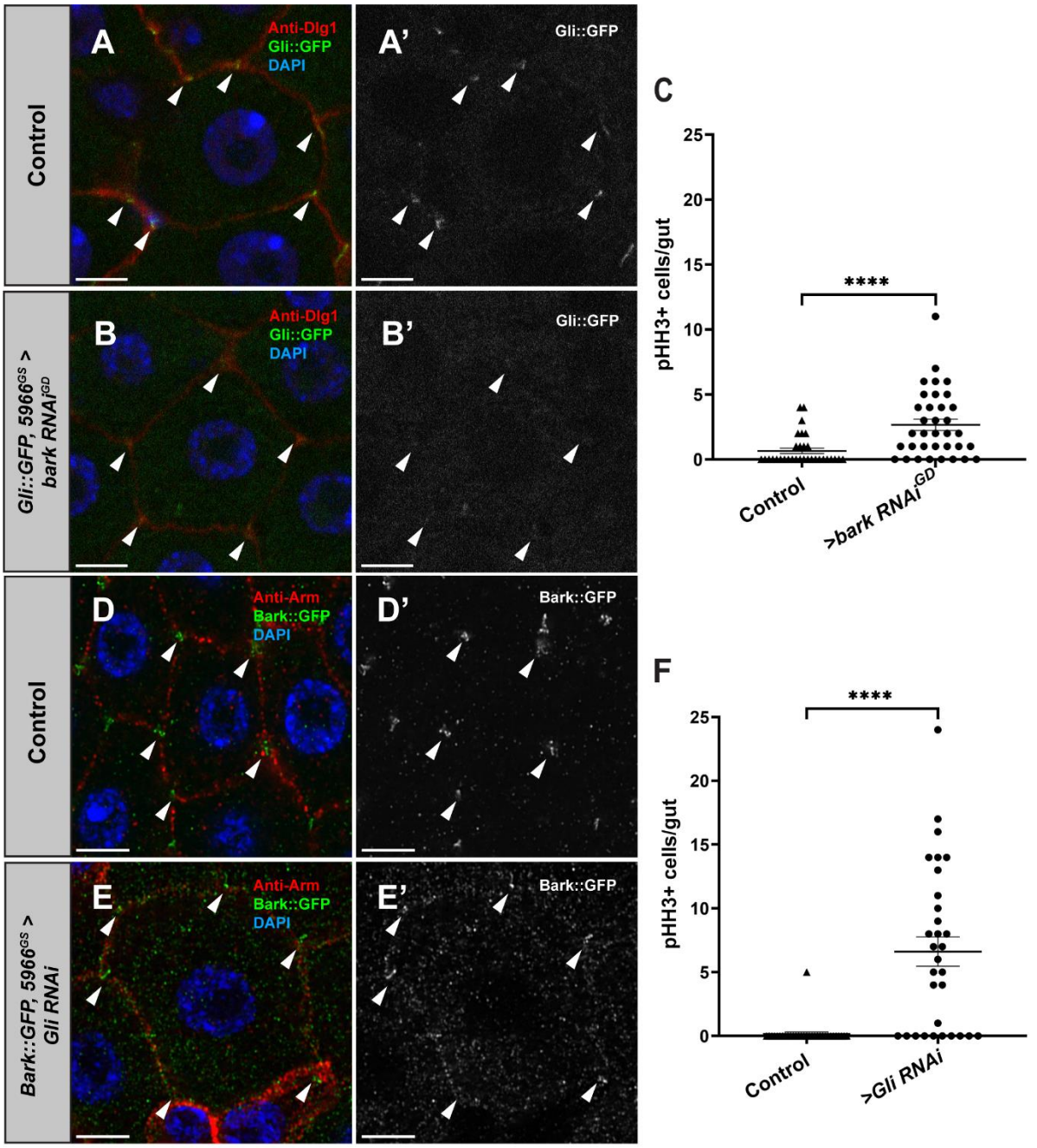

Figure 2-S2: Depletion of Gli results in loss of Bark from the TCJ in the adult posterior midgut. (**A-A'**) In young outcrossed (7 do) fly PMGs, Bark is localized exclusively to the tSJ. (**B-B'**) Depletion of Gli expression in ECs of young (7 do) flies leads to loss of Bark from the tSJ and an increase in Bark on the bicellular junction and cytoplasm. Genotypes: *w; 5966^{GS}* (control); *w; Bark::GFP, 5966^{GS}:Gli RNAi*. All flies are fed RU-486 for 5 days to

induce transgene expression. Bark (GFP, green); Armadillo (Arm, adherens junctions, red); DNA (DAPI, blue). Scale bars, 20 μm. (**C**) Quantification of mitotic events in the posterior midguts of *5966^{GS}:Gli RNAi* and outcrossed controls. Statistical significance was determined by Mann-Whitney test. **, P < 0.01. (**D-D'**) In young outcrossed fly PMGs, Gli localizes exclusively to the tSJ. (**E-E'**) EC-specific depletion of Bark protein by *5966^{GS}:bark RNAi^{GD}* expression causes mislocalization of Gli to cytoplasmic puncta, indicating Bark is required for Gli localization to the TCJ in the PMG. Genotypes: *w; Gli-GFP; bark RNAi^{GD}* (control); *w; Gli-GFP; 5966^{GS}:bark RNAi^{GD}*. All flies are fed RU-486 for 7 days to induce transgene expression. Scale bars, 20 μm. (**F**) Quantification of mitotic events in the posterior midguts of *5966^{GS}:bark RNAi^{GD}* and outcrossed controls. Statistical significance was determined by Mann-Whitney test. ****, P < 0.0001.

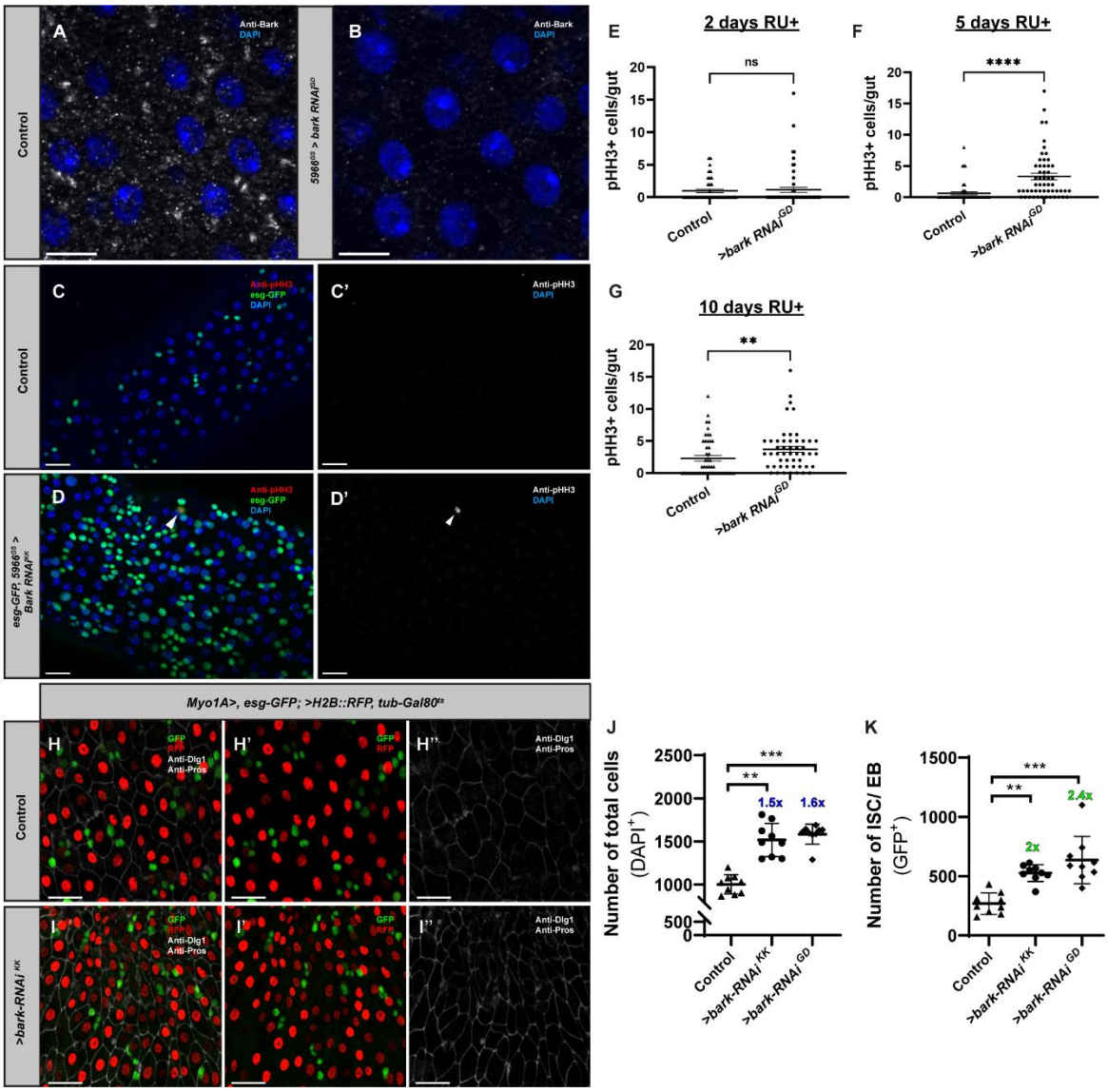

Figure 2-S3: Depletion of bark in mature EC non-autonomously stimulates stem cell proliferation. Induced expression of *5966^{GS}:bark RNAi^{GD}* by RU-486 feeding (11d) successfully depletes Bark protein from ECs in PMGs from young (2 do) flies (**B**) compared to uninduced siblings (**A**). Scale bar, 10 µm. (**C-D'**) Depletion of *bark* by induced expression of *5966^{GS}:bark RNAi^{KK}* in young flies results in an increase in esg+ cells and mitotic events in the PMG (n = 22) compared to outcrossed controls (n = 26), similarly to *5966^{GS}:bark RNAi^{GD}* as measured by phospho-histone H3 (arrowhead).

Genotypes: *w; esg-GAL4, UAS-GFP, 5966^{GS}* (outcrossed control); *w; esg-GAL4, UAS-GFP, 5966^{GS}:bark RNAi^{KK}* All flies are fed RU-486 for 5 days to induce transgene expression. Scale bars, 20 µm. (**E-G**) Depletion of Bark leads to a significant increase in ISC proliferation over time**.** Depletion of Bark protein from young fly PMG enterocytes by induced expression of *5966^{GS}:bark RNAi^{GD}* results in an increase in esg+ cells and mitotic events in the PMG compared to outcrossed controls 2d (**E**), 5d (**F**) and 10d (**G**) following RU-486 induction. Genotypes: *w; esg-GAL4, UAS-GFP, 5966^{GS}* (outcrossed control); *w; esg-GAL4, UAS-GFP, 5966^{GS}:bark RNAi^{GD}.* 2d induction (**E**): *>bark RNAi^{GD}* n = 58; *w^{1118}* n = 36. 5d induction (**F**): *>bark RNAi^{GD}* n = 54; *w^{1118}* n = 48. 10d induction (**G**): *>bark RNAi^{GD}* n = 50; *w^{1118}* n = 49. Data shown is combined from two independent trials. Error bars represent mean with SEM. Significance was determined by Mann-Whitney test. ns, not significant; **, P < 0.005; ****, P < 0.0001. Knockdown of *bark* in ECs using *Myo1A-GAL4^{ts}* (*Myo1A>, esg-GFP; H2B::RFP, tub-GAL80^{ts}*) increases progenitor cells. **(H-H'')** Confocal images of control PMG in the R5 region after 7 days of tracing. **(I-I'')** Knockdown of *bark* increases the total number of cells and the number of ISC/ EB (GFP^{+}). Anti-Dlg1 marks bSJs and anti-Pros marks EE nuclei. **(J, K)** Quantifications of the total cell number (DAPI^{+}) **(J)** and ISC/ EB **(K)** upon *bark* knockdown after 7 days of tracing. (n= 9, 9, 9). Statistical significance determined by Kruskal-Wallis test. **, P < 0.01; ***, P < 0.001. Scale bar, 20 µm.

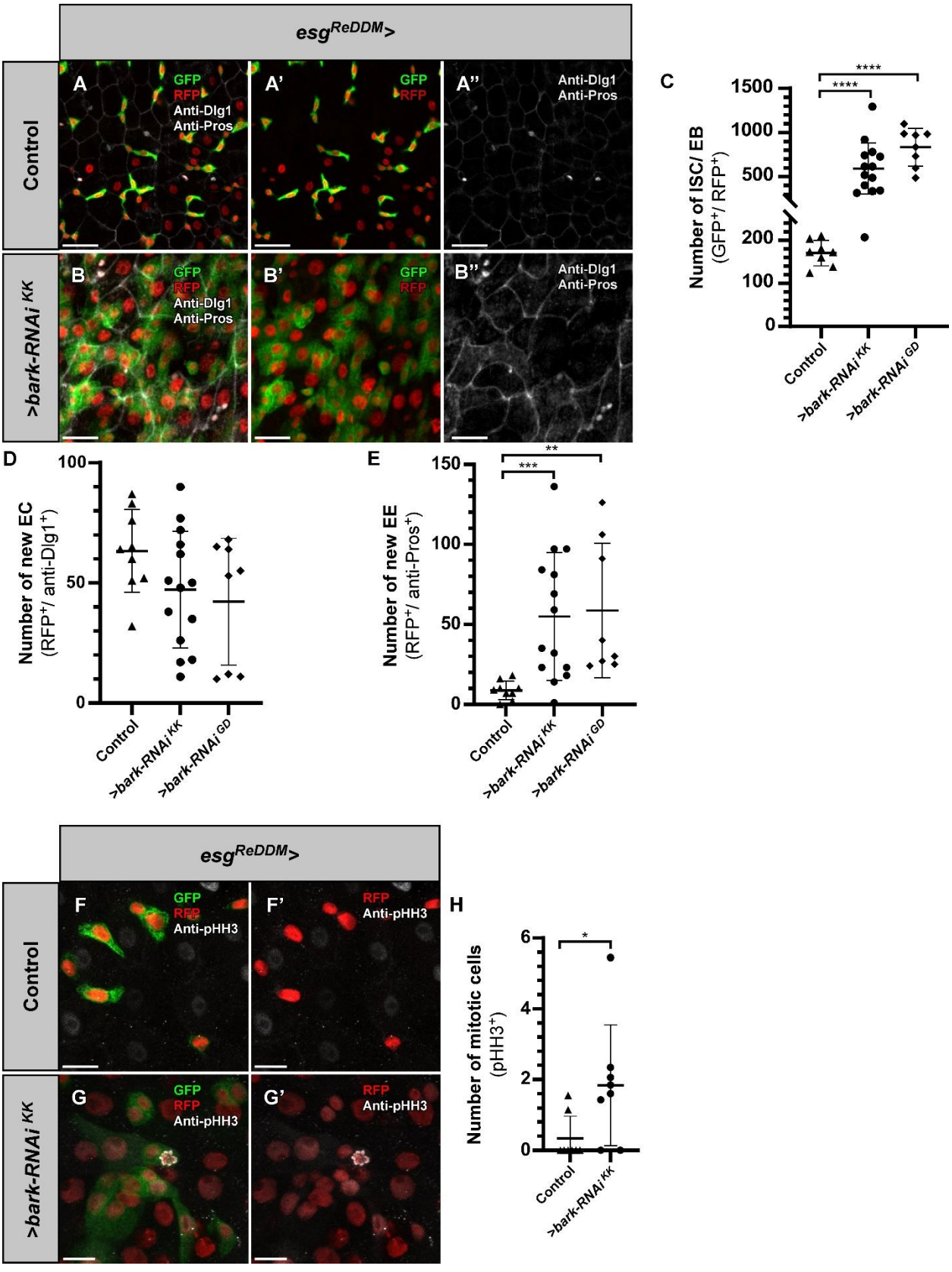
esgReDDM>
Control
>bark-RNAi KK
A
A'
A''
B
B'
B''
GFP
RFP
Anti-Dlg1
Anti-Pros
C
Number of ISC/ EB
(GFP+/ RFP+)
1500
1000
500
200
100
0
****
****
Control
>bark-RNAi KK
>bark-RNAi GD
D
Number of new EC
(RFP+/ anti-Dlg1+)
100
50
0
E
Number of new EE
(RFP+/ anti-Pros+)
150
100
50
0
**
***
esgReDDM>
Control
>bark-RNAi KK
F
F'
G
G'
Anti-pHH3
H
Number of mitotic cells
(pHH3+)
6
4
2
0
*

Figure 2-S4: ISC/EB specific depletion of *bark* results in ISC proliferation and increase in progenitor cells and EE differentiation. *esg^{ReDDM}* (*w; esg-GAL4, UAS-CD8::GFP; UAS-H2B::RFP, tub-GAL80^{ts}*) tracing and the knockdown of *bark* in ISCs/EBs leads to an increase in progenitor cells and EEs. **(B-B'')** Compared with controls **(A-A'')**, knockdown of *bark* in the R5 region following 7d of temperature shift increases the number of newly differentiated EEs (GFP$^-$/RFP$^+$/anti-Pros$^+$) and the number of progenitor cells (GFP$^+$/RFP$^+$) but no significant change in the number of ECs (GFP$^-$/RFP$^+$/anti-Dlg1$^+$). **(C-E)** Quantifications of ISCs/EBs **(C)**, new ECs **(D)** and new EEs. **(E)** Quantification of new ECs upon *bark* knockdown after 7 days of tracing. (n= 9, 8, 14). Statistical significance determined by one-way ANOVA. **, P < 0.01; ***, P < 0.001. Scale bar, 20 µm. **(F-G')** Knockdown of *bark* **(G-G')** leads to an increase in the number of proliferating cells (marked by pHH3) as compared to the controls **(F-F')**. **(H)** Quantification of the number of mitotic cells upon *bark* depletion after 7 days of tracing. (n= 8, 8). Statistical significance determined by Mann-Whitney test. ****, P < 0.0001. Scale bar 10 µm.

Chapter 3: Vesicular trafficking appears altered in the aged *Drosophila melanogaster* intestine

Introduction

Dietary restriction delays age-related septate junction component mislocalization

Our lab has previously explored potential causes of age-related mislocalization of SJ components in the PMG (Resnik-Docampo *et al.*, 2017). To find if mislocalization of SJ components is truly age-linked, we decided to artificially extend lifespan and determine if this also delayed SJ component mislocalization. Dietary restriction (DR), the restriction of daily caloric consumption, is well-known to extend lifespan across many species, including yeast, *C. elegans, Drosophila,* and mice (Kapahi *et al.*, 2017; Weindruch *et al.*, 1986). We utilized DR in wild-type *Drosophila* across their lifetime and found that lifespan was significantly extended (**Fig. 3-1A**) (Resnik-Docampo *et al.*, 2017). Using immunofluorescence, we found that DR flies have delayed mislocalization of Gli protein, based on tSJ/cytoplasm fluorescence intensity ratios (**Fig. 3-1B**). Therefore, we concluded that the observed mislocalization of SJ components in aged fly intestines is linked with the aging process. However, it should be noted that because DR is based on changes in feeding, this may inherently alter intestinal health outside of a lifespan increase, and thus could affect SJ integrity through another mechanism.

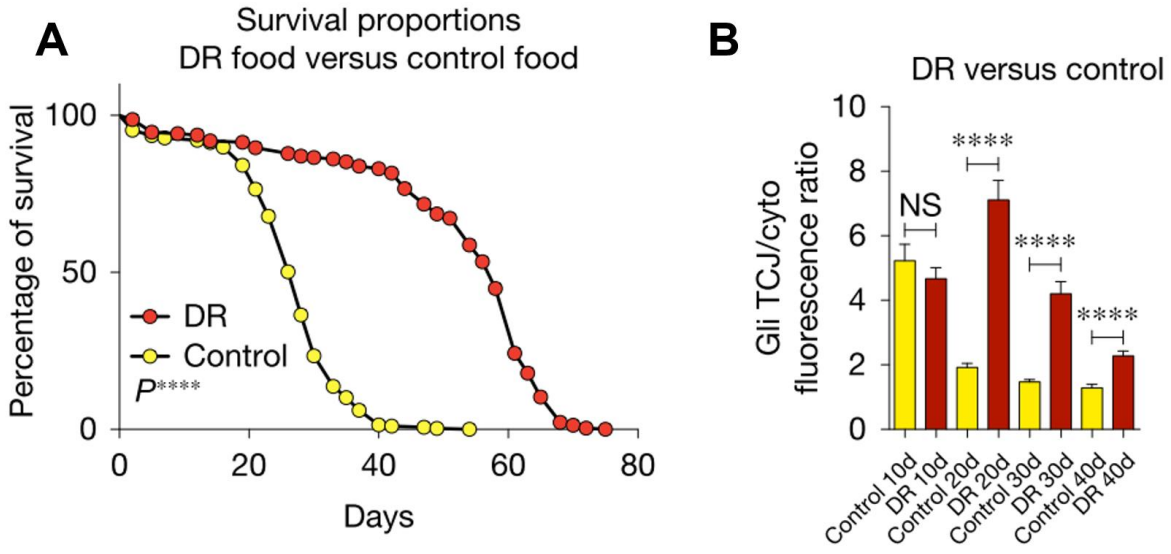

Figure 3-1: Dietary restriction delays age-related mislocalization of Gliotactin protein in *Drosophila* enterocytes. Figure adapted from Resnik-Docampo *et al.*, 2017. (**A**) Dietary restriction in wild-type *Drosophila* significantly extends lifespan (red) compared with controls fed *ad libitum* (yellow). (**B**) In DR flies, Gliotactin tSJ/cytoplasm fluorescence intensity ratio is significantly higher in old age than controls fed *ad libitum,* indicating that age-related mislocalization of Gliotactin has been delayed.

Axenic conditions do not delay age-related septate junction component mislocalization

The microbiome is known to play a significant role in overall intestinal health, and aging is associated with dysbiosis, an abnormal microbiome. It was previously demonstrated that age-associated dysbiosis contributes to intestinal barrier failure (Clark *et al.*, 2015; Rera *et al.*, 2012). When a microbiome sample from an aged fly is transplanted into a young fly, intestinal barrier loss and death occur significantly sooner. Using the Smurf assay, which identifies “Smurfs” as having severe intestinal barrier loss,

“pre-Smurfs” were found to have a small increase in bacterial load. Shortly after becoming “Smurfs,” a second, larger increase in bacterial load was observed (Clark *et al.*, 2015). Additionally, aging in both *Drosophila* and mammals is associated with an increase in immunity-related gene expression. In *Drosophila*, it has been demonstrated that increased antimicrobial peptide (AMP) expression and defective insulin/insulin-like growth factor signaling are tightly linked to Smurf status regardless of age (Rera *et al.*, 2012).

Because age-associated dysbiosis was shown to accelerate intestinal barrier loss (Clark *et al.*, 2015), our lab investigated if the presence of a microbiome is required for age-associated SJ component mislocalization. When wild-type flies were raised in axenic conditions, their lifespan was slightly increased (**Fig. 3-2A**). However, localization of Gli protein based on immunofluorescence in young and old flies did not significantly differ from age-matched controls (**Fig. 3-2B**). This indicated that presence of a microbiome is not required for age-associated SJ component mislocalization in the aged fly intestine. However, the relationship between SJ component localization and age-associated dysbiosis has not yet been investigated.

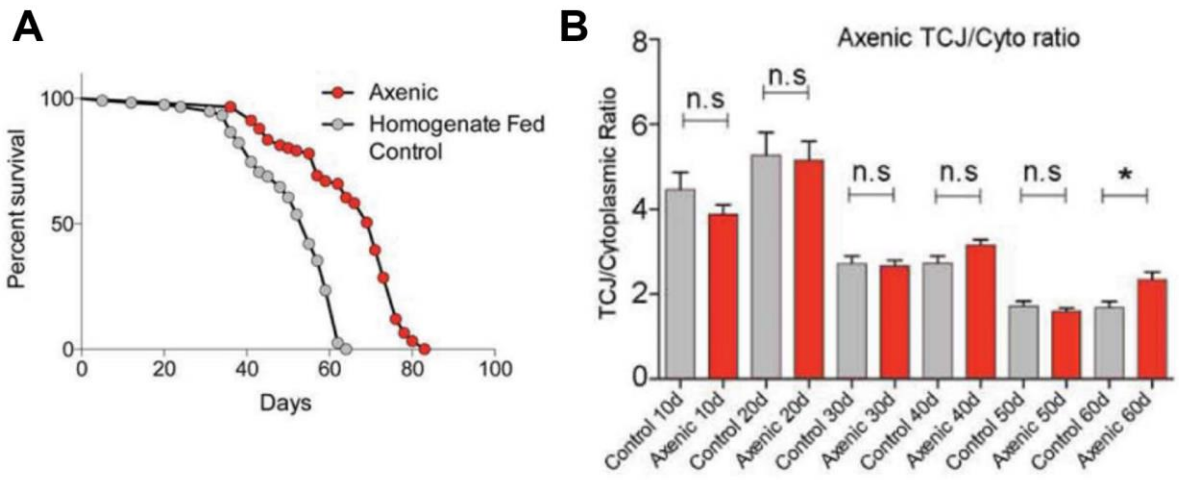

Figure 3-2: Presence of a microbiome is not required for age-related mislocalization of Gli protein in the *Drosophila* intestine. Figure adapted from Resnik-Docampo *et al.*, 2018. (**A**) Wild-type flies raised under axenic conditions have slightly longer lifespans than their control counterparts. (**B**) Gli-GFP tSJ/cytoplasm fluorescence intensity ratio in ECs across the adult lifetime is not significantly changed by axenic conditions.

Intestinal stem cell ablation does not delay age-related septate junction component mislocalization

The increase in intestinal stem cell (ISC) proliferation, based on an increase in *esg*+ cells, in the aged *Drosophila* intestine has been well documented (Resnik-Docampo *et al.*, 2017; Choi *et al.*, 2011; Biteau *et al.*, 2008). Our lab had previously observed that in the *Drosophila* hindgut, which has no ISCs, no age-related change in SJ protein localization occurs (Resnik-Docampo *et al.*, 2017). Additionally, age-associated increase in ISC proliferation seems to be accompanied by an accumulation of misdifferentiated cells (e.g., polyploid *esg*+ cells) in the gut, whose identities are currently unknown. It is possible that if these cells are misdifferentiated, normal SJ maintenance could also be

disrupted, especially if these cells express traits associated with ISCs/EBs, which have no SJs. Sufficiently high accumulation of these misdifferentiated cells could then result in disruption of intestinal barrier function. Therefore, our lab hypothesized that ISC overproliferation could be contributing to age-associated SJ component mislocalization, and that ISC ablation could potentially benefit SJ component localization.

Headcase (*Hdc*) expression is a marker for ISCs/EBs, and is required for their maintenance (Resende *et al.*, 2017). Therefore, *esg>Hdc RNAi* expression was induced in young flies to ablate ISCs/EBs beginning in adulthood (**Fig. 3-3**). No significant change was observed in localization of SJ components Snakeskin (Ssk) or Discs large (Dlg) in young or old flies, suggesting that age-associated ISC overproliferation does not contribute to age-associated SJ component mislocalization (Jones lab, unpublished data). However, it should be noted that ISCs/EBs were ablated at the start of adulthood, before aging phenotypes set in, which may have had unknown harmful effects. This experiment does not rule out the possibility that ISC/EB ablation starting in midlife, or modulation of ISC activity throughout life, could be beneficial to SJ component localization in old fly intestines.

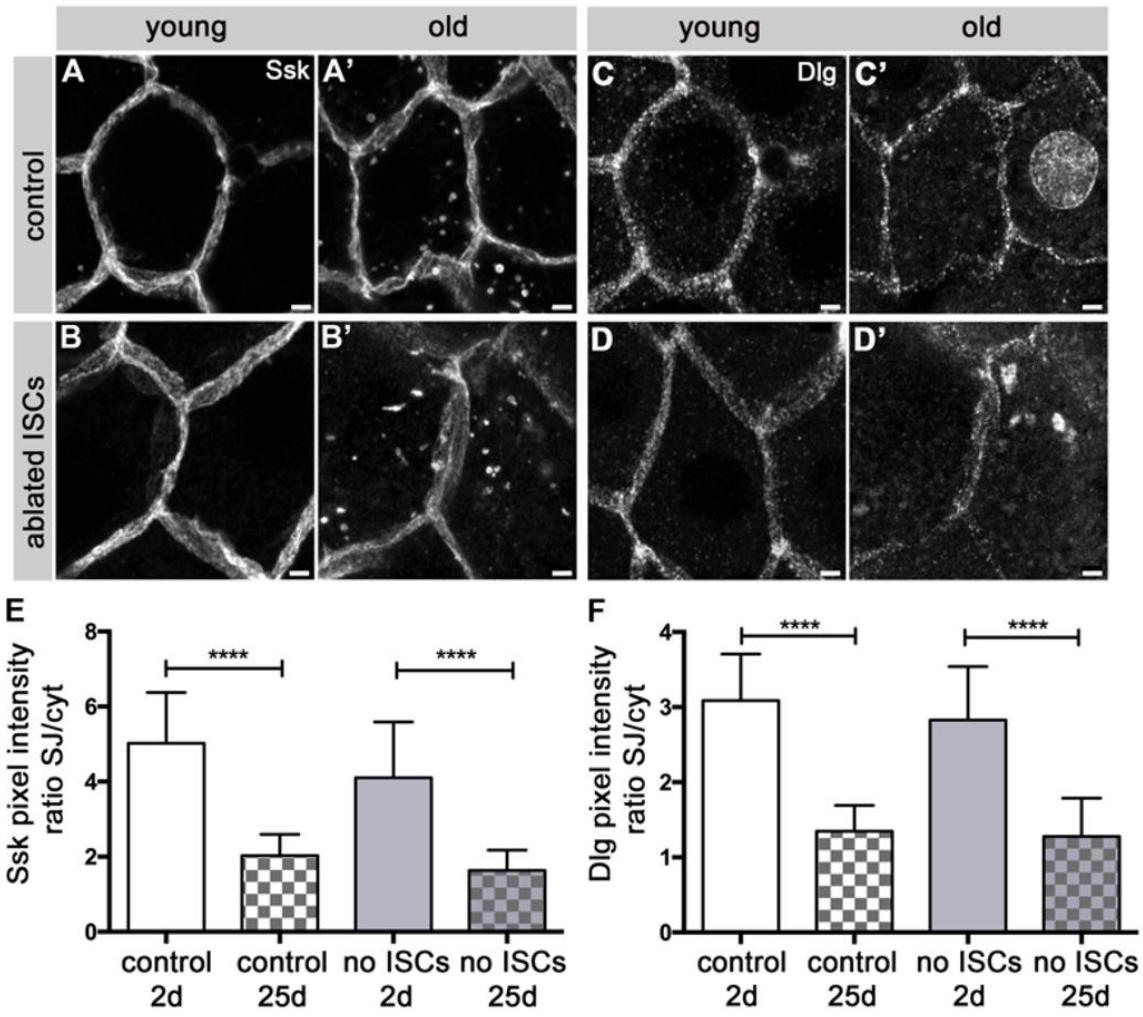

Figure 3-3: Intestinal stem cell (ISC) ablation does not delay age-related mislocalization of SJ components in the *Drosophila* intestine. ISCs/EBs were depleted from fly PMGs at the start of adulthood (2 do) using transient *esg>Hdc RNAi* expression, and PMGs were assessed in midlife (25 do). No significant difference was observed in localization of Ssk and Dlg protein compared to controls, based on the SJ:cytoplasm fluorescence intensity ratios. Error bars represent standard deviation. Statistical significance was determined by Mann-Whitney test. ****, $P < 0.0001$. Scale bars, 2 µm. (Jones lab, unpublished data).

Septate junction components have been observed in trafficking compartments

There are previous observations of SJ components localizing to trafficking compartments based on immunofluorescence staining. This provided us with candidate SJ components to co-stain with trafficking compartments to screen for age-related changes in their colocalization. For example, cytoplasmic tetraspanin 2A (Tsp2A), a transmembrane SJ protein that forms a complex with Mesh and Snakeskin (Ssk), was found to colocalize with the early endosome marker Hrs and the late endosome marker Rab7 in the fly PMG (Xu *et al.*, 2019; Riedel *et al*., 2016). The SJ protein Neuroglian (Nrg) associates with Rab5-GFP and Rab11-GFP in the embryo, based on immunoprecipitation (Tiklová *et al.*, 2010). Gli has also been observed colocalizing with the early endosome marker Hrs and the lysosome marker Lamp1 in the fly wing disc (Padash-Barmchi *et al.*, 2010). While extensive screens have not been performed to track SJ proteins' localization to every known vesicular trafficking compartment, these data indicated to us that immunofluorescence studies of SJ proteins in the PMG would likely reveal colocalization with vesicular trafficking markers.

Integrity of vesicular trafficking is required for septate junction assembly and maintenance

SJ components are regularly turned over, although this process is slow for SJ core complex components (Oshima & Fehon, 2011) compared to turnover of adherens junction components (Yamada *et al.*, 2005) and tight junction components (Shen *et al.*, 2008). Multiple studies have demonstrated that SJ assembly requires functional vesicular trafficking, and that SJ maintenance requires turnover of SJ components via vesicular trafficking. Expression of *Rab5 RNAi* in the PMG, which disrupts early endosome function, decreases cytoplasmic Tsp2A, while disruption of recycling endosome function by *Rab11*

RNAi expression increases cytoplasmic Tsp2A. In both cases, Tsp2A protein is lost from the SJ based on immunofluorescence, indicating that the endocytosis and recycling pathways are required for Tsp2A to be maintained at the SJ in the PMG (Xu *et al.*, 2019). Notably, *Tsp2A RNAi* expression in the PMG may also lead to defects in endocytosis (Xu *et al.*, 2019), suggesting that age-related mislocalization of Tsp2A in the PMG (data not shown) may contribute to age-related endocytosis defects. Additionally, $Rab5^{DN}$ expression causes Gli to spread along the bSJ and into the cytoplasm. Interestingly, this study also revealed constitutively dephosphorylated Gli cannot be endocytosed (Padash-Barmchi *et al.*, 2010), and it may be useful to investigate in the future if post-translational modification of SJ proteins becomes dysfunctional with age.

Like SJ maintenance, initial SJ assembly in *Drosophila* embryos requires endocytosis. In late embryogenesis, SJs are assembled as individual or small groups of septa that gradually have additional septa added on (Tepass & Hartenstein, 1994). When endocytosis is inhibited by $Rab5^{DN}$ or $Rab11^{DN}$ expression in the embryo, SJ proteins fail to accumulate properly on the apicolateral membrane (Tiklová *et al.*, 2010). It may be useful in further studies to determine if SJ assembly in pre-EC or pre-EE cells similarly requires endocytosis.

Aging and disease are associated with changes in vesicular trafficking in mammals

Our initial observation that SJ proteins increasingly localize to cytoplasmic puncta in the aged fly PMG (Resnik-Docampo *et al.*, 2017) did not give insight into what specific vesicular trafficking compartments could be affected by age and contributing to this phenotype. Vesicular trafficking of proteins and other cellular components within and between cells is an essential and dynamic function in every animal cell, and includes

diverse, complex processes such as clathrin-mediated endocytosis (CME), recycling, exocytosis, and others. Previously collected RNAseq data in young and old fly PMGs revealed most known vesicular trafficking marker genes are only slightly upregulated with age (Resnik-Docampo *et al.*, 2017). The initial broad scope of this study, along with no significant change in transcription of known vesicular trafficking markers, led us to search for pre-existing evidence of specific vesicular trafficking pathways that are altered with age or disease.

There is evidence in mammals that endocytosis is altered with age, even in the absence of known disease. Aged rat liver sinusoidal endothelial cells have reduced endocytic and degradative rates, suggesting a loss of function phenotype (Simon-Santamaria *et al.*, 2010). Additionally, total Rab5 protein and total clathrin protein levels increase with age in human brains without known neurological disease (Alsaqati *et al.*, 2018). Age-associated disease has also been associated with changes in endocytosis and recycling. Antibody staining for Rab5, an early endosome marker, indicated that neurons in human brains with early Alzheimer's disease have enlarged or aggregated early endosomes (Cataldo *et al.*, 2000). Decreased immunostaining for Rab11, a recycling endosome marker, has also been observed in human colon cancer, and studies in the *Drosophila* PMG suggest this Rab11 depletion may enhance cancer progression (Nie *et al.*, 2019).

Taken together, these studies on vesicular trafficking in aging and age-related disease, SJ protein colocalization with vesicular trafficking markers, and the requirement for endocytosis in SJ maintenance indicated to us that focusing on changes in CME and

recycling would be a reasonable first step in identifying the cause of age-related mislocalization of SJ proteins in the fly PMG.

Results

Aging may be associated with changes in early and late endosomes in the Drosophila posterior midgut

The SJ component cytoplasmic puncta observed in aged fly PMG enterocytes could be localizing to any one or multiple types of vesicular trafficking compartments. Additionally, this phenotype could be due to any one or multiple steps of vesicular trafficking stalling, slowing or accelerating. We chose initially to focus on clathrin-mediated endocytosis (CME) in enterocytes, due to the availability of *Drosophila* genetic tools and evidence for age- and disease-related change in CME in mammals. We then decided to conduct a screen of CME compartments in aged fly PMGs, to identify targets for further study.

Hepatocyte growth factor regulated tyrosine kinase substrate (Hrs) is an early endosome marker in *Drosophila* (Lloyd *et al.*, 2002). We stained with anti-Hrs antibody in young and old *Drosophila* PMGs, and identified possible changes in Hrs staining. Hrs+ vesicles appear to be larger in size and increasingly localize near the membrane (**Figs. 3-4A-A', 3-6A-A'**) in the aged fly PMG. If future quantification confirms this phenotype, it could indicate that CME is altered around the early endosome stage in the aged fly PMG. Early endosomes may have increased in number, increased their cargo, or stalled. Validity of the anti-Hrs antibody was confirmed by *UAS-Hrs RNAi* expression reducing antibody staining in the wing disc (**Fig. 3-S1**).

Rab7 is a marker for late endosomes in *Drosophila* (Vanlandingham & Ceresa, 2009). Similar to our observations of anti-Hrs staining, anti-Rab7 staining in old fly PMGs suggests that Rab7+ vesicles are enlarged (**Fig. 3-4B-B'**). If this observation is confirmed by quantification, this could indicate that the late endosome stage of CME is affected by age. Validity of the anti-Rab7 antibody was confirmed by *UAS-Rab7 RNAi* expression reducing antibody staining in the wing disc (**Fig. 3-S2**).

Additional vesicular trafficking markers were screened using antibodies and protein trap lines in young and old fly PMGs. We observed that flies expressing *Rab4-YFP*, a marker for recycling endosomes (Sorvina *et al.*, 2016), show what appear to be increased numbers of Rab4+ vesicles in diploid ISCs/EBs in aged fly PMGs (**Fig. 3-S3**), which may be a topic for further investigation. Observations of other vesicular trafficking markers, including RabX4 (neural early endosome marker) (Zhang *et al.*, 2007), Rab5 (early endosome marker) (Bucci *et al.*, 1992), Rab11 (recycling endosome marker) (Ullrich *et al.*, 1996), Rab35 (fast recycling marker) (Kouranti *et al.*, 2006), Lamp1 (lysosome marker) (Kannan *et al.*, 1996), Ref(2)p (autophagosome marker) (Nezis *et al.*, 2008), Atg1 (autophagosome marker) (Chang & Neufeld, 2009), and Atg8a (autophagosome marker) (Alemu *et al.*, 2012), revealed no obvious change in apparent vesicle size or localization (data not shown).

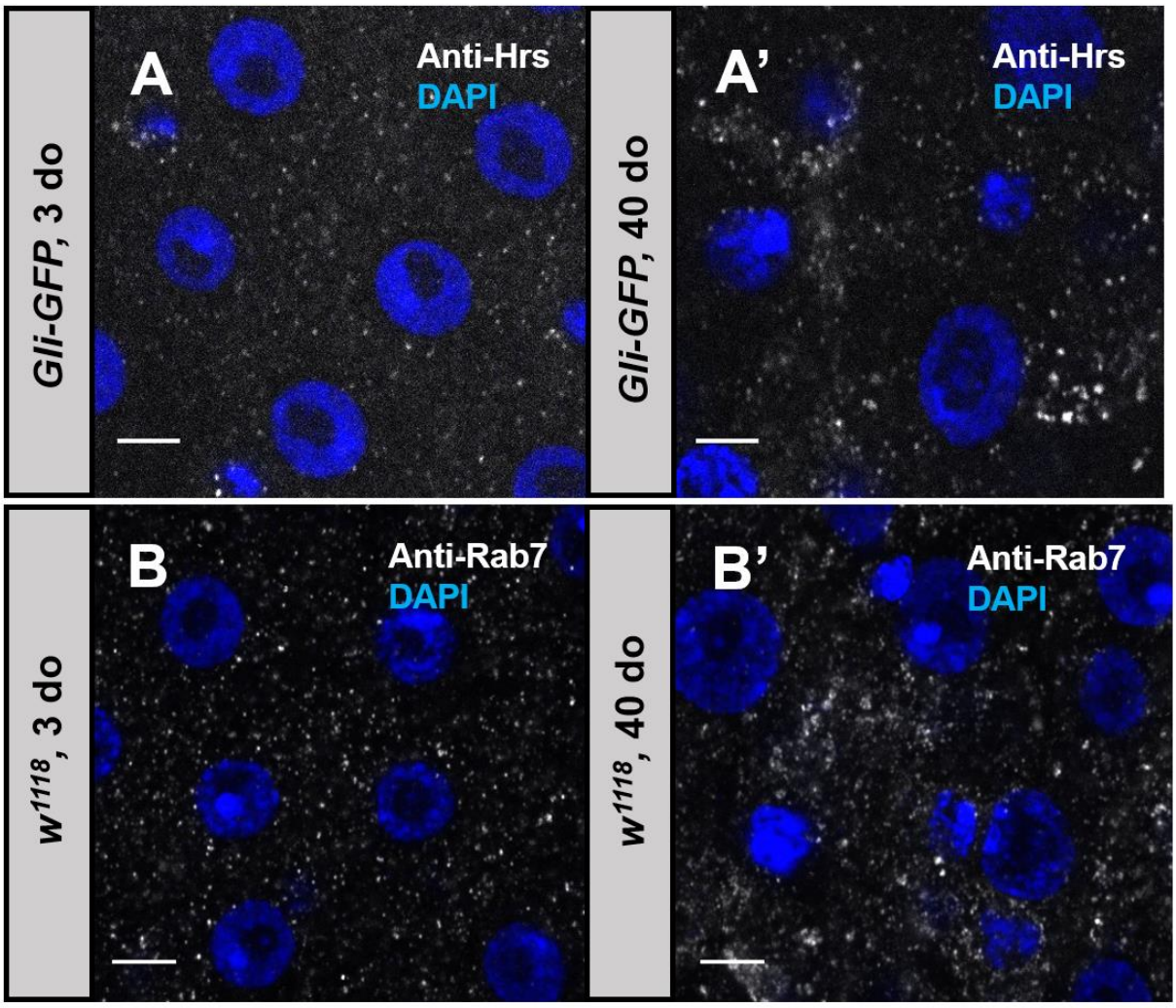

Figure 3-4: Anti-Hrs and anti-Rab7 staining are altered in aged fly PMGs. (**A**) In the young (3 do) fly PMG, Hrs+ vesicles are uniform in size and distribution across the EC cytoplasm (n = 6). (**A'**) Aged (40 do) fly PMGs appear to have Hrs+ vesicles that are sometimes larger in size, and may occasionally localize along the membrane (top left) (n = 7). (**B**) In the young (3 do) fly PMG, Rab7+ vesicles are uniform in size and distribution across the EC cytoplasm (n = 8). (**B'**) Aged (40 do) fly PMGs appear to have Rab7+ vesicles that are sometimes larger in size, and are less uniformly distributed across the cytoplasm (n = 10). Scale bars, 5 µm.

Trafficking of Gliotactin and Mesh proteins may be altered with age in the Drosophila posterior midgut

After we detected possible changes in size or aggregation in early and late endosomes in the aged fly PMG, we decided to screen for changes in their colocalization with SJ proteins based on immunofluorescence. If certain SJ proteins increasingly or decreasingly colocalize with certain CME markers in the EC cytoplasm, this could give insight into which CME stages have changed with age, how they have changed, and whether certain SJ protein types are affected differently. This screen also identified targets that should be prioritized in the future *Mesh-APEX2-GFP* screen which will search for Mesh-associated proteins in young and old fly PMGs.

In young (3 do) fly PMGs, anti-Hrs and anti-Rab7, staining rarely colocalize with anti-Mesh and Gli-GFP staining, respectively (**Fig. 3-5A, B**). However, in aged (35 do, 40 do) PMGs, anti-Hrs and anti-Mesh staining often colocalize (**Fig. 3-5A'**), as do anti-Rab7 and Gli-GFP staining (**Fig. 3-5B'**). These data suggest that trafficking of Mesh protein has been altered around the early endosome stage, and that trafficking of Gli protein has been altered around the late endosome stage. In both cases, increasing colocalization could indicate that CME has stalled at or downstream of these stages, causing accumulation; alternatively, it could indicate CME has accelerated at these stages, and production of early endosomes and late endosomes has increased. However, it should be noted that these trends are not consistent across SJ proteins tested. For example, no change in anti-Ssk colocalization with anti-Hrs or anti-Rab7 was noted in aged PMGs. Additionally, anti-Mesh staining does not change in colocalization with anti-Rab7 staining in the aged PMG, and anti-Tsp2A staining decreases in colocalization with anti-Rab7 in aged PMGs

(data not shown). Quantification of these results, and expansion of the screen to include other known SJ proteins such as Discs large, will be necessary before conclusions can be made about changes in SJ trafficking in the aged PMG.

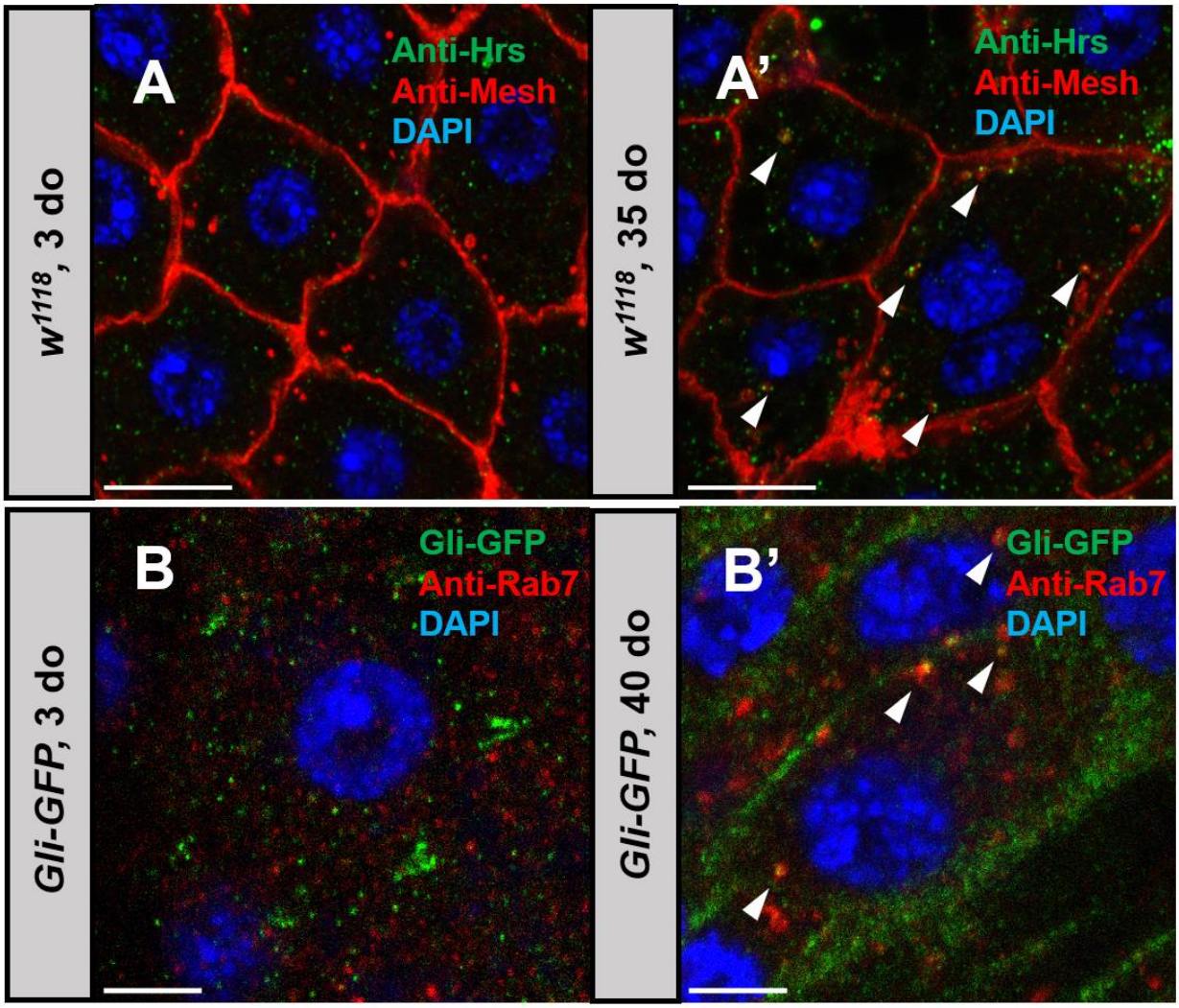

Figure 3-5: CME marker and SJ component staining appear to increasingly colocalize in aged fly PMG enterocytes. In young fly PMGs (3 do) (**A**), no colocalization of anti-Hrs and anti-Mesh staining is visible (n = 9). In old fly PMGs (40 do) (**A'**), Hrs+ vesicles and Mesh protein appear to colocalize in the EC cytoplasm (arrowheads) (n = 12). Scale bars, 10 µm. In young fly PMGs (3 do) (**B**), no colocalization of anti-Rab7 and Gli-GFP staining is

visible (n = 8). In old fly PMGs (40 do) (**B'**), Rab7+ vesicles and Gliotactin protein appear to colocalize in the EC cytoplasm (arrowheads) (n = 10). Scale bars, 5 μm.

Depletion of endocytic proteins disrupts septate junction component localization in the Drosophila posterior midgut

After we determined that CME of SJ proteins appears to be altered with age, we decided to investigate the requirement of vesicular trafficking in SJ maintenance. We depleted vesicular trafficking markers in ECs of young PMGs by inducing RNAi or dominant negative gene expression. Multiple SJ proteins, including Ssk and Tsp2A, had noticeable changes in localization following depletion of functional trafficking markers including Hrs, Rab5, Rab7, and Rab11 (**Fig. 3-6**). Based on immunofluorescence staining, SJs appeared to be disrupted in a way reminiscent of the aging phenotype (**Fig. 1-6**). Additionally, depletion of vesicular trafficking markers from ECs led to an increase in *esg*+ cells and dysplasia in the PMG (data not shown). Notably, Ssk seems to increasingly localize to cytoplasmic puncta when trafficking markers are depleted (**Fig. 3-6A-C**). This could be because removing one vesicular compartment causes accumulation of the preceding vesicular compartment, which could be confirmed by additional immunofluorescence experiments. Overall, these data indicate that the integrity of vesicular trafficking pathways is required for normal localization of SJ proteins.

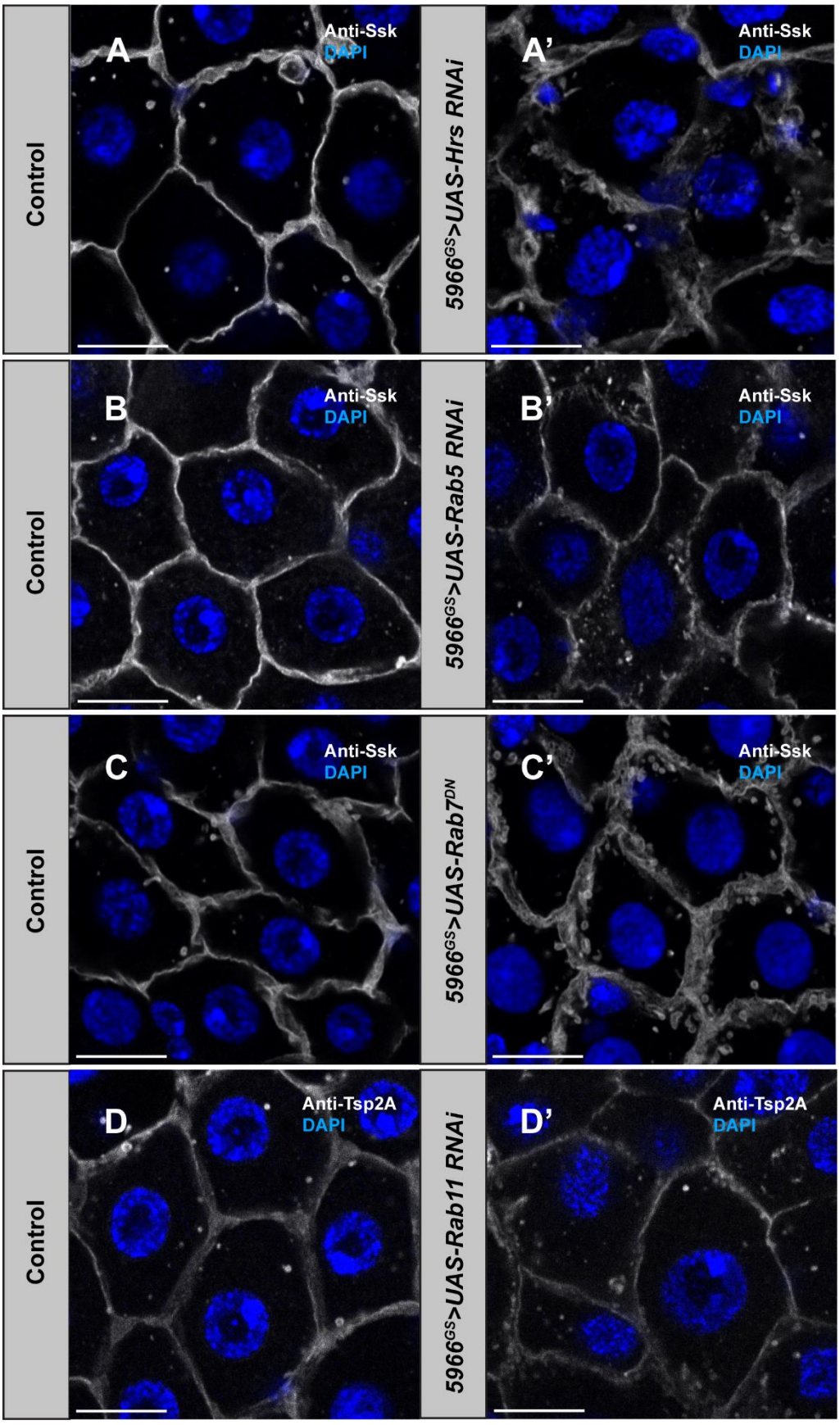
Control
A
Anti-Ssk
DAPI
5966GS>UAS-Hrs RNAi
A'
Anti-Ssk
DAPI
Control
B
Anti-Ssk
DAPI
5966GS>UAS-Rab5 RNAi
B'
Anti-Ssk
DAPI
Control
C
Anti-Ssk
DAPI
5966GS>UAS-Rab7DN
C'
Anti-Ssk
DAPI
Control
D
Anti-Tsp2A
DAPI
5966GS>UAS-Rab11 RNAi
D'
Anti-Tsp2A
DAPI

Figure 3-6: Integrity of vesicular trafficking is required for normal localization of SJ proteins. Induced *5966^{GS}:UAS-Hrs RNAi* expression in ECs (n = 6) (**A'**), induced *5966^{GS}:UAS-Rab5 RNAi* expression in ECs (n = 10) (**B'**), and induced *5966^{GS}:UAS-Rab7^{DN}* expression in ECs (n = 10) (**C'**) disrupts localization of the bSJ protein Snakeskin (Ssk) compared with outcrossed controls (**A**, n = 6; **B**, n = 12, **C**, n = 12). Induced expression of *5966^{GS}:UAS-Rab11 RNAi* in ECs disrupts localization of the bSJ protein Tetraspanin 2A (Tsp2A) (n = 9) (**D'**) compared with outcrossed controls (n = 12) (**D**). Scale bars, 10 µm. (B, D: Christopher Ochoa).

Discussion

Occluding junctions, referred to as septate junctions (SJs) in *Drosophila* and tight junctions (TJs) in mammals, contribute significantly to intestinal barrier function. There is evidence that in mammals, TJs in the small intestine lose physical integrity with age (Ren *et al.*, 2014). Correspondingly, our lab has previously found that SJs in the fly intestine lose physical integrity with age, and SJ components appear to mislocalize away from the SJ (Resnik-Docampo *et al.*, 2017). This mislocalization does not require the presence of a microbiome (Resnik-Docampo *et al.*, 2018, **Fig. 3-2**) or intestinal stem cells (**Fig. 3-3**) and is correlated with age, even when lifespan is manipulated (**Fig. 3-1**). Due to SJ components in the aged fly intestine appearing to increasingly localize to cytoplasmic puncta, we hypothesized that this age-related mislocalization was due to dysfunctional vesicular trafficking of SJ components. We began a study to identify and broadly characterize these potential defects, with the hope that future investigations will be able to rescue these vesicular trafficking defects and restore intestinal barrier function. In humans, such a treatment may help promote gastrointestinal health and longevity.

Previous evidence suggests that clathrin-mediated endocytosis (CME) and recycling endosomes become dysfunctional with age and age-related disease in mammals (Cataldo *et al.*, 2000; Simon-Santamaria *et al.*, 2010; Alsaqati *et al.*, 2018; Nie *et al.*, 2019). Therefore, we screened fly PMGs for age-related change in vesicular trafficking compartments based on immunofluorescence staining with a focus on CME and adjacent compartments. We found that antibody staining for Hrs, an early endosome marker (Lloyd *et al.*, 2002), and Rab7, a late endosome marker (Vanlandingham & Ceresa, 2009), is altered with age (**Fig. 3-4**). Hrs+ and Rab7+ vesicles appear to be enlarged or aggregated in ECs of the aged fly PMG. If quantification of puncta number and size confirm this, early and late endosomes could be dysfunctional in the aged PMG. Additionally, electron microscopy could be used to determine if these vesicles have enlarged or aggregated. This would give insight into how these compartments or their regulation have become dysfunctional. Other compartments such as recycling endosomes and autophagosomes appeared not to change in size or aggregation with age (data not shown), although this does not rule out the possibility that they undergo other forms of age-related change.

Next, we screened young and old PMGs for changes in SJ component and vesicular compartment colocalization based on immunofluorescence staining, with a particular focus on early and late endosomes in accordance with our previous findings. Hrs and the SJ component Mesh increasingly colocalize in ECs in the aged PMG, as do Rab7 and the SJ component Gliotactin (Gli) (**Fig. 3-5**). If this is confirmed by quantification of colocalization, these data could indicate that the trafficking of Mesh and Gli is impacted in the early and late endosome stages, respectively. Additionally, it would suggest that

Mesh and Gli trafficking is not impacted by aging in the same way, since in young PMGs, Mesh and Gli are rarely seen colocalizing with vesicular trafficking markers in EC cytoplasm. SJ proteins such as Ssk also exhibited no change in colocalization with vesicular trafficking markers (data not shown), despite Ssk protein mislocalization to cytoplasmic puncta with age (Resnik-Docampo *et al.*, 2017). In the future, our lab will perform a screen using a *Mesh-APEX2-GFP* line to biotinylate Mesh-associated proteins in young and old fly PMGs, then identify these proteins via mass spectrometry. *Mesh-APEX2-GFP* was validated by its colocalization with anti-Mesh antibody at the SJ in young fly PMGs (**Fig. 3-S4**). If Mesh-associated proteins are different in young and old fly PMGs, especially vesicular trafficking markers, this could provide insight into how trafficking of Mesh is altered with age.

Because we observed SJ proteins appearing to localize to trafficking compartments associated with CME, we decided to test the requirement for CME and other trafficking pathways in SJ protein localization to the plasma membrane. Depletion of early endosome, late endosome, or recycling endosome markers by RNAi expression in ECs resulted in a dysplastic phenotype (**Fig. 3-6**) and disruption of normal SJ protein localization based on immunofluorescence. This indicates that CME and recycling pathways are required for SJ proteins to localize normally. However, because this experiment depleted vesicular trafficking markers from all ECs in the PMG, this would almost certainly disrupt many other processes required for homeostasis on a cellular and tissue level. This tissue-wide disruption may have also contributed to the dysplastic phenotype and SJ protein mislocalization observed. Future studies will include depleting

vesicular trafficking markers in individual ECs to assess changes in SJ protein localization while avoiding confounding effects from tissue-wide dysplasia.

Age-related mislocalization of SJ proteins may be due to slowed or stalled delivery to the SJ. Therefore, we wanted to transiently deplete Mesh protein from the SJs of ECs in young and old fly PMGs by RNAi expression, then allow Mesh protein to be recovered at the SJ. We hypothesized that ECs from old PMGs would recover less Mesh protein at the SJ than young PMGs, due to age-related defects in vesicular trafficking of Mesh. Although unquantified, it does not appear that *5966^{GS}>UAS-Mesh RNAi* expression for 5 days drastically depleted Mesh protein from the SJ (**Fig. 3-S5**). Additionally, there was no clear difference in Mesh protein level at the SJ in young and old flies following the 7 day recovery period. The failure to substantially deplete Mesh from the SJ was surprising, given that *5966^{GS}>UAS-Mesh RNAi* expression for 5 days is sufficient to cause dysplasia (data not shown). However, SJ protein turnover is slow (Oshima & Fehon, 2011) and Mesh delivery to the SJ may not have been drastically impacted. Interestingly, this suggests that even minor disruptions to the SJ can significantly disrupt homeostasis. A longer depletion time, higher RU-486 dosage, and shorter recovery time could help reveal differences in Mesh recovery at the SJ in young and old PMGs.

As well as electron microscopy studies, use of mass spectrometry, and SJ protein recovery experiments, future studies will follow up on the hypothesis that early and late endosomes are disrupted in the aged fly PMG. For example, forcing endocytosis by induced *Rab5^{CA}* expression in middle-aged or old flies could be tested to find if this rescues SJ protein mislocalization to the cytoplasm. Additionally, given the recent development of a protocol to image fly PMGs *in vivo* (Martin *et al.*, 2018), tracking

vesicular trafficking dynamics could provide fascinating insight into which compartments are affected by aging. For example, monitoring fluorescently tagged Mesh, Hrs, and Rab7 proteins could show whether Mesh successfully passes from early to late endosomes, or is stalling in early endosomes.

In summary, our lab has found that SJ proteins mislocalize with age in the *Drosophila* PMG, and hypothesized that this is due to dysfunctional vesicular trafficking of SJ proteins. While this work is broad and preliminary, we believe we have identified meaningful age-related changes in vesicular trafficking of SJ proteins in ECs, specifically in early and late endosomes. Dysfunctional vesicular trafficking may contribute to age-related intestinal barrier loss via loss of SJ integrity. Since vesicular trafficking is essential for many cellular processes in all tissue types, it will be important to screen for other processes that are disrupted by this age-related change in the PMG, as well as if age-related change in vesicular trafficking occurs in other organs in both *Drosophila* and mammals.

Acknowledgments

The Jones lab is thanked for their support and comments on experiments. Christopher Ochoa is thanked for his contributions to experiments and data analysis. This work was supported by the UCLA Cell and Molecular Biology Training Program (Ruth L. Kirschstein National Research Service Award GM007185), and the NIH: AG040288, AG028092 and DK105442 (D.L.J.).

Methods

Fly food and husbandry: Flies were cultured in vials containing standard cornmeal medium (1.1% agar, 2.9% baker's yeast, 9.2% maltose, and 7.1% cornmeal; all concentrations given in wt/vol). Propionic acid (0.5%) and TegoSept (methylparaben, Sigma, 0.16%) were added to adjust pH and prevent fungal growth, respectively. Newly eclosed adults were kept for an additional 1–2 days before inducing transcription activation by placement on food containing the steroid hormone mifepristone (RU-486; Sigma M8046) in a 25 µg/ml concentration and flipped every 2 days thereafter. All analyses for these studies were performed on female flies, as age-related gut pathology has been well established in females (Biteau *et al.*, 2008; Rera *et al.*, 2012).

Immunofluorescence: All images were taken in the P3–P4 regions of the *Drosophila* PMG, located by centering the pyloric ring in a ×40 field of view (fov) and moving 1–2 fov toward the anterior. PMGs were dissected into ice-cold PBS/4% formaldehyde and incubated for 1 h in fixative at room temperature. Samples were then washed three times, for 10 min each, in PBT (PBS containing 0.5% Triton X-100), 10 min in Na-deoxycholate (0.3%) in PBT (PBS with 0.3% Triton X-100), and incubated in block (PBT-0.5% bovine serum albumin) for 30 min at room temperature. Samples were immunostained with primary antibodies overnight at 4ºC, washed 3 × 10 min at room temperature in PBT (PBS containing 0.5% Triton X-100), incubated with secondary antibodies (1:500, Invitrogen) at room temperature for 2 h, washed 3 × 10 min with PBT and mounted in Vecta-Shield/DAPI (Vector Laboratories, H-1200). Images were acquired on a Zeiss LSM780 or LSM880 inverted confocal microscope (UCLA MCDB/BSCRC Microscopy Core), and on a Zeiss Axio Observer Z1 with Apotome 2 using the ZEN Black v.2.0 (Zeiss) software.

Images were processed with Fiji/ImageJ and Zen software. Final figures were assembled using Adobe Illustrator.

pHH3 Quantification: Quantification of mitotic events, as measured by $pHH3^{+}$ cells per gut, was performed by acquiring 4 independent images at 40X magnification per gut in the P3-P4 region. Images were taken in directly adjacent fields of view on each side of the gut. Quantification of progenitor cell number and epithelial renewal and fluorescence intensity measurements were performed as described previously (Zipper *et al.*, 2020).

Statistical Analysis: GraphPad Prism 8.0.2 was used to run statistical analysis and create graphs of quantifications. For single comparisons, data sets were analyzed by two-sided unpaired *t*-test or Mann-Whitney test. Multiple comparisons were analyzed by one-way ANOVA or Kruskal-Wallis tests. For survival analyses, Mantel-Cox log-rank test was performed. Significant differences are displayed as * for $P \leq 0.05$, ** for $P \leq 0.01$, *** for $P \leq 0.001$ and **** for $P \leq 0.0001$.

Fly stocks used:

Stock	Source	ID
5966-GAL4^{GS}	Gift from H. Jasper[1]	n/a
mex^{ts}	Phillips & Thomas, 2006	n/a
Gli::GFP	DGRC	115-332
Su(H)lacZ; esg:GFP, 5966-GAL4^{GS}	Gift from B. Ohlstein[2]	n/a
w^{1118}	Gift from L. Wang[3]	n/a
UAS-Hrs RNAi (TRiP.HMS00841 attP2)	Bloomington	33900
UAS-Rab5 RNAi (TRiP.JF03335 attP2)	Bloomington	30518
y, v; Rab7-RNAi (TRiP.JF02377)	Bloomington	27051
y v; Rab11-RNAi (TRiP.JF02812)	Bloomington	27730
y,w; UAS-YFP.Rab7.T22N (DN)	Bloomington	9778
UAS-Atg1[GD7149]	VDRC	16133
UAS-Atg8a RNAi [GD4654]	VDRC	43097
ptc-GAL4	Bloomington	65661
UAS-Mesh-APEX-GFP/Cyo	V. Sauer[4]	n/a
Rab11-YFP	Bloomington	62599
Rab35-YFP	Bloomington	62559
Rab5-YFP	Bloomington	62543
RabX4-EYFP	Bloomington	62563
y,w; Rab4-YFP	Bloomington	62542
Rab7-YFP	Bloomington	42705
UAS-Ref(2)p-GFP/(Cyo)	Chang *et al*., 2009	n/a
UAS-GFP:LAMP/Cyo	Pulipparacharuvil *et al*., 2005	n/a

Table 3-1: List of antibodies used.

[1]Genentech and Buck Institute for Research on Aging, USA; [2]UT Southwestern Medical Center, USA; [3]UCLA, USA; [4]UCLA, USA.

Antibodies used:

Antibody	Manufacturer	Catalog #	Species	Clonality	Dilution
Anti-Armadillo	DSHB	N2 7A1	Mouse	Monoclonal	1:20
Anti-Atg8a	Gift from D. Walker[1]	n/a	Rabbit	Polyclonal	1:125
Anti-Discs large	DSHB	4F3	Mouse	Monoclonal	1:250
Anti-GABARAP	Abcam	ab109364	Rabbit	Monoclonal	1:200
Anti-GFP	Aves Labs	GFP-1010	Chicken	Polyclonal	1:500
Anti-GFP	Molecular Probes	A-11122	Rabbit	Polyclonal	1:3000
Anti-Hrs	DSHB	27-4	Mouse	Monoclonal	1:10
Anti-Mesh	Gift from M. Furuse[2]	n/a	Rabbit	Polyclonal	1:1000
Anti-pHH3	Millipore	06-570	Rabbit	Polyclonal	1:200
Anti-Rab5	Abcam	ab31261	Rabbit	Polyclonal	1:100
Anti-Rab7	DSHB	n/a	Mouse	Monoclonal	1:50
Anti-Rab11	Gift from M. Gaitan[3]	n/a	Rabbit	Polyclonal	1:50
Anti-Ref(2)p	Abcam	ab178440	Rabbit	Polyclonal	1:250
Anti-Snakeskin	Gift from M. Furuse[2]	n/a	Rabbit	Polyclonal	1:1000
Anti-Tsp2A	Gift from M. Furuse[2]	n/a	Rabbit	Polyclonal	1:1500
Anti-Chicken Alexa488	Invitrogen	A-11039	Goat	Polyclonal	1:500
Anti-Rabbit Alexa488	Invitrogen	A-11008	Goat	Polyclonal	1:500
Anti-Mouse Alexa568	Invitrogen	A-11004	Goat	Polyclonal	1:500
Anti-Rabbit Alexa568	Invitrogen	A-11011	Goat	Polyclonal	1:500
Anti-Rabbit Alexa647	Invitrogen	A-31573	Donkey	Polyclonal	1:500

Table 3-2: List of antibodies used.

[1]UCLA, USA; [2]National Institute for Physiological Sciences, Japan; [3]University of Geneva, Switzerland.

Supplemental information

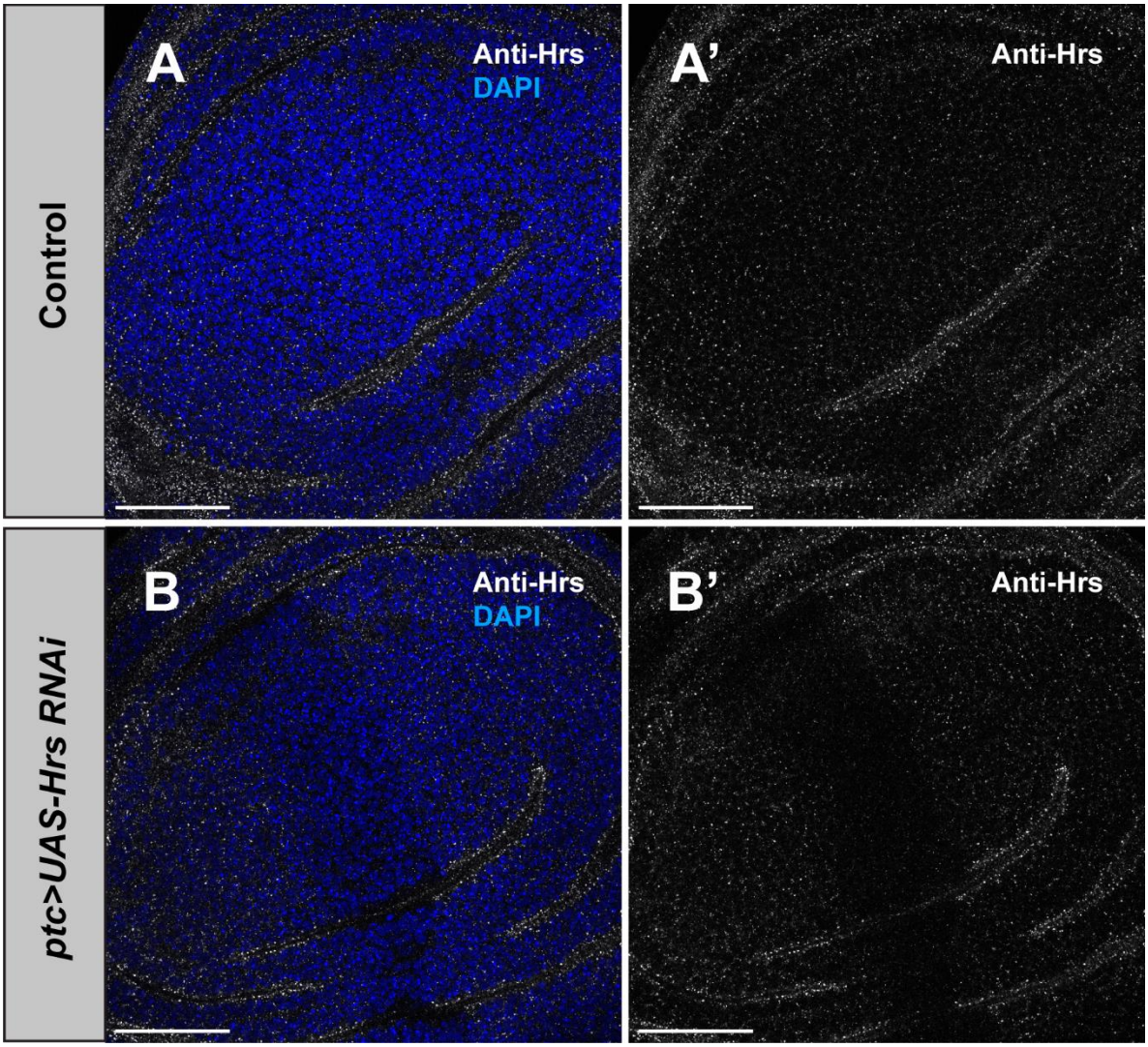

Figure 3-S1: Validation of *UAS-Hrs RNAi* line and anti-Hrs antibody. Expression of *ptc-GAL4>UAS-Hrs RNAi* decreases anti-Hrs antibody staining in the third instar wing disc (n = 8) (**B**) compared with control (n = 11) (**A**). Scale bars, 50 µm.

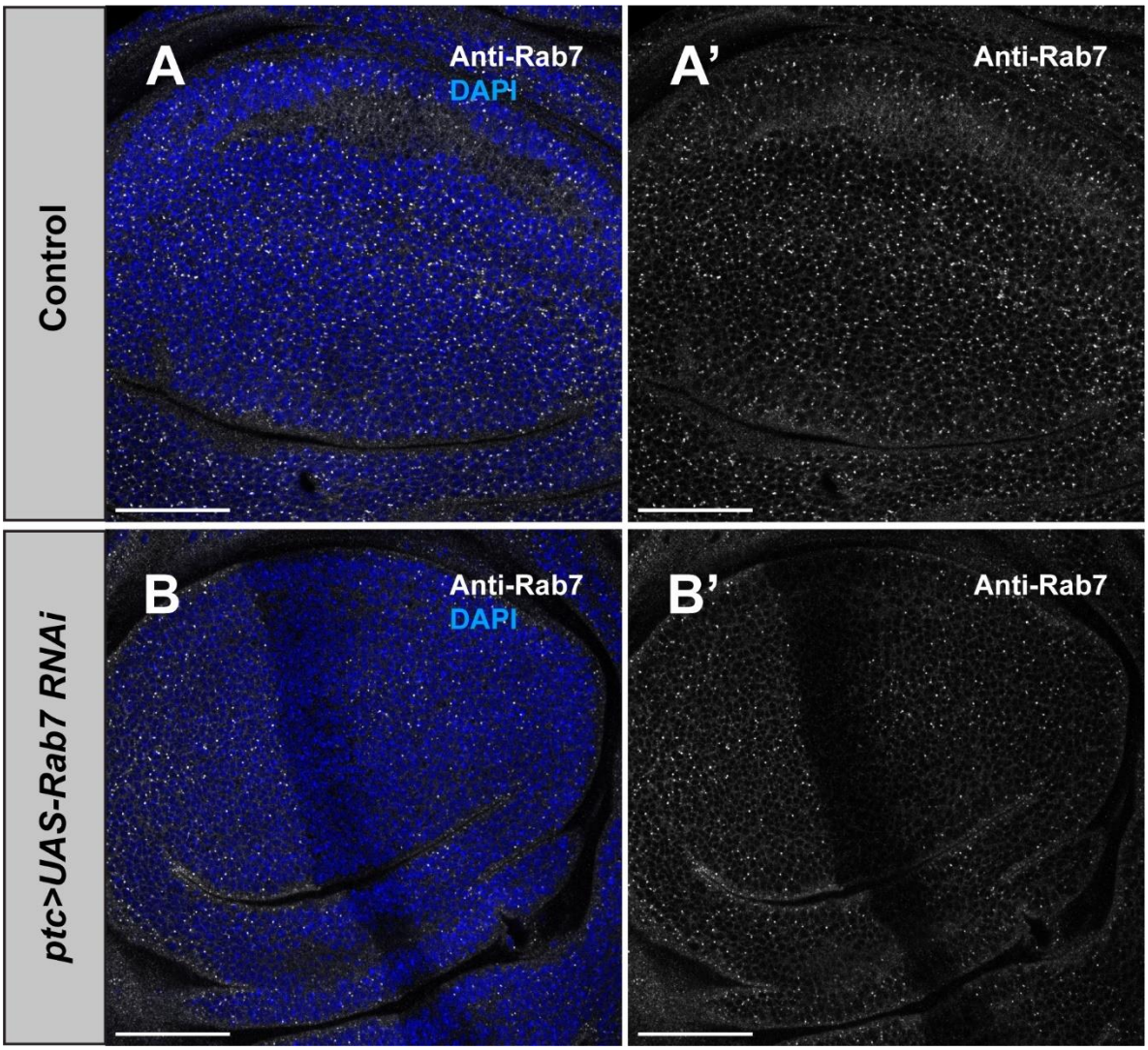

Figure 3-S2: Validation of *UAS-Rab7 RNAi* line and anti-Rab7 antibody. Expression of *ptc-GAL4>UAS-Rab7 RNAi* decreases anti-Rab7 antibody staining in the third instar wing disc (n = 9) (**B**) compared with control (n = 10) (**A**). Scale bars, 50 µm.

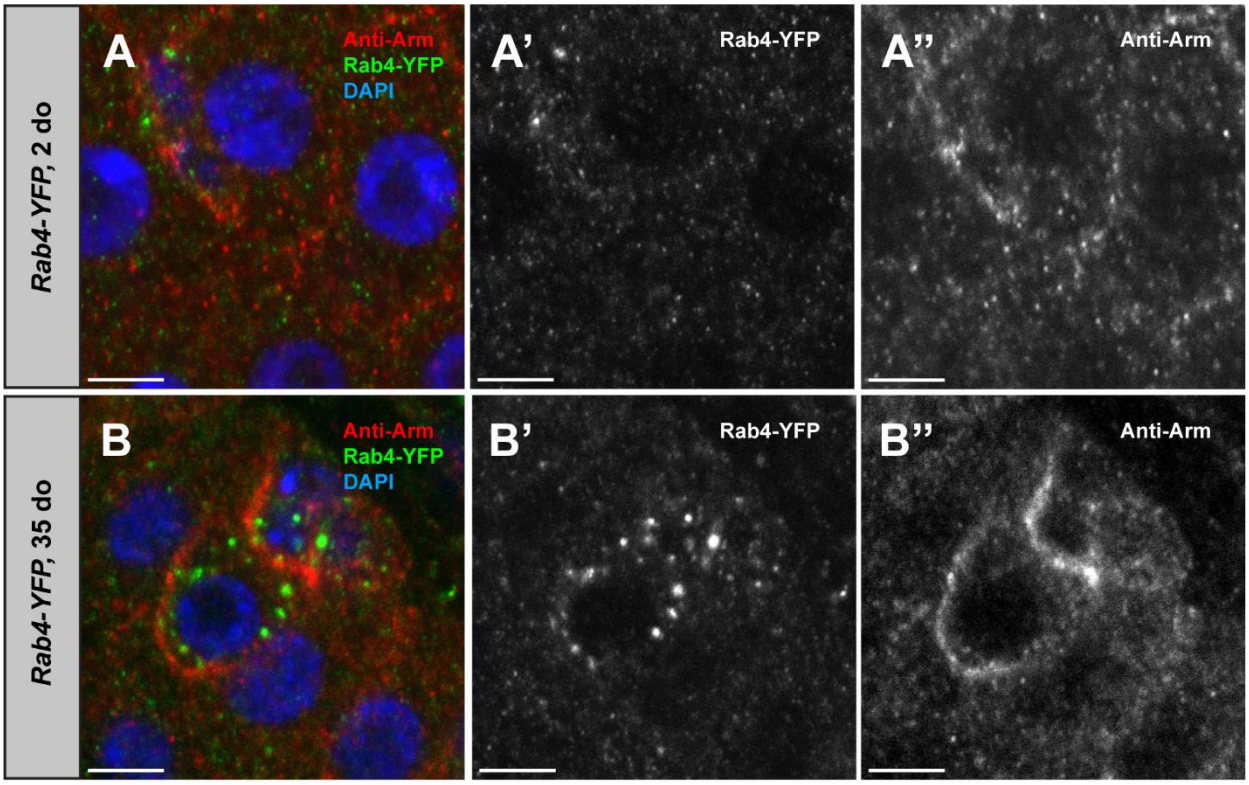

Figure 3-S3: Rab4+ vesicles appear to increase in size and number in different cell types in the aged fly PMG. (**A**) In young (2 do) fly PMGs, Rab4+ vesicles appear to be uniformly distributed in ECs, and slightly larger in size in diploid cells (upper left) (n = 7). (**B**) In aged (35 do) fly PMGs, Rab4+ vesicles appear to increase in size (n = 7). Additionally, these larger Rab4+ vesicles seem to be present in both diploid and polyploid cells. Scale bars, 5 µm.

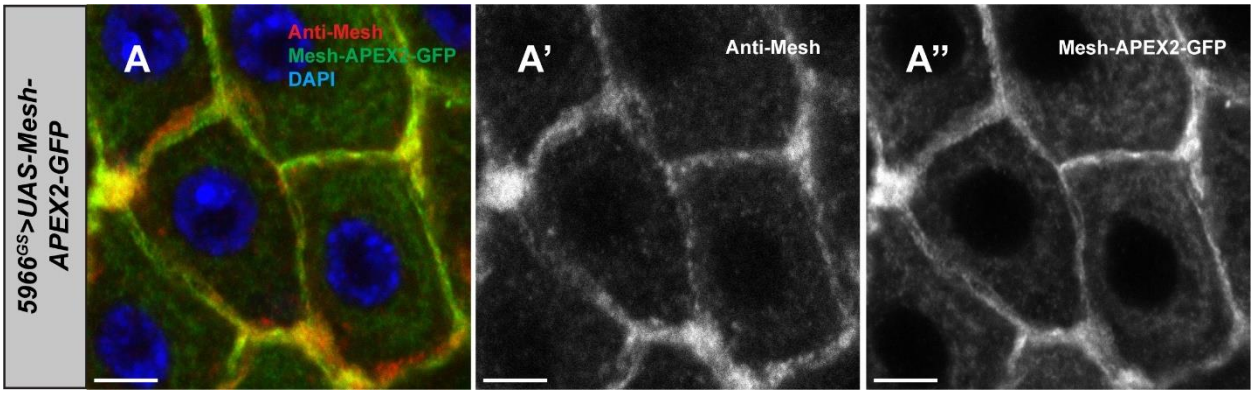

Figure 3-S4: Validation of the Mesh-APEX2-GFP tool for identification of Mesh-associated proteins. Induced expression of *5966^{GS}>Mesh-APEX2-GFP* produces Mesh-APEX2-GFP protein (green) which localizes to the SJs of ECs and colocalizes with anti-Mesh antibody (red) (n = 3) (**A**). Scale bars, 5 µm.

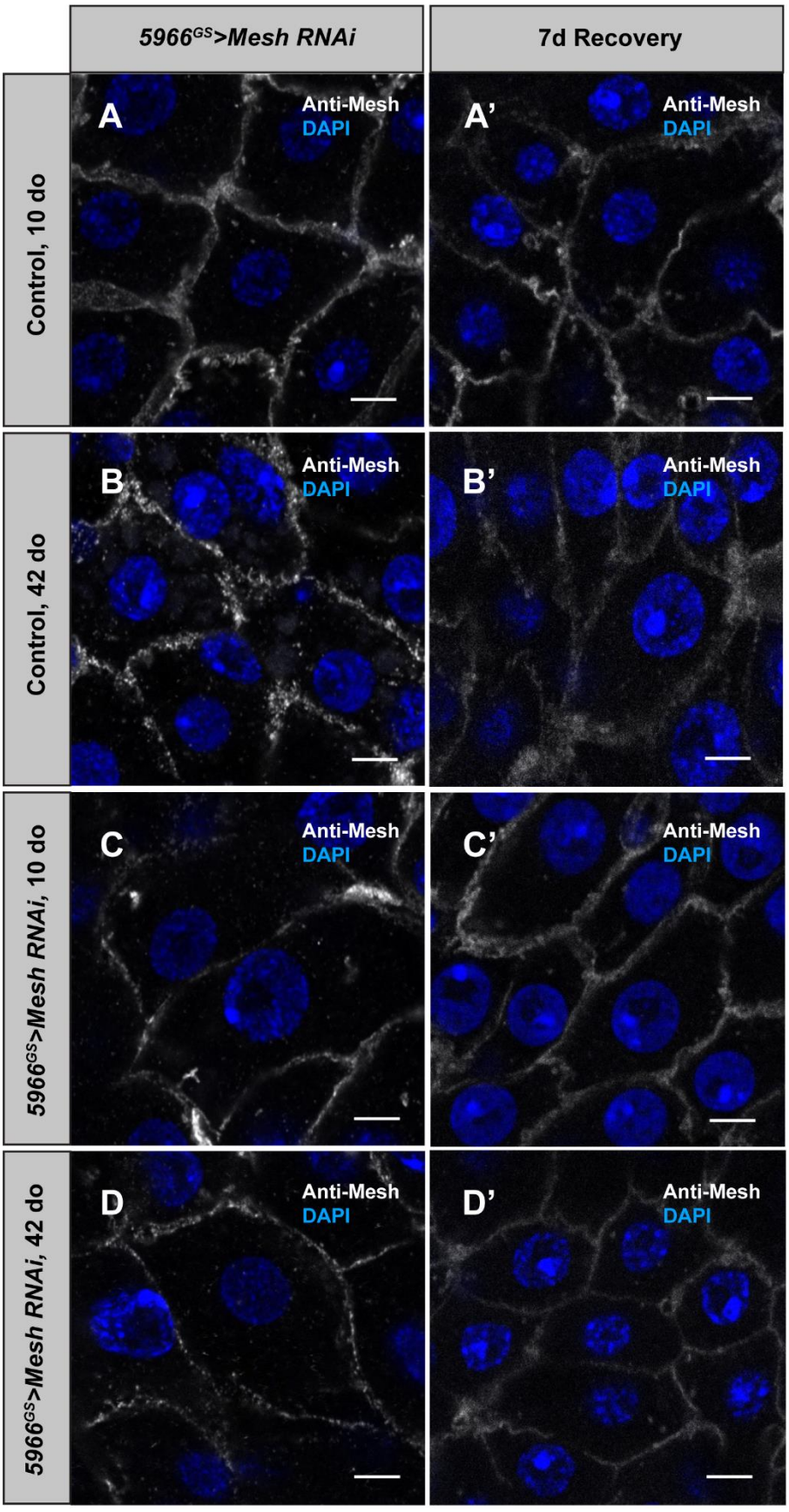
5966GS>Mesh RNAi
7d Recovery
Control, 10 do
Control, 42 do
5966GS>Mesh RNAi, 10 do
5966GS>Mesh RNAi, 42 do
A
A'
B
B'
C
C'
D
D'
Anti-Mesh
DAPI

Figure 3-S5: Recovery of Mesh protein at the EC sSJ following RNAi depletion of Mesh in young and old fly PMGs. Mesh protein was depleted from ECs using *5966^{GS}>UAS-Mesh RNAi* expression induced for 5 days in young (2 do) (n = 7) (**C**) and old (40 do) (n = 7) (**D**) flies. Flies were then allowed to recover for 7 days (**C',** n = 10; **D',** n = 11). Based on immunofluorescence, no significant difference in Mesh recovery was observed in young and old flies, or compared with young (**A,** n = 5, **A'**, n = 11) and old (**B,** n = 5, **B'**, n = 12) outcrossed controls. Scale bars, 5 µm.

Chapter 4: Conclusion

Across multiple species, intestinal barrier function declines with age or inflammatory bowel disease. This has potentially significant implications for systemic aging and gastrointestinal disease. While multiple factors contribute to intestinal barrier function, such as the microbiome, occluding junctions appear to play an especially important role. Occluding junctions, referred to as tight junctions (TJs) in mammals and septate junctions (SJs) in arthropods, regulate passive paracellular transport of water, ions, and nutrients across the intestinal epithelium.

Our lab became focused on SJs in *Drosophila* upon finding that SJs in enterocytes (ECs) of aged fly posterior midguts (PMGs), analogous to the mammalian small intestine, appear to lose physical integrity with age (Resnik-Docampo *et al.*, 2017). A similar discovery was made in aged rat small intestine TJs (Ren *et al.*, 2014), suggesting that this age-related decline occurs across species. We hypothesized that age-related decline of occluding junctions contributes to intestinal barrier decline in *Drosophila.* If this phenotype is also present in humans, intestinal TJs could become a significant therapeutic target in aging and gastrointestinal disease.

Because SJ proteins appear to mislocalize in the aged fly PMG (Resnik-Docampo *et al.*, 2017), our lab decided to investigate the requirement of specific SJ proteins for maintenance of intestinal homeostasis. We reasoned that if SJ proteins are required at the SJ to maintain intestinal homeostasis, their age-related mislocalization could be contributing to the overall aging phenotype. We concentrated our efforts on a specific region of the occluding junction known as the tricellular junction (TCJ). TCJs are found where three adjacent cells meet, and have unique proteins not found in the bicellular junction (BCJ). The first-discovered tricellular septate junction (tSJ) protein, Gliotactin

(Gli), was found to be required in ECs at the tSJ to maintain intestinal homeostasis. Additionally, Gli mislocalizes from the tSJ with age, which may contribute to age-related phenotypes in the fly PMG (Resnik-Docampo *et al.*, 2017).

Given that Gli depletion from the SJ produces a robust phenotype despite the tSJ being a relatively small portion of the SJ, we decided to investigate the requirement of another tSJ protein in the maintenance of intestinal homeostasis. Bark beetle (Bark) was the second-discovered tSJ protein in *Drosophila*, and is hypothesized to form a trimer that creates a diaphragm-like structure in the TCJ canal (Byri *et al.*, 2015; Hildebrandt *et al.*, 2015). Bark is also required for Gli to be recruited to the tSJ in the embryonic epithelium (Byri *et al.*, 2015). We decided to investigate the role of Bark in the maintenance of intestinal homeostasis, as well as its relationship to Gli in the adult PMG.

Chapter 2 of this manuscript demonstrates that Bark is required in tSJs in ECs to maintain intestinal barrier function in *Drosophila*. Upon depletion of Bark from ECs in young fly PMGs, intestinal homeostasis is disrupted: intestinal stem cell (ISC) proliferation increases, intestinal barrier function is severely compromised, and total lifespan is shortened. Our collaborators also demonstrated that Bark is similarly required in progenitor enteroblast (EB) cells in the PMG to maintain intestinal homeostasis. Like Gli, Bark mislocalizes from the tSJ in the aged PMG. Overexpression of *bark* across the adult lifetime fails to rescue aging phenotypes, and *bark* overexpression in young flies appears to disrupt ISC homeostasis. Paired with our lab's previous RNAseq data indicating *bark* transcription is upregulated with age (Resnik-Docampo *et al.*, 2017), this suggests that rescuing age-related SJ protein mislocalization will require a different technique.

Additionally, we investigated the relationship between Gli and Bark in the adult fly PMG. Since both play a key role in the maintenance of intestinal homeostasis and mislocalize with age, understanding their relationship could provide valuable insight into why they mislocalize with age. We found that unlike in the embryonic epithelium, Gli and Bark appear mutually dependent on one another to be recruited to the tSJ. Gli and Bark were also found to have a similar relationship in the pupal notum (de Bournonville & Le Borgne, 2020). While these differing findings in the pupal notum, PMG and embryonic epithelium could be experimental artifacts, there may be key differences in SJs in different tissue types or life stages that could be interesting to investigate in the future.

Given our finding that SJ proteins are required to maintain homeostasis in the PMG, it was apparent that the cause of SJ protein mislocalization with age in the PMG should be identified to begin finding a way to slow or reverse this process in *Drosophila*. In Chapter 3 of this manuscript, we found that antibody staining for Hrs, an early endosome marker, and Rab7, a late endosome marker, is altered in aged PMGs. Both early and late endosomes appear to be enlarged or aggregated, suggesting these stages of clathrin-mediated endocytosis have become disrupted with age. Additionally, anti-Hrs antibody staining and anti-Mesh antibody staining appear to increasingly colocalize in the aged PMG, as do anti-Rab7 antibody staining and Gli-GFP staining. This could indicate that trafficking of Mesh and Gli has been impacted in the early and late endosome stages, respectively. We also found that depletion of endocytosis and recycling markers by induced RNAi expression appears to cause SJ protein mislocalization, although this could be due to tissue-wide endocytosis knockdown causing a dysplastic phenotype.

While much of our work characterizing changes in vesicular trafficking in the aged PMG is preliminary, our findings combined with evidence from other groups indicate that this field of study has significant potential to impact our understanding of a key basic cellular process may be altered by an individual's age. If the specific ways SJ protein trafficking is altered in the aged PMG can be found – for example, if Mesh trafficking stalls in early endosomes, and a similar phenotype is found in humans – therapeutics could be developed that restore early endosome function. Our findings in the *Drosophila* PMG can also be used as a starting point to search for changes in SJ protein localization and vesicular trafficking in the mammalian small intestine. Additionally, given previous work which indicates age-related changes in vesicular trafficking in the human brain (Alsaqati *et al.*, 2018; Cataldo *et al.*, 2000), it seems likely that age-related changes in vesicular trafficking occur in other organs in both *Drosophila* and humans.

In summary, we have demonstrated that SJ proteins in the *Drosophila* PMG must be present at the SJ to maintain intestinal homeostasis. In particular, the tricellular septate junction protein Bark beetle is required in enterocytes and enteroblasts to maintain ISC homeostasis, maintain intestinal barrier function, and have a normal lifespan. Because Bark beetle mislocalizes with age in the PMG, this may contribute to the overall PMG aging phenotype. We have previously hypothesized that age-related mislocalization of Bark and other SJ proteins in the PMG is due to dysfunctional vesicular trafficking, and we now have preliminary evidence that early and late endosomes are altered with age in the PMG. Our studies will provide insight into the relationship between occluding junctions, gastrointestinal disease, and aging.

References

Alemu E.A., Lamark T., Torgersen K.M., Birgisdottir A.B., Larsen K.B., Jain A., Olsvik H., Øvervatn A., Kirkin V. & Johansen T. (2012) ATG8 family proteins act as scaffolds for assembly of the ULK complex: Sequence requirements for LC3-interacting region (LIR) motifs. *Journal of Biological Chemistry* 287: 39275–39290

Alsaqati M., Thomas R.S. & Kidd E.J. (2018) Proteins Involved in Endocytosis Are Upregulated by Ageing in the Normal Human Brain: Implications for the Development of Alzheimer's Disease. *The Journals of Gerontology: Series A* 73: 289–298

Antonello Z.A., Reiff T., Ballesta-Illan E. & Dominguez M. (2015) Robust intestinal homeostasis relies on cellular plasticity in enteroblasts mediated by miR-8–Escargot switch. *EMBO J* 34: 2025–2041

Apidianakis Y. & Rahme L.G. (2011) *Drosophila* melanogaster as a model for human intestinal infection and pathology. *Dis Model Mech* 4: 21

Bagnat M., Cheung I.D., Mostov K.E. & Stainier D.Y.R. (2007) Genetic control of single lumen formation in the zebrafish gut. *Nature Cell Biology 2007 9:8* 9: 954–960

Bilder D., Li M. & Perrimon N. (2000) Cooperative Regulation of Cell Polarity and Growth by *Drosophila* Tumor Suppressors. *Science (1979)* 289: 113–116

Biteau B., Hochmuth C.E. & Jasper H. (2008) JNK Activity in Somatic Stem Cells Causes Loss of Tissue Homeostasis in the Aging *Drosophila* Gut. *Cell Stem Cell* 3: 442–455

Biteau B., Karpac J., Supoyo S., DeGennaro M., Lehmann R. & Jasper H. (2010) Lifespan Extension by Preserving Proliferative Homeostasis in *Drosophila*. *PLoS Genet* 6: e1001159

Brand A.H. & Perrimon N. (1993) Targeted gene expression as a means of altering cell fates and generating dominant phenotypes. *Development* 118: 401–415

Bucci C., Parton R.G., Mather I.H., Stunnenberg H., Simons K., Hoflack B. & Zerial M. (1992) The small GTPase rab5 functions as a regulatory factor in the early endocytic pathway. *Cell* 70: 715–728

Byri S., Misra T., Syed Z.A., Bätz T., Shah J., Boril L., Glashauser J., Aegerter-Wilmsen T., Matzat T., Moussian B., *et al.* (2015) The Triple-Repeat Protein Anakonda Controls Epithelial Tricellular Junction Formation in *Drosophila*. *Dev Cell* 33: 535–548

Cataldo A.M., Peterhoff C.M., Troncoso J.C., Gomez-Isla T., Hyman B.T. & Nixon R.A. (2000) Endocytic Pathway Abnormalities Precede Amyloid β Deposition in Sporadic Alzheimer's Disease and Down Syndrome: Differential Effects of APOE Genotype and Presenilin Mutations. *Am J Pathol* 157: 277–286

Chang Y-Y. & Neufeld T.P. (2009) An Atg1/Atg13 Complex with Multiple Roles in TOR-mediated Autophagy Regulation. *Mol Biol Cell* 20: 2004–2014

Choi N.H., Lucchetta E. & Ohlstein B. (2011) Nonautonomous regulation of *Drosophila* midgut stem cell proliferation by the insulin-signaling pathway. *Proc Natl Acad Sci USA* 108: 18702–18707

Choi Y.J., Hwang M.S., Park J.S., Bae S.K., Kim Y.S., Yoo M.A. (2008) Age-related upregulation of *Drosophila* caudal gene via NF-kappaB in the adult posterior midgut. *Biochim Biophys Acta* 1780: 1093–1100

Clark R.I., Salazar A., Yamada R., Fitz-Gibbon S., Morselli M., Alcaraz J., Rana A., Rera M., Pellegrini M., Ja W.W., *et al.* (2015) Distinct Shifts in Microbiota Composition during *Drosophila* Aging Impair Intestinal Function and Drive Mortality. *Cell Rep* 12: 1656–67

Condette C.J., Khorsi-Cauet H., Morlière P., Zabijak L., Reygner J., Bach V. & Gay-Quéheillard J. (2014) Increased Gut Permeability and Bacterial Translocation after Chronic Chlorpyrifos Exposure in Rats. *PLoS One* 9: e102217

Dutta D., Dobson A.J., Houtz P.L., Gläßer C., Revah J., Korzelius J., Patel P.H., Edgar B.A. & Buchon N. (2015) Regional Cell-Specific Transcriptome Mapping Reveals Regulatory Complexity in the Adult *Drosophila* Midgut. *Cell Rep* 12: 346–358

Esmangart de Bournonville T. & le Borgne R. (2020) Interplay between Anakonda, Gliotactin, and M6 for Tricellular Junction Assembly and Anchoring of Septate Junctions in *Drosophila* Epithelium. *Current Biology* 30: 4245-4253.e4

Furriols M. & Bray S. (2000) Dissecting the Mechanisms of Suppressor of Hairless Function. *Dev Biol* 227: 520–532

Furuse M. & Tsukita S. (2006) Claudins in occluding junctions of humans and flies. *Trends Cell Biol* 16: 181–188

Guo L., Karpac J., Tran S.L. & Jasper H. (2014) PGRP-SC2 Promotes Gut Immune Homeostasis to Limit Commensal Dysbiosis and Extend Lifespan. *Cell* 156: 109–122

Hildebrandt A., Pflanz R., Behr M., Tarp T., Riedel D. & Schuh R. (2015) Bark beetle controls epithelial morphogenesis by septate junction maturation in *Drosophila*. *Dev Biol* 400: 237–247

Hung R.J., Li J.S.S., Liu Y. & Perrimon N. (2021) Defining cell types and lineage in the *Drosophila* midgut using single cell transcriptomics. *Curr Opin Insect Sci* 47: 12–17

Izumi Y., Furuse K. & Furuse M. (2019) Septate junctions regulate gut homeostasis through regulation of stem cell proliferation and enterocyte behavior in *Drosophila*. *J Cell Sci*: jcs.232108

Izumi Y., Yanagihashi Y. & Furuse M. (2012) A novel protein complex, Mesh-Ssk, is required for septate junction formation in the *Drosophila* midgut. *J Cell Sci* 125: 4923–33

Jiang H. & Edgar B.A. (2009) EGFR signaling regulates the proliferation of *Drosophila* adult midgut progenitors. *Development* 136: 483–493

Jiang H., Patel P.H., Kohlmaier A., Grenley M.O., McEwen D.G. & Edgar B.A. (2009) Cytokine/Jak/Stat signaling mediates regeneration and homeostasis in the *Drosophila* midgut. *Cell* 137: 1343

Kannan K., Stewart R.M., Bounds W., Carlsson S.R., Fukuda M., Betzing K.W. & Holcombe R.F. (1996) Lysosome-Associated Membrane Proteins h-LAMP1 (CD107a) and h-LAMP2 (CD107b) Are Activation-Dependent Cell Surface Glycoproteins in Human Peripheral Blood Mononuclear Cells Which Mediate Cell Adhesion to Vascular Endothelium. *Cell Immunol* 171: 10–19

Kapahi P., Kaeberlein M. & Hansen M. (2017) Dietary restriction and lifespan: Lessons from invertebrate models. *Ageing Res Rev* 39: 3–14

Kirkwood T.B.L. (2004) Intrinsic ageing of gut epithelial stem cells. *Mech Ageing Dev* 125: 911–915

Korzelius J., Azami S., Ronnen-Oron T., Koch P., Baldauf M., Meier E., Rodriguez-Fernandez I.A., Groth M., Sousa-Victor P. & Jasper H. (2019) The WT1-like transcription factor Klumpfuss maintains lineage commitment of enterocyte progenitors in the *Drosophila* intestine. *Nature Communications 2019 10:1* 10: 1–13

Kouranti I., Sachse M., Arouche N., Goud B. & Echard A. (2006) Rab35 Regulates an Endocytic Recycling Pathway Essential for the Terminal Steps of Cytokinesis. *Current Biology* 16: 1719–1725

Lane N.J. & Skaer H. (1980) Intercellular Junctions in Insect Tissues. In pp 35–213.

Li H. & Jasper H. (2016) Gastrointestinal stem cells in health and disease: from flies to humans. *Dis Model Mech* 9: 487–99

Lloyd T.E., Atkinson R., Wu M.N., Zhou Y., Pennetta G. & Bellen H.J. (2002) Hrs Regulates Endosome Membrane Invagination and Tyrosine Kinase Receptor Signaling in *Drosophila*. *Cell* 108: 261–269

MacMillan H.A., Yerushalmi G.Y., Jonusaite S., Kelly S.P. & Donini A. (2017) Thermal acclimation mitigates cold-induced paracellular leak from the *Drosophila* gut. *Scientific Reports 2017 7:1* 7: 1–11

Marchiando A.M., Graham W.V. & Turner J.R. (2010) Epithelial Barriers in Homeostasis and Disease. *Annual Review of Pathology: Mechanisms of Disease* 5: 119–144

Mariano C., Sasaki H., Brites D. & Brito M.A. (2011) A look at tricellulin and its role in tight junction formation and maintenance. *Eur J Cell Biol* 90: 787–796

Martin J.L., Sanders E.N., Moreno-Roman P., Jaramillo Koyama L.A., Balachandra S., Du X. & O'Brien L.E. (2018) Long-term live imaging of the *Drosophila* adult midgut reveals real-time dynamics of division, differentiation and loss. *Elife* 7

Martín-Blanco E., Gampel A., Ring J., Virdee K., Kirov N., Tolkovsky A.M. & Martinez-Arias A. (1998) puckered encodes a phosphatase that mediates a feedback loop regulating JNK activity during dorsal closure in *Drosophila*. *Genes Dev* 12: 557

Martins R.R., McCracken A.W., Simons M.J.P., Henriques C.M. & Rera M. (2018) How to Catch a Smurf? - Ageing and Beyond… In vivo Assessment of Intestinal Permeability in Multiple Model Organisms. *Bio Protoc* 8

Micchelli C.A. & Perrimon N. (2006) Evidence that stem cells reside in the adult *Drosophila* midgut epithelium. *Nature* 439: 475–479

Michielan A. & D'Incà R. (2015) Intestinal Permeability in Inflammatory Bowel Disease: Pathogenesis, Clinical Evaluation, and Therapy of Leaky Gut. *Mediators Inflamm* 2015

Mu Q., Kirby J., Reilly C.M. & Luo X.M. (2017) Leaky Gut As a Danger Signal for Autoimmune Diseases. *Front Immunol* 8: 598

Mullin J.M., Valenzano M.C., Verrecchio J.J. & Kothari R. (2002) Age- and diet-related increase in transepithelial colon permeability of Fischer 344 rats. *Dig Dis Sci* 47: 2262–2270

Nezis I.P., Simonsen A., Sagona A.P., Finley K., Gaumer S., Contamine D., Rusten T.E., Stenmark H. & Brech A. (2008) Ref(2)P, the *Drosophila* melanogaster homologue of mammalian p62, is required for the formation of protein aggregates in adult brain. *J Cell Biol* 180: 1065–1071

Nie Y., Yu S., Li Q., Nirala N.K., Amcheslavsky A., Edwards Y.J.K., Shum P.W., Jiang Z., Wang W., Zhang B., *et al.* (2019) Oncogenic pathways and loss of the Rab11 GTPase synergize to alter metabolism in *Drosophila*. *Genetics* 212: 1227–1239

Odenwald M.A. & Turner J.R. (2017) The intestinal epithelial barrier: a therapeutic target? *Nat Rev Gastroenterol Hepatol* 14: 9–21

Ohlstein B. & Spradling A. (2005) The adult *Drosophila* posterior midgut is maintained by pluripotent stem cells. *Nature 2005 439:7075* 439: 470–474

Ohlstein B. & Spradling A. (2007) Multipotent *Drosophila* intestinal stem cells specify daughter cell fates by differential Notch signaling. *Science* 315: 988–992

Oshima K. & Fehon R.G. (2011) Analysis of protein dynamics within the septate junction reveals a highly stable core protein complex that does not include the basolateral polarity protein Discs large. *J Cell Sci* 124: 2861–2871

Osterwalder T., Yoon K.S., White B.H. & Keshishian H. (2001) A conditional tissue-specific transgene expression system using inducible GAL4. *Proc Natl Acad Sci U S A* 98: 12596–601

Padash-Barmchi M., Browne K., Sturgeon K., Jusiak B. & Auld V.J. (2010) Control of Gliotactin localization and levels by tyrosine phosphorylation and endocytosis is necessary for survival of polarized epithelia. *J Cell Sci* 123: 4052–62

Park J., Kim Y. & Yoo M. (2009) The role of p38b MAPK in age-related modulation of intestinal stem cell proliferation and differentiation in *Drosophila*. *Aging* 1: 637

Phillips M.D. & Thomas G.H. (2006) Brush border spectrin is required for early endosome recycling in *Drosophila*. *J Cell Sci* 119: 1361–1370

Pulipparacharuvil S., Akbar M.A., Ray S., Sevrioukov E.A., Haberman A.S., Rohrer J. & Krämer H. (2005) *Drosophila* Vps16A is required for trafficking to lysosomes and biogenesis of pigment granules. *J Cell Sci* 118: 3663–3673

Reiff T., Antonello Z.A., Ballesta-Illán E., Mira L., Sala S., Navarro M., Martinez L.M. & Dominguez M. (2019) Notch and EGFR regulate apoptosis in progenitor cells to ensure gut homeostasis in *Drosophila*. *EMBO J* 38: e101346

Ren W., Wu K., Li X., Luo M., Liu H., Zhang S. & Hu Y. (2014) Age-related changes in small intestinal mucosa epithelium architecture and epithelial tight junction in rat models. *Aging Clin Exp Res* 26: 183–191

Rera M., Bahadorani S., Cho J., Koehler C.L., Ulgherait M., Hur J.H., Ansari W.S., Lo T., Jones D.L. & Walker D.W. (2011) Modulation of Longevity and Tissue Homeostasis by the *Drosophila* PGC-1 Homolog. *Cell Metab* 14: 623–634

Rera M., Clark R.I. & Walker D.W. (2012) Intestinal barrier dysfunction links metabolic and inflammatory markers of aging to death in *Drosophila*. *Proceedings of the National Academy of Sciences* 109: 21528–21533

Resende L.P.F., Truong M.E., Gomez A. & Jones D.L. (2017) Intestinal stem cell ablation reveals differential requirements for survival in response to chemical challenge. *Dev Biol* 424: 10–17

Resnik-Docampo M., Koehler C.L., Clark R.I., Schinaman J.M., Sauer V., Wong D.M., Lewis S., D'Alterio C., Walker D.W. & Jones D.L. (2017) Tricellular junctions regulate intestinal stem cell behaviour to maintain homeostasis. *Nat Cell Biol* 19: 52–59

Resnik-Docampo M., Sauer V., Schinaman J.M., Clark R.I., Walker D.W. & Jones D.L. (2018) Keeping it tight: The relationship between bacterial dysbiosis, septate junctions, and the intestinal barrier in *Drosophila*. *Fly (Austin)* 12: 34–40

Riedel F., Gillingham A.K., Rosa-Ferreira C., Galindo A. & Munro S. (2016) An antibody toolkit for the study of membrane traffic in *Drosophila* melanogaster. *Biol Open*: bio.018937

Salazar A.M., Resnik-Docampo M., Ulgherait M., Clark R.I., Shirasu-Hiza M., Jones D.L. & Walker D.W. (2018) Intestinal Snakeskin Limits Microbial Dysbiosis during Aging and Promotes Longevity. *iScience* 9: 229–243

Sarov M., Barz C., Jambor H., Hein M.Y., Schmied C., Suchold D., Stender B., Janosch S., Vinay Vikas K.J., Krishnan R.T., *et al.* (2016) A genome-wide resource for the analysis of protein localisation in *Drosophila*. *Elife* 5

Schiffrin E.J., Morley J.E., Donnet-Hughes A. & Guigoz Y. (2010) The inflammatory status of the elderly: The intestinal contribution. *Mutation Research/Fundamental and Molecular Mechanisms of Mutagenesis* 690: 50–56

Schuppan D., Junker Y. & Barisani D. (2009) Celiac Disease: From Pathogenesis to Novel Therapies. *Gastroenterology* 137: 1912–1933

Shen L., Weber C.R. & Turner J.R. (2008) The tight junction protein complex undergoes rapid and continuous molecular remodeling at steady state. *Journal of Cell Biology* 181: 683–695

Simon-Santamaria J., Malovic I., Warren A., Oteiza A., le Couteur D., Smedsrød B., McCourt P. & Sørensen K.K. (2010) Age-Related Changes in Scavenger Receptor–Mediated Endocytosis in Rat Liver Sinusoidal Endothelial Cells. *The Journals of Gerontology: Series A* 65A: 951–960

Sorvina A., Shandala T., Brooks D. (2016) *Drosophila* Pkaap regulates Rab4/Rab11-dependent traffic and Rab11 exocytosis of innate immune cargo. *Biol Open* 5 (6): 678–688.

Sugawara T., Furuse K., Otani T., Wakayama T. & Furuse M. (2021) Angulin-1 seals tricellular contacts independently of tricellulin and claudins. *Journal of Cell Biology* 220

Tepass U. & Hartenstein V. (1994) The Development of Cellular Junctions in the *Drosophila* Embryo. *Dev Biol* 161: 563–596

Tiklová K., Senti K.A., Wang S., Gräslund A. & Samakovlis C. (2010) Epithelial septate junction assembly relies on melanotransferrin iron binding and endocytosis in *Drosophila*. *Nat Cell Biol* 12: 1071–1077

Tran L. & Greenwood-Van Meerveld B. (2013) Age-Associated Remodeling of the Intestinal Epithelial Barrier. *J Gerontol A Biol Sci Med Sci* 68: 1045

Ullrich O., Reinsch S., Urbe S., Zerial M. & Parton R. (1996) Rab11 regulates recycling through the pericentriolar recycling endosome. *J Cell Biol* 135: 913–924

Vanlandingham P.A. & Ceresa B.P. (2009) Rab7 regulates late endocytic trafficking downstream of multivesicular body biogenesis and cargo sequestration. *J Biol Chem* 284: 12110–24

Weindruch R., Walford R.L., Fligiel S. & Guthrie D. (1986) The Retardation of Aging in Mice by Dietary Restriction: Longevity, Cancer, Immunity and Lifetime Energy Intake. *J Nutr* 116: 641–654

Willott E., Balda M.S., Fanning A.S., Jameson B., van Itallie C. & Anderson J.M. (1993) The tight junction protein ZO-1 is homologous to the *Drosophila* discs-large tumor suppressor protein of septate junctions. *Proc Natl Acad Sci U S A* 90: 7834

Wittek A., Hollmann M., Schleutker R. & Luschnig S. (2020) The Transmembrane Proteins M6 and Anakonda Cooperate to Initiate Tricellular Junction Assembly in Epithelia of *Drosophila*. *Current Biology* 30: 4254-4262.e5

Xu C., Tang H., Hung R., Hu Y., Ni X., Housden B.E. & Perrimon N. (2019) The Septate Junction Protein Tsp2A Restricts Intestinal Stem Cell Activity via Endocytic Regulation of aPKC and Hippo Signaling. *Cell Rep* 26: 670-688.e6

Yamada S., Pokutta S., Drees F., Weis W.I. & Nelson W.J. (2005) Deconstructing the cadherin-catenin-actin complex. *Cell* 123: 889–901

Zhai Z., Kondo S., Ha N., Boquete J.P., Brunner M., Ueda R. & Lemaitre B. (2015) Accumulation of differentiating intestinal stem cell progenies drives tumorigenesis. *Nature Communications 2015 6:1* 6: 1–13

Zhang J., Schulze K.L., Hiesinger P.R., Suyama K., Wang S., Fish M., Acar M., Hoskins R.A., Bellen H.J. & Scott M.P. (2007) Thirty-One Flavors of *Drosophila* Rab Proteins. *Genetics* 176: 1307–1322

Zihni C., Mills C., Matter K. & Balda M.S. (2016) Desmosomes Tight junctions: from simple barriers to multifunctional molecular gates. *Nature Publishing Group*

Zipper L., Jassmann D., Burgmer S., Görlich B. & Reiff T. (2020) Ecdysone steroid hormone remote controls intestinal stem cell fate decisions via the PPARγ-homolog Eip75B in *Drosophila*. *Elife* 9: 1–27